NTNU – Trondheim
Norwegian University of
Science and Technology

Cenozoic Seismic Stratigraphy of the Northern North Sea

The Application of Regional Scale 3D Data.

Anders Ringen

Geology
Submission date: December 2012
Supervisor: Stephen John Lippard, IGB
Co-supervisor: Wim Lekens, GDF Suez E&P Norge AS

Norwegian University of Science and Technology
Department of Geology and Mineral Resources Engineering

Acknowledgements

I would like to express my gratitude towards my supervisor at the Norwegian University of Science and Technology (NTNU) Professor Stephen John Lippard for helping me with thoughtful and constructive comments to the manuscript. I would also like to express my gratitude towards GDF SUEZ E&P Norge AS for providing me with an excellent data set and unparalleled working conditions within their office facilities. I wish to thank the whole Exploration department for including me in their great environment. Special thanks go to external supervisor Wim Lekens. Through the entire process he has been of great support and acted as a motivator providing enthusiasm towards my work and have encouraged me to lay down the best possible effort. Appreciations are also handed to my friends and family, and my fellow students at NTNU for great times during the years at the university.

Abstract

Purpose: To apply regional 3D seismic data within a stratigraphic framework for the Cenozoic northern North Sea. The objective is to interpret the depositional history of the Neogene stratigraphy and to investigate its effects on the underlying Palaeogene strata.

Methodology: Seismic interpretation using seismic- and sequence stratigraphic principles and well data. Calculations of thicknesses, volumes and accumulation rates using depth converted interpretations.

Results/Findings: A depositional model confirming previous work. The post-rift subsiding northern North Sea Basin accommodated thick sedimentary successions. The sediments were supplied by progradation from the basin margins during periods of uplift and lowstand. Three regional erosional surfaces are related to uplift in the Palaeocene, Miocene and Pliocene-Pleistocene. The supply from the eastern basin margin created the largest sedimentary wedges in the Palaeocene, Pliocene and Pleistocene. During the Miocene deltas supplied sand to the Utsira Formation. Two large incised valleys formed from Western Norway into the Møre Basin prior to the onset of Pliocene progradation. Dramatically increasing accumulation rates in the Pliocene are thought to be related to glacial erosion and sediment supply from the Western Norway through the Sognefjord. The Palaeogene stratigraphy has been deformed by polygonal faulting and shale diapirism. The shale diapirs formed in the same time interval as the deposition of the Utsira Formation. The polygonal faulting is thought to have occurred prior to the diapirism.

Implications: Established methodologies of seismic stratigraphy, sequence stratigraphy and shelf edge trajectories have been better constrained with 3D seismic data. Mapping and visualisation in 3D improves the evaluation of time and space relationships of geological events.

Table of Contents

List of Figures

List of Tables

Appendices

1. Introduction

The Cenozoic era is a geological time period marked by changes that have sculptured the world as we know it today. Through the last 65 Ma the landscape of Europe has emerged. The Alpine orogeny has produced spectacular mountain ranges (Coward et al., 2003). The North Atlantic rifting culminated in crustal separation of the European and North American continents. The northern European region has been influenced by periods of uplifts, volcanism and glaciations (e.g. Anell et al., 2009; Hansen et al., 2009; Sejrup et al., 2000). Through all this time the North Sea has been filled with considerable amounts of sediments. The Norwegian continental shelf subsequently contains an outstanding record of the combined effects of tectonic and climatic processes on sediment depositional patterns.

The North Sea has through 45 years of continuous hydrocarbon exploration become one of the most thoroughly investigated continental shelves in the world (Gabrielsen et al., 2001). Due to the interests of petroleum companies vast amounts of excellent data has been acquired. Substantial seismic surveying has been carried out and numerous wells have been drilled. The industrial backdrop provides outstanding conditions for research. The main focus for the petroleum industry has been on the Jurassic, Cretaceous and Palaeocene strata, where most of the major oil and gas discoveries have been made (e.g. Gabrielsen et al., 2001). In sediments younger than Palaeocene, fewer discoveries have been made. Hence, the sedimentary history of the youngest North Sea stratigraphy has been less well documented (Martinsen & Dreyer, 2001)

The depositional history of the shallowest stratigraphy is often considered primarily of academic interest, but for a number of reasons it is also of great importance for the petroleum industry. Firstly, the accumulation of late Cenozoic sediments has strongly contributed to burying source rocks to depths suitable for generating hydrocarbons (Martinsen & Dreyer, 2001). For modelling purposes the industry needs knowledge of the quantity and timing of sediment deposition. Secondly, gas reservoirs at shallow depths in the North Sea constitute hazard when drilling for deeper targets and need to be avoided. Thirdly, there is a potential commercial interest, proven by shallow gas discovered in a commercially viable quantity in 2005 in the Peon discovery made in

Pleistocene sediments of the northern North Sea. The reservoir is located just 200 m below the sea bed and Statoil is currently planning to put the discovery into production (Kristing & Andersen, 2007).

1.1 Confidentiality

Permission is granted from GDF SUEZ E&P Norge AS for usage of proprietary seismic and well data. An agreement is made for the academic work to be subject to one year delayed publication. The following proprietary data has been used: released well and seismic data, the Carmot seismic survey ‘CS02 v.04’, velocity model ‘Vstack NNS Calibrated v.4’ and the Ichron North Viking Graben and Tampen Spur Stratigraphic Database study. Permission is granted from Carmot Seismic AS for usage and presentation of figures of the seismic survey and the velocity model. Additional Permission is granted from Ichron Limited to use the data from the North Viking Graben and Tampen Spur Stratigraphic Database study without releasing any of the underlying data. Permission for the usage of the Ichron sequences scheme and approval of the figures presented in this thesis has been granted.

A confidentiality agreement is made with Ichron Limited to not publish their biostratigraphic markers and sequence boundary depths from wells. Figures with well correlation panels and well sections displaying Ichron sequence well tops and have been made, but are not shown in this thesis.

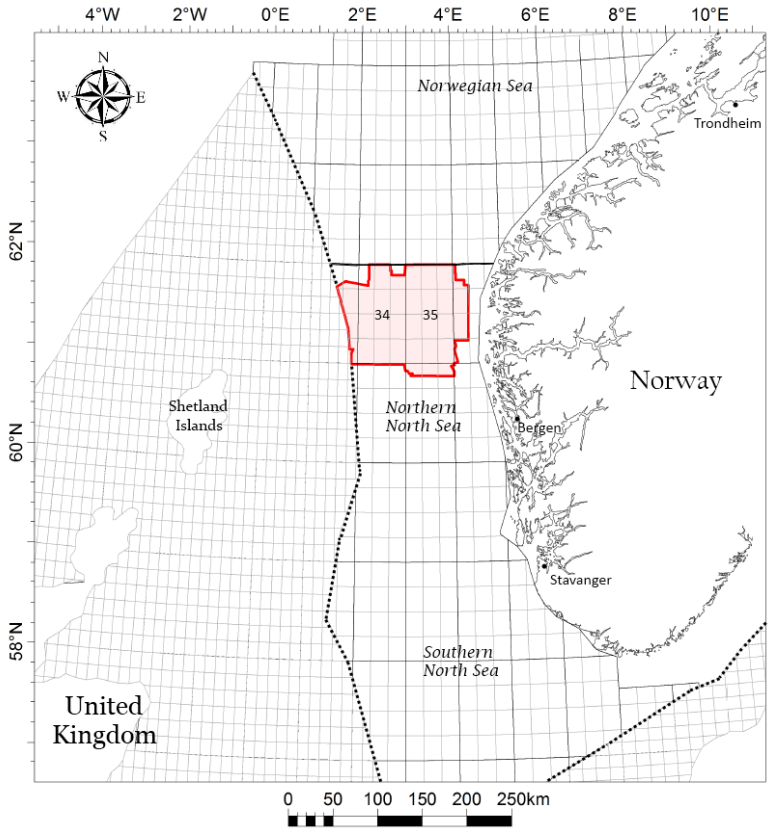

Figure 1. Map showing Norway, offshore dividing lines, blocks and quadrants. Area of interest in red covers Quadrants 34 and 35, in addition to some neighbouring blocks.

1.2 Area of interest

The area of interest is located in the northern North Sea. It covers nearly the whole of Quadrants 33-36, in addition to the northernmost part of Quadrant 31 (Figure 1). Seismic acquisition in the North Sea started already in 1963 (Johansen, 2012). In the northern North Sea, which is considered a mature oil province, modern seismic acquisition is mostly performed in 3D (NPD, 2010). In the time period from 1998 to 2007, 7 2D seismic surveys and 49 3D seismic surveys were acquired north of 60°N (Stenløk, 2008). Within the area of interest oil and gas production started over 30 years ago and currently 18 fields are producing (NPD, 2010; NPD FactPages, 2012) (Table 1). A total of 284 exploration wells and 984 production wells have been drilled within the area of study (NPD FactPages, 2012).

Producing fields within the area of interest					
Fram	Gullfaks	Snorre	Statfjord Øst	Troll	Vigdis
Gimle	Gullfaks Sør	Statfjord	Sygna	Valemon	Visund
Gjøa	Kvitebjørn	Statfjord Nord	Tordis	Vega	Visund Sør

Table 1. Overview over producing fields within the area of interest (NPD FactMap).

1.3 Objectives

The objective is to use regional 3D seismic data along with shallow depth well data to map the Cenozoic stratigraphy of the Norwegian sector in the northern North Sea. The primary objective of this thesis is to interpret the depositional history of the Neogene stratigraphy. The goal is to provide insights into processes that controlled the vast deposition and increasing accumulation rates in the Pliocene epoch. The geological history is interpreted in terms of sediment provenance area, tectonic processes and relative sea-level changes. A secondary objective is to investigate what effects the rapid deposition of Neogene strata may have had on underlying Palaeogene strata. The Quaternary glacial processes are not covered as they would require additional site survey and shallow technical well data.

2. Regional setting

2.1 The North Sea physiography

The North Sea is an intracratonic basin located on the North Atlantic margin. At the present day it is surrounded by landmasses on three sides, the British Isles, Scandinavia and mainland Europe. To the north there is an open connection to the Norwegian Sea. The North Sea is also narrowly connected to the Baltic Sea in the east and to the Atlantic Ocean, through the English Channel, to the south-west. With an average depth of 90 m the North Sea is considered a shallow sea (Walday & Kroglund, 2002). As can be seen from Figure 2, water depths close to the coastlines in the south and at the Dogger Bank area are less than 20 m. To the north of the Dogger Bank water depths gradually increase towards 200 m of the eastern coast of the Shetland Islands. The deepest parts of the North Sea are located within the Norwegian Trench along the Norwegian coast line. The trench was formed by the Norwegian Channel Ice Stream (NCIS) (Sejrup et al., 2000). Along the south-western coast of Norway water depths in the trench reach about 300-400 m. In the Skagerrak the trench reaches its maximum depth of 725 m (Walday & Kroglund, 2002).

The North Sea waters are affected by strong tidal action, a hostile climate, input of fresh water and water inflows from the Atlantic Ocean. The inflowing waters mainly enter the North Sea through its northern opening. The main water current moves south- and eastwards along the western slope of the Norwegian Trench. Smaller inflowing currents also enter through the English Channel and south of the Shetland Islands. In the Skagerrak, the North Sea water mixes with less saline water sourced from the Baltic. The brackish water subsequently moves into the Norwegian Trench and flows back to the Atlantic Ocean. The general circulation pattern of the North Sea moves in an anti-clockwise direction (Figure 2) (Walday & Kroglund, 2002).

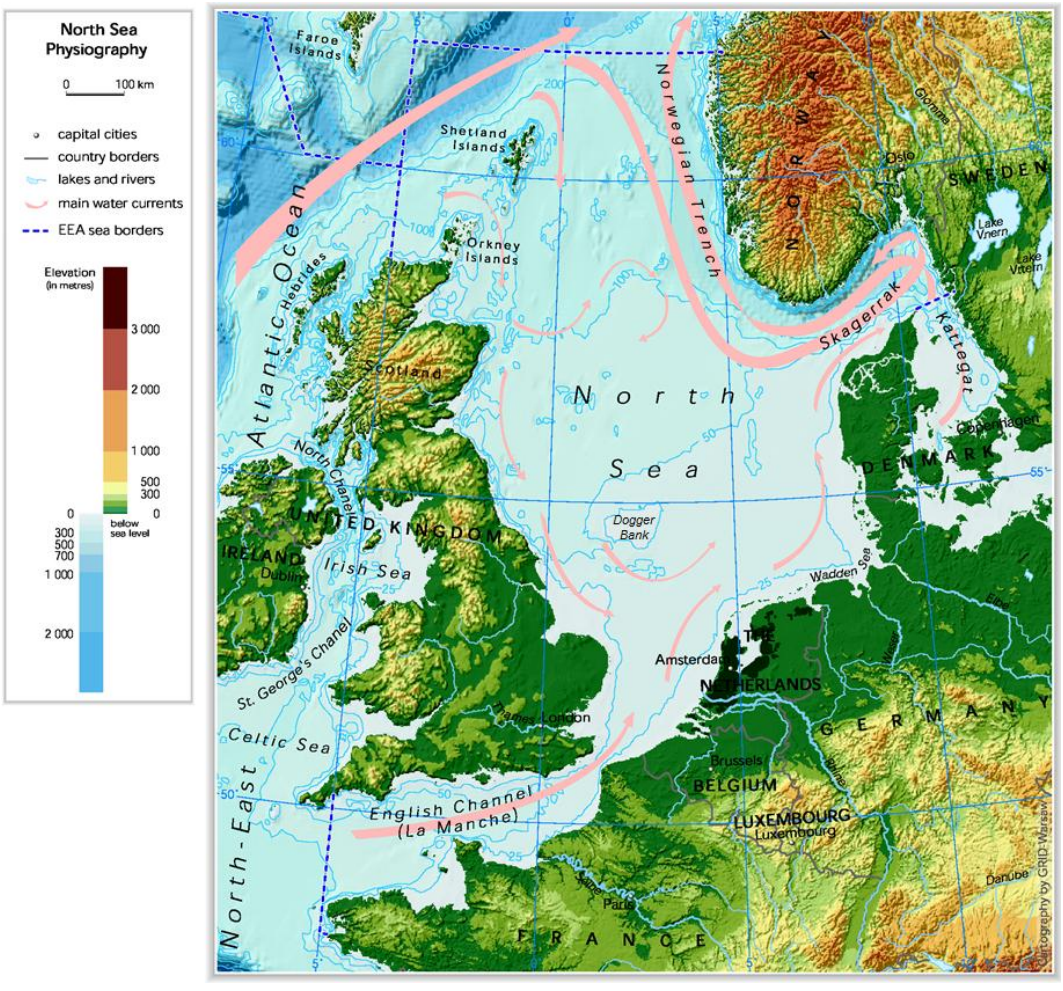

Figure 2. The North Sea Physiography with depth distribution and main currents (After Walday & Kroglund, 2002).

2.2 Crustal structure

The crust beneath the North Sea Basin sedimentary succession is of Precambrian to Lower Palaeozoic age. The Caledonian orogeny, caused by the continental collision between Laurentia, Baltica and Avalonia, culminated in Late Silurian-Early Devonian crustal deformation (Zanella et al., 2003). The crust was generally thickened. Subsequent mainly Mesozoic crustal extension has thinned the crust (Ziegler & Dèzes, 2006). As a result, the depth to the Moho is variable beneath the North Sea. On the platforms, on both sides of the Mesozoic rift system, the depth to the Moho is around 33-34 km, while beneath the Viking and Central Grabens it is 24 km or less. In local areas the depth is as low as 20 km. Late Cretaceous and Cenozoic post-rift thermal subsidence has contributed in lowering the depth to the Moho by over 4 km (Ziegler & Dèzes, 2006). It is in the areas of extensive crustal thinning that the thickest successions of post-rift sediments have been deposited (Zanella et al., 2003).

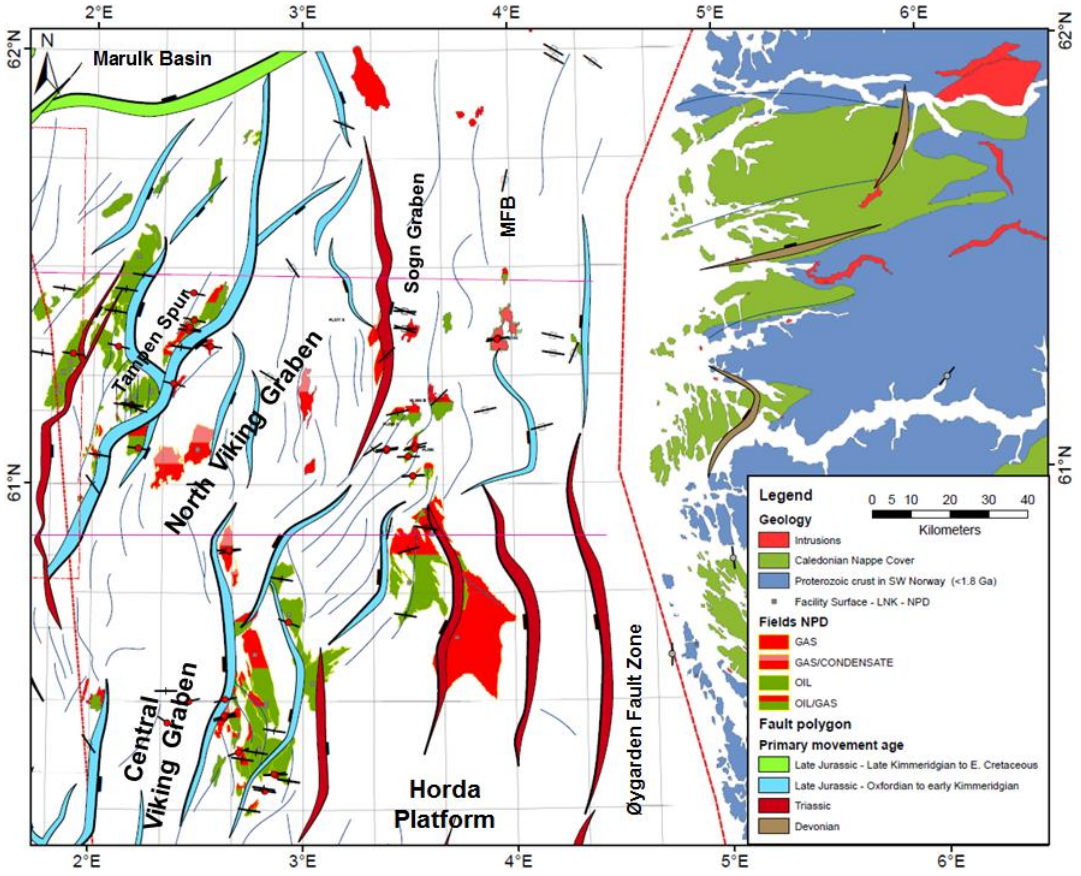

Figure 3. Stress and tectonics map of the northern North Sea illustrating the main tectonic elements. Major faults are colour coded corresponds to their principal age of movement. MFB = Måløy Fault Blocks (Data based on Zanella & Coward, 2003).

2.3 Tectonic setting

The tectonic setting in the North Sea is sculptured by a long history of several extensional phases following the Caledonian crustal accretion. Several episodes of extensional tectonism have prevailed in the Devonian, Permian-Early Triassic and Late Jurassic-Early Cretaceous. The principal structural features that were formed in the northern North Sea are illustrated in Figure 3. The major faults' principal timing and their relative magnitude of displacement is displayed as by fault polygons with colour coding. The Caledonian continental collision ceased during the late Silurian to Early Devonian after having formed major low angle thrust faults in the Scottish and Norwegian mainland. A large basin developed in the northern North Sea following the continental collision, probably caused by gravitational subsidence of a thickened crust. A deep pull-apart basin developed in the Devonian, with low-angle detachment faults connected by NE trending, crustal scale strike-slip faults. These large faults are known as the Møre-Trøndelag/Great-Glen fault zone and the Midland Valley basin fault system further south (Figure 4). Baltica and Laurentia were moving laterally to each other and the associated sense of displacement of Devonian and Early Carboniferous age was sinistral. In the Carboniferous the large faults were reactivated, but with a reversed movement. Devonian faults are recorded onshore in the western parts of Norway (Figure 3) (Zanella & Coward). After the Carboniferous inversion volcanism and intrusions prevailed and a period of uplift and subsequent thermal subsidence followed (Coward et al., 2003). During the Carboniferous the Mid North Sea High was uplifted and the Northern and Southern Permian basins were formed (Figure 4).

Triassic rifting activity generated deep half grabens, located in the eastern parts of the northern North Sea. The major Triassic structures that were formed are the Sogn Graben, the Horda Platform, and the Stord Basin. The eastern limit of the Triassic basins is defined by the north-trending Øygarden Fault Zone, where the basement is offset by up to 8 km. The western limit of the Sogn Graben is an eastern dipping fault that has been offset by about 4.5 km, where 2 km offset is accounted to Triassic extension.

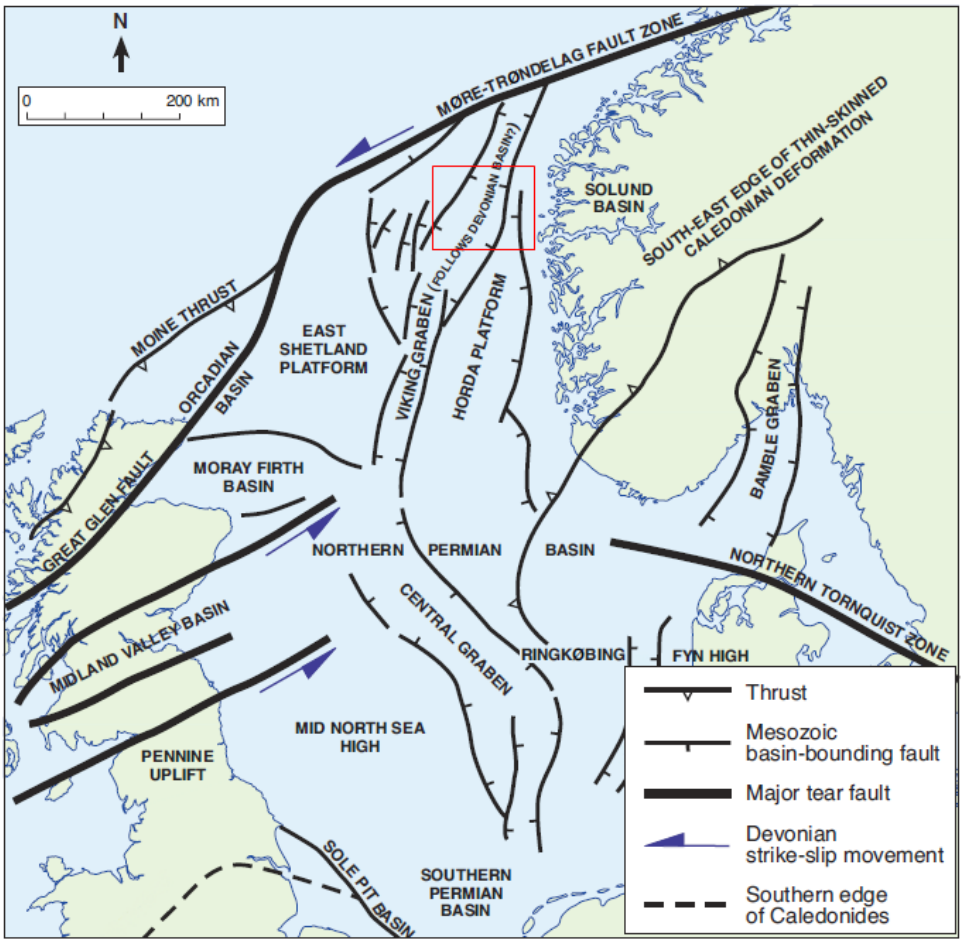

Figure 4. Tectonic framework of north-west Europe. The area of study is marked with a red square (After Zanella & Coward, 2003).

During the Late Jurassic a triple junction rift system developed in the North Sea, with arms forming the major structures of the Viking Graben, the Central Graben and the Moray Firth Basins. The centre of the triple junction was located at the same position as a preceding Middle Jurassic thermal dome. Together with pre-existing basement lineaments of Caledonide and Tornquist origin zones of structural weakness was provided (Fraser et al., 2003). The rifting underwent as multiple pulses of faulting with intervening stages of relative tectonic quiescence. In the northern North Sea the North Viking Graben forms a major asymmetric structure trending north to north-east with major faults dipping to the east or east-south-east (Zanella & Coward, 2003). On the western side of the Viking Graben the East Shetland Basin and the elevated East Shetland Platform are located. Towards the east, neighbouring structures are the Sogn Graben, the Horda Platform, the Måløy Fault Blocks and the Øygarden Fault Zone (Figure 3) (Fraser et al., 2003).

A Late Cretaceous inversion phase created inverted structures in the southern North Sea. The influence of the inversion phase was very weak in the northern North Sea (Zanella & Coward, 2003). The Cretaceous to Cenozoic periods were dominated by regional thermal subsidence, in addition to periods of basin flank uplifts. In Eocene and Oligocene local inversion was associated with the opening of the Labrador Sea, west of Greenland. The present day stress regime in the North Sea is characterised by an average maximum horizontal stress orientated north-west to south-east, which is consistent with the stress field active in north-western Europe (Zanella & Coward, 2003).

2.4 Regional development

2.4.1 Late Palaeozoic-Triassic – terrestrial to marine strait

During Late Silurian to Early Devonian times the continental collision between Baltica and Laurentia came to an end. The continental collision had formed the Caledonian orogeny (Coward et al., 2003). Sediments of Devonian age have been recorded in local detachment basins onshore western Norway, but not offshore (Marshall & Hewett, 2003). Rifting activity started during the latest Devonian to Middle Carboniferous. Sediments of Carboniferous and Permian age have not been encountered in the northern North Sea (Glennie et al., 2003), but in the southern and northern Permian basins the Rotliegend and Zechstein Groups were deposited (Coward et al., 2003). From the Late Permian-Early Triassic and onwards the Pangaean supercontinent was progressively broken up by successive rifting events (Martinsen & Dreyer, 2005). The area of the northern North Sea developed from terrestrial to becoming a narrow marine strait from the Late Triassic to the Early Jurassic (Figure 5). A multi-directional rift system developed in Western and Central Europe. In the North Sea the Horn, Moray Firth, Central and Viking Grabens developed in the Early Triassic. The North Danish-Polish Trough developed and the rift systems of the Alpine domain, the Bay of Biscay and the Western Shelves were activated (Ziegler & Dèzes, 2006).

2.4.2 Early-Mid Jurassic – thermal doming

The Early Jurassic is referred to as a time of tectonic quiescence in the North Sea. To the south of the Gibraltar Transfer Zone sea-floor spreading was ongoing in the Central Atlantic (Figure 5). The Triassic to Early Jurassic formed basins thermally subsided. The subsidence allowed for a continuous deposition of Lower Jurassic sediments, conformably over the Triassic strata. The uplift of the North Sea Dome during the Mid-Jurassic created the Intra-Aalenian Unconformity. The doming is suggested to be caused of a thermal effect of a hot mantle plume leading on to volcanism. Much of the Early Jurassic strata were eroded due to subaerial exposure (Husmo et al., 2003). The exposed North Sea Dome sediments sourced the sands of the Brent Delta in the northern North Sea (Zanella & Coward, 2003). The clastic sediments of the Brent Group are preserved in great thicknesses (100-500 m) to the north of the North Sea Dome, where they today make up some of the most important hydrocarbon reservoirs in the North Sea (Husmo et al., 2003).

2.4.3 Late Jurassic – extensive rifting

Crustal extension with the formation of rotational fault blocks in the northern Viking Graben was initiated in the late Middle-Jurassic (Bathonian). The majority of extension underwent in the Late Jurassic (Calovian-Kimmeridgian). Major faults developed and the younger sedimentary sequences were tilted forming suitable structural traps for later hydrocarbon accumulation. The rifting activity was a controlling factor for the coeval Late Jurassic sedimentation. Late Jurassic deposits display great variations in depositional facies from coastal, shelf and deep-water systems to mud-dominated marine facies (Fraser et al., 2003). At the centre of extension a series of grabens and half grabens were formed. In the area of interest the Viking Graben and its northern extension, the Sogn Graben, now represent a 25–40 km wide NNE–SSW-trending depression in the northern North Sea (Dmitrieva et al., 2012). The transition between syn-rift and post-rift deposition is marked by unconformity in the North Sea, commonly referred to as the “Base Cretaceous Unconformity” (BCU) (Gabrielsen et al., 2001). Limited extension still occurred at the transition to the Cretaceous, but ceased completely during the Early Cretaceous (Coward et al., 2003).

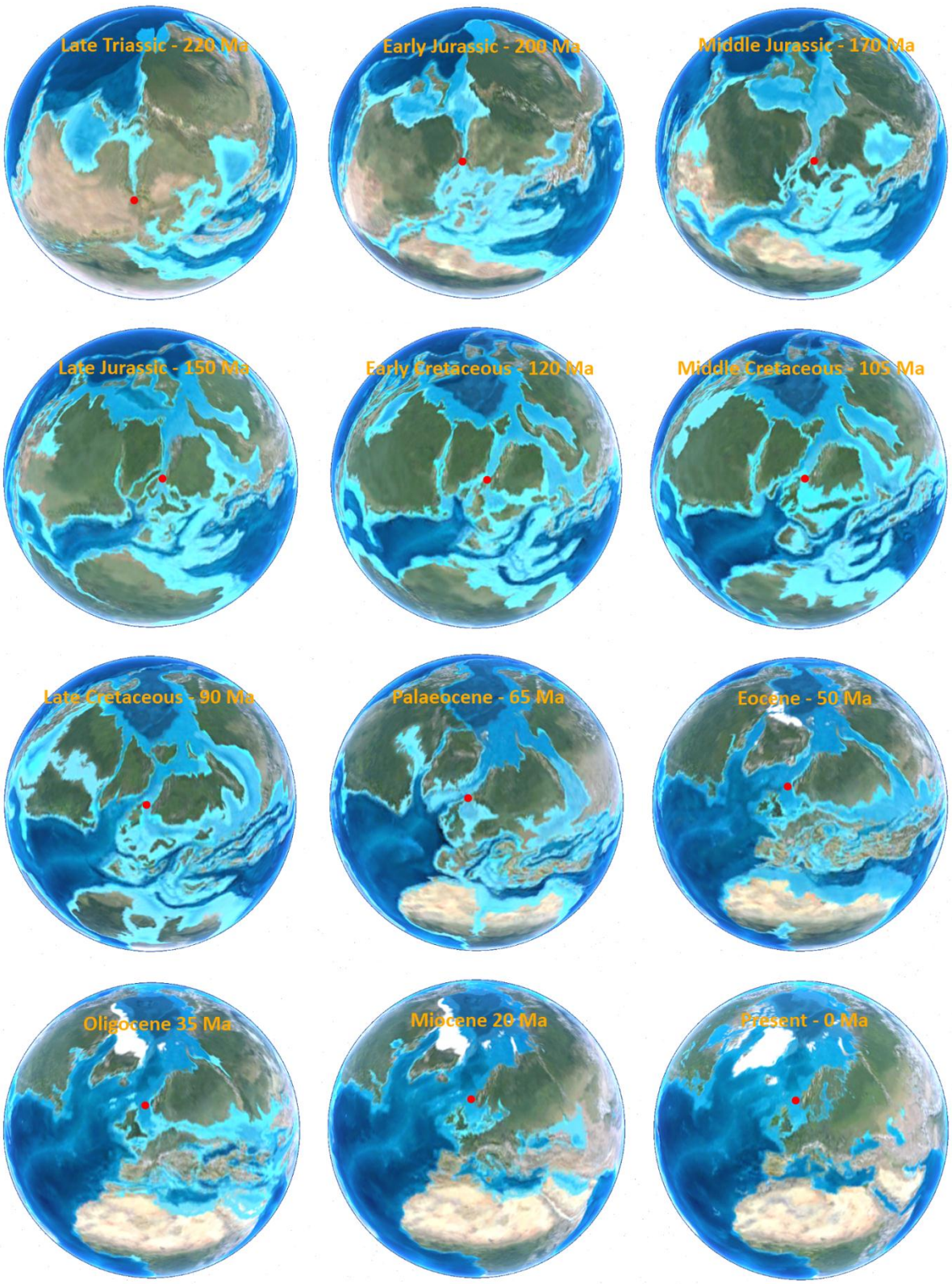

Figure 5. Paleogeographic overview from Triassic times to Present. Northern North Sea location is marked with a red dot. Produced using Google Earth (Hronusov, 2006).

2.4.4 Cretaceous – subsidence and infill

During Early Cretaceous the oceanic spreading in the Central Atlantic broke through the Gibraltar Transfer Zone and a northward continuation of the spreading ridge was made up into the Labrador Sea and the Rockall Trough, west of the British Isles. The rifting activity in the North Atlantic was however modest in the Cretaceous (Coward et al., 2003). As the crustal extension became focused in the Atlantic rift system, the tectonic activity in the North Sea rift system subsequently waned. Post-rift thermal subsidence of the failed rift system began in the Early Cretaceous (Ziegler & Dèzes, 2006). During Cretaceous times the deposition in the northern North Sea was characterized by deep marine infill (Wien & Kjennerud, 2005). The North Sea Basin subsidence was amplified by the continuous sediment loading (Gabrielsen et al., 2001). Seafloor spreading in the Atlantic with subsequent volcanism increased the CO_2 content in the atmosphere and raised the global temperature. Deposition of chalk was widespread in the southern part of the North Sea. However, in the northern North Sea deposition of shale dominated (Brekke & Olaussen, 2007). The tectonic structures were gradually onlapped and covered (Coward et al., 2003). The sedimentation was more or less continuous throughout the period and by the end of the Cretaceous the Jurassic rift relief had almost completely diminished (Wien & Kjennerud, 2005).

2.4.5 Palaeocene – uplift and volcanism

Throughout the Cenozoic the North Sea area developed as a passive continental margin (Brekke et al., 2001). Sediments were deposited, largely accumulating over the continuously subsiding graben structures (Anell et al., 2012). In Palaeocene the North Atlantic rifting activity started causing volcanism that formed the Northern Atlantic Igneous Province (NAIP). Volcanic rocks were formed in the western and eastern parts of Greenland and around the NW British Isles, Faroe Islands and over to the Møre and Vøring margins (Figure 6) (Hansen et al., 2009). The Iceland Plume hot spot developed in Early Palaeocene and generated a regional thermal uplift. Adjacent to the North Sea, an area extending down towards the Shetland Platform and the UK was elevated (Martinsen & Nøttvedt, 2007). The flanks on both sides of the Viking and Central Grabens were uplifted (Ahmadi et al., 2003). Consequently older Mesozoic hinterlands and basin margins were eroded and supplied sand to the

subsiding basins turning them into major depocentres of large deltas and submarine-fan systems (Bowman, 1998). The majority of input in the Palaeocene and Eocene derived from the western margin of the North Sea. The Scotland and Shetland Platform areas were significantly more uplifted and exposed to erosion than Scandinavia. Only minor sand systems were fed from the Norwegian side (Ahmadi et al., 2003). The volume and grain size of the Palaeocene deposits were at their greatest towards the end of the period (Bowman, 1998).

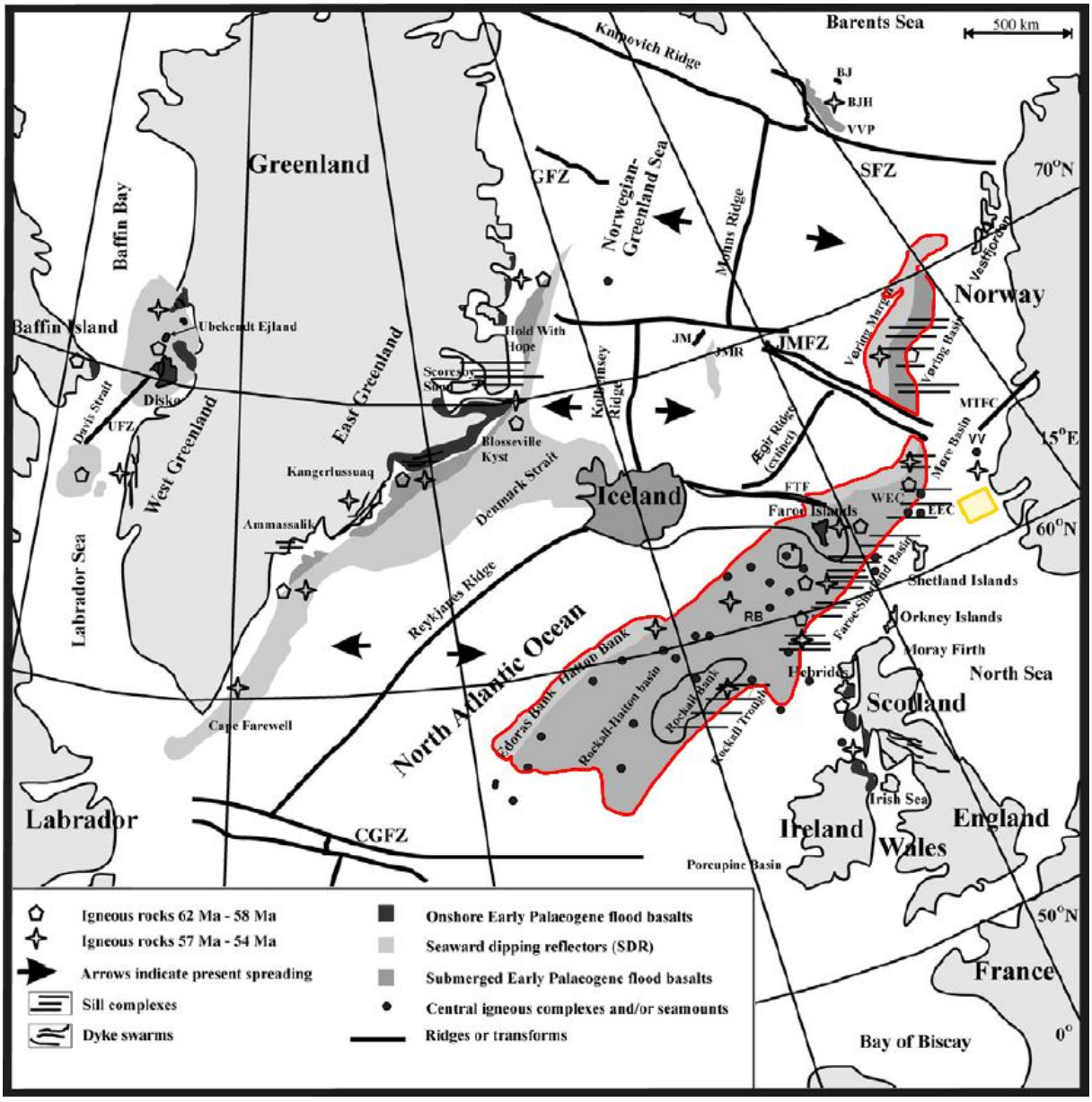

Figure 6. Map of the North Atlantic Igneous Province (NAIP). The area of interest is marked in yellow and the igneous rocks closest to the North Sea are marked in red (After Hansen et al., 2009).

2.4.6 Eocene – opening of the Norwegian-Greenland Sea

At the transition from Palaeocene to Eocene (56 Ma) final crustal separation was achieved between Greenland and Europe in the Norwegian-Greenland Sea and west of the British Isles. The volcanic activity consequently ceased at the margins and remained centred over the spreading axes and on Iceland (Ziegler, 1988; Skogseid et al., 2000; Ziegler & Dèzes, 2006). The Early Eocene volcanism caused the deposition of the widespread tuffaceous Balder Formation in the North Sea (Galloway et al., 1993). Because of the sea-floor spreading to the north-west and the ongoing Alpine orogeny to the south-east, the North Sea Basin was placed in compression (Knott et al., 1993). The compression provided a mechanism for basin margin uplift and amplified the relief to the basin centre (Galloway et al., 1993). The thermal subsidence created a marine connection between the North Sea and the North Atlantic Ocean along the failed rift system (Bowman, 1998). Following the opening of the North Atlantic the Scotland-Shetland Platform subsided, which in terms reduced the sediment source area for the North Sea (Galloway et al., 1993). The sedimentary fill in Eocene time was much more mud prone than during the Palaeocene. The sediment supply, and especially the sand fraction, gradually decreased throughout the Eocene. The submarine fans in the Eocene were much smaller than the large, stacked submarine fans of the Palaeocene. Mid- to Late Eocene sedimentation was typically more channelized (Jones et al., 2003). The main part of the Eocene succession is a slope/basin floor system downlapping and thinning towards the east in the northern North Sea (Martinsen et al., 1999). The eastward thinning indicates a near absence of sediment input from the eastern margin. Only the occasional sand deposit was sourced from Norway in the northern North Sea (Jordt et al., 1995).

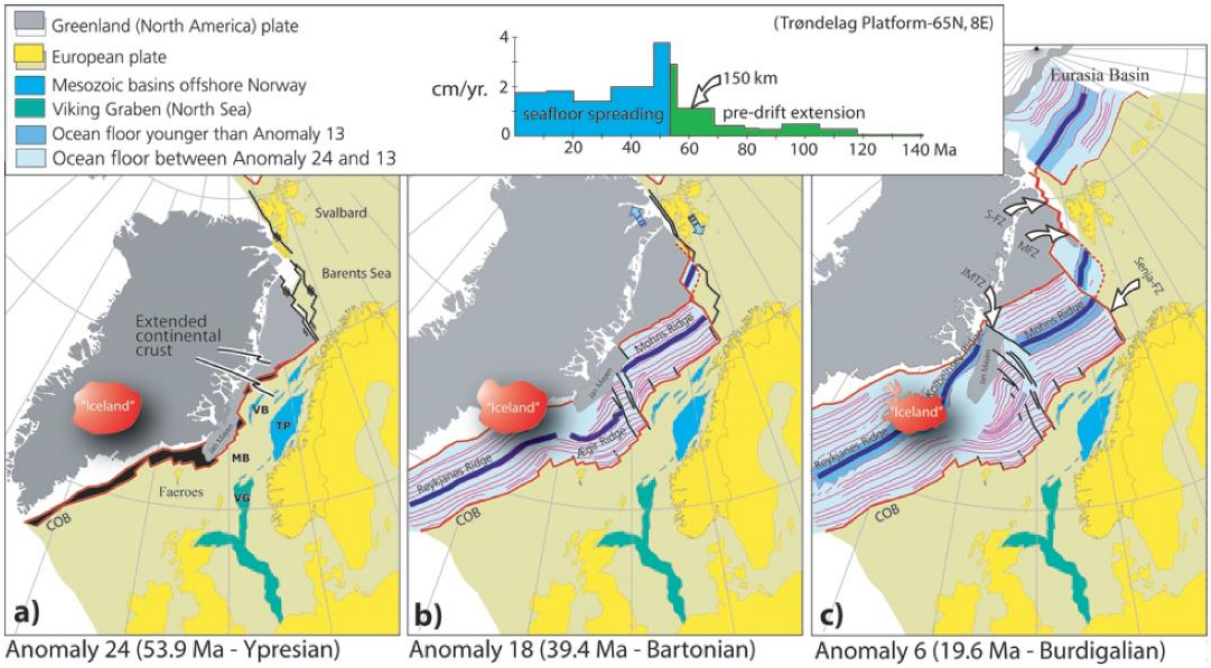

Figure 7. Opening of the Norwegian-Greenland Sea as documented by magnetic seafloor anomalies (Torsvik & Crocks, 2005).

2.4.7 Oligocene – from greenhouse to icehouse

In the North Sea the Oligocene was a time of tectonic quiescence (Anell et al., 2009). To the north-west the opening of the North Atlantic was ongoing, focused over three interconnected spreading ridges, the Reykjanes, Ægir and Mohns Ridges (Figure 7). About 35 Ma, at the transition to the Oligocene, the Ægir ridge to the south-east of the Jan Mayen microcontinent was abandoned. The Reykjanes Ridge had propagated further north- and westwards and as an accommodation for this movement a new ridge, the Kolbeinsey Ridge, was formed on the north-western side of Jan Mayen. The Jan Mayen microcontinent rotated away from Greenland in an anticlockwise direction and started following the Eurasian plate movement. The seafloor spreading in the Labrador Sea west of Greenland ceased and Greenland became attached to the North Atlantic plate (Torsvik & Cocks, 2005). For the North Sea the effect may have been some localized uplift due to compression and the changes in the North Atlantic spreading dynamics (Anell et al., 2009). In the Early Oligocene the global climate changed from a greenhouse environment into an icehouse environment (Zachos et al., 2001). Substantial amounts of ice were accumulating in the Antarctic which forced the global sea levels to fall (Martinsen &

Nøttvedt, 2007). In the North Sea Basin the gentle and steady thermal subsidence proceeded (Fyfe et al., 2003). Over most parts of the northern North Sea deposition was dominantly argillaceous and thick layers of clay were deposited. The Palaeocene and Eocene land-laid ash deposits and volcanic rocks were eroded and transported into the North Sea basin. The volcanic rocks have sourced the large amount of smectite deposited at this time (Løseth et al., 2003). Initially the majority of Oligocene sediments were supplied from the west (Martinsen & Nøttvedt, 2007). This dominant supply direction then ceased. Central Europe emerged during the Eocene-Oligocene. The erosion and drainage of the emerged landmass created a supply of sediment to the North Sea basin coming from the south-east (Fyfe et al., 2003). In addition, the first substantial influx of sediment from Norway started in the Oligocene (Galloway et al., 1993).

2.4.8 Miocene – uplift and erosion

The Miocene was, just as the Oligocene, characterized by regional tectonic quiescence in the North Sea (Anell et al., 2009). However, the climatic setting of the region changed. The newly formed mountain ranges, consisting of the Alpine and Himalayan chains, affected the atmospheric circulation. The mountains prevented the exchange of polar and tropical air and the altered circulation pattern terminated the relatively hot and wet climate, and led to the onset of a cooling period (Martinsen & Nøttvedt, 2007). Climatic cooling was accompanied by an uplift of the eastern basin margin and southern Norway (Galloway et al., 1993; Anell et al., 2009).The relative sea level in the North Sea basin was lowered. A regional unconformity in the northern North Sea corresponding to the uplift was formed. The unconformity is interpreted to have lasted from the latest Oligocene (ca. 25 Ma) and to the Late Miocene (ca. 8-9 Ma). During this period it is estimated that the erosion lasted for 2-3 Ma with subsequent non-deposition for 12 Ma (Martinsen et al., 1999). The uplift of the shelf area resulted in increased sediment input to the North Sea basin. The sand-rich Utsira Formation was deposited overlying the mid-Miocene unconformity (Galloway et al., 1993). The Utsira Formation consists of several sand bodies sourced from the basin margins. In the northern North Sea the thick main quartzose sand unit pinches out and a thinner glauconitic sand unit dominates (Eidvin & Rundberg, 2001). Along

the eastern basin margin a partly time equivalent Utsira Sand East unit has been deposited (Gregersen & Johannesen, 2007).

2.4.9 Pliocene – stacking of clinoforms

At the beginning of Pliocene the climate was relatively warm (Zachos et al., 2001; Anell et al., 2009) On the Norwegian margin, the first glacial influence is thought to be simultaneous with the northern hemisphere major glaciation at 2.74 Ma (Eidvin et al., 2000). The following periods of glaciation significantly increased the sediment supply to the continental shelf. Deep mainland erosion led to deposition of huge sediment volumes on the adjacent shelf (Martinsen et al., 1999). A period of regression caused regional erosion and a hiatus (Eidvin et al., 2000). Uplift of the near coastal and onshore areas, forced sediments to prograde towards the basin centre and thereby formed the Upper Pliocene succession of clinoforms. By building out at a level several hundred meters above the Utsira Formation (Gregersen & Johannessen, 2007) the generally regressive successions of sedimentary wedges (Gregersen et al., 1997) record the highest sedimentation rates on the Norwegian shelf (Martinsen & Dreyer, 2001). The wedges mainly consist of clay and silt and the uppermost parts have been erosionally truncated (Gregersen, 1997). Relative sea-level changes, probably controlled by glacio-eustacy, ended the general Pliocene progradation (Gregersen, 1998). The relative sea level fell toward the end of the Pliocene (Zachos et al., 2001). Tilting of the Neogene deposits along with widespread erosion in the North Sea indicates an uplift phase in Scandinavia (Japsen et al. 2011). A marked angular unconformity was formed at the top of the Pliocene deposits (Wien & Kjennerud, 2005; Brekke et al. 2001).

2.4.10 Pleistocene – glaciation

The global climate continued to cool into the Pleistocene. The cooling caused the development of a Scandinavian ice cap (Sejrup et al., 2000). On occasions the North Sea climate was more temperate giving alternations of periglacial, glacial and glaciomarine conditions. The Scandinavian and Scottish ice sheets repeatedly advanced and retreated into the sea leading to both erosion and deposition of a range of ice-related sediments (Fyfe et al., 2003). Ice sheets probably covered the

area between Scotland and Norway at some point. At times of lower sea levels, the North Sea basin floor may also have been exposed as ice-free tundra (Lambeck, 1993). A regional angular unconformity was formed over the tilted Neogene sediments, removing the upper parts of the prograding Pliocene deposits. Some of the ice from the Scandinavian ice cap is believed to have drifted from the Oslofjord, through Skagerrak and northwards along the Norwegian shoreline. The flowing ice transported and deposited large amounts of sediments (Sejrup et al., 1996). This Norwegian Channel Ice Stream (NCIS) has created an N-NW-S-SE deepening trench which is the prominent morphological feature on the present bathymetry (Wien & Kjennerud, 2005). The Norwegian Channel stratigraphy is characterised by extensive flat lying, relatively uniform Quaternary deposits. Tills are overlain by glaciomarine and marine sediments. Frequently, solely tills separated by Glacial Erosion Surfaces (GES) are preserved (Sejrup et al., 1996). A widespread regional uplift on the north western Atlantic margin has been interpreted as an isostatic response to the glacial erosion and rebound, following the ice sheet melting. Thermal effects following the North Atlantic opening have also been proposed (Riis & Fjeldskaar, 1992), but the tectonic influence on the uplift is uncertain (Anell et al., 2009).

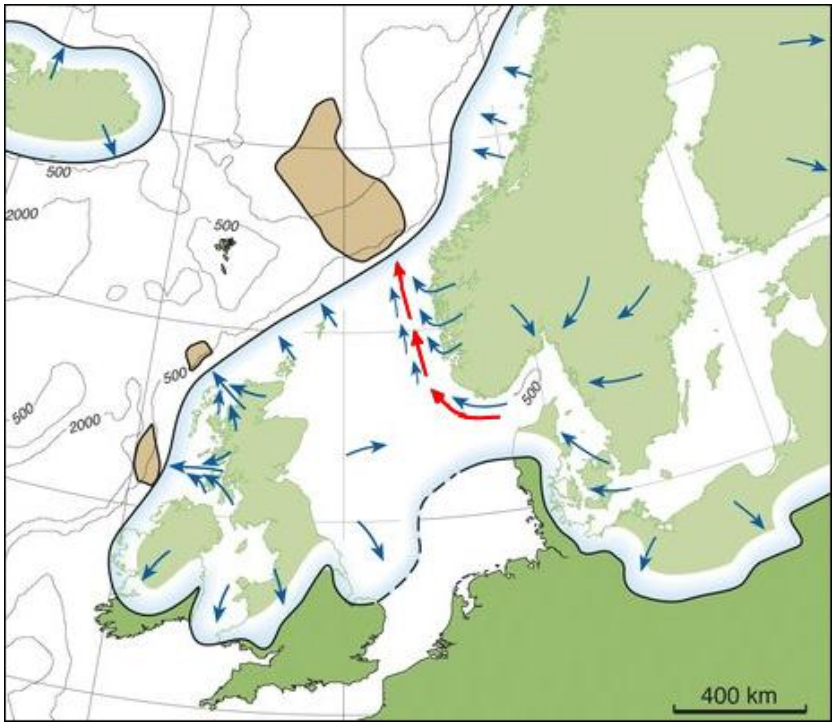

Figure 8. Model of the British and Scandinavian ice sheets. The blue arrows show ice flows and the red arrows mark the Norwegian Channel Ice Stream (NCIS). The brown areas on the continental margins mark large depositional areas of the continental slope related to the ice streams including the large North Sea Fan (After Sejrup et al., 2000).

2.5 Chronostratigraphy

Chronostratigraphy is the element of stratigraphy that deals with the relative time relations and ages of rock bodies. The geochronology is ranked in a hierarchy starting with Eon which is subdivided into Era, Period, Epoch and Age (Stage) (Salvador, 1994). The chronostratigraphic scheme of this thesis matches the numerical ages of the Ichron report and the International Stratigraphic Chart 2010. All are based on Gradstein et al., (2004) and Ogg et al., (2008) (Ichron, 2010; ICS, 2010). The chronostratigraphic column, along with sequence- and lithostratigraphy, is illustrated in Figure 9.

2.6 Lithostratigraphy

Stratigraphy is the science of describing rock bodies based on properties or attributes the rocks possess. Lithostratigraphy defines and characterises rock bodies on the basis of observable lithological properties. Units are systematically organized referring to their lithological composition and stratigraphic position. The primary units of lithostratigraphy are called formations. Several associated formations with significant and diagnostic lithological properties in common are gathered in groups. The unit next in rank below a formation is called a member. A member is always part of a formation, but possesses lithological properties that distinguishes it from adjacent parts of the formation (Salvador, 1994).

The lithostratigraphy of the central and northern North Sea was described by Deegan & Scull (1977). Dalland et al. (1988) published, on behalf of the Norwegian Petroleum Directorate (NPD), a lithostratigraphic scheme for the Mesozoic and Cenozoic succession offshore of mid- and northern Norway. Isaksen & Tonstad (1989) published on the behalf of the NPD, a revision of the Cretaceous and Cenozoic nomenclature that was first introduced by Deegan & Scull. The area of interest lies within the North Sea. The northern limit of the area of interest borders the Norwegian Sea, for this reason the lithostratigraphy of Dalland et al. (1988) is also relevant. The Norwegian Offshore Stratigraphic Lexicon (NORLEX) project, led by the Geology Museum at the University of Oslo, undertakes a systematic update of the offshore lithostratigraphy, based on updated geologic information. They have revised the

regional lithostratigraphy following the guidelines of the International Stratigraphic Guide. A significant difference to the NPD schemes is the classification of siliciclastic units with limited distribution within marine shales as members and not as formations (Gradstein et al., 2010). An illustrative comparison of the lithostratigraphic schemes is seen from Figure 9. The lithostratigraphic well tops from NPD used in this thesis are based on Isaksen & Tonstad (1989) (Section 3.3.2).

2.6.1 The Cromer Knoll and Shetland Groups

The Cretaceous deposits have been divided into two major groups corresponding with the division between the Early and Late Cretaceous epochs. The Cromer Knoll Group is of Early Cretaceous age and consists of fine-grained, argillaceous, marine sediments with varying content of chalk. It is widely distributed in the Norwegian sector but the thickness varies as it was deposited over an irregular topography formed during Late Jurassic rifting. The Cromer Knoll Group is thickest in the northern North Sea in the Sogn Graben where it is thought to be close to 1400 m thick. The Shetland Group is of Late Cretaceous age. It consists mostly of chalk in central parts of the North Sea, in the northern North Sea however it is mainly siliciclastics and marls. The thickness of the package ranges from 1000 to 2000 m (Isaksen & Tonstad, 1989).

2.6.2 The Rogaland Group

The Cenozoic stratigraphy of the North Sea has been divided into three groups: the Rogaland, Hordaland and Nordland Groups. The Rogaland Group was deposited from Palaeocene to Early Eocene. In most of the Norwegian North Sea it consists mainly of argillaceous sediments. In some areas sandstones interbedded with shales are also observed. The sediments were deposited in a relatively deep marine environment characterized by submarine fans built out from the west. The Rogaland Group is subdivided into 12 formations. Three of the formations are represented in the study area. The Våle Formation is the oldest; it typically consists of marls and claystones interbedded with limestones, sandstones and siltstone. It has been recognised in the northern North Sea, it is however very thin in this area. The overlying Lista Formation is widespread in the North Sea. It consists of poorly laminated brown to grey-brown shales. Thin sandstone layers are locally developed.

The upper part of the Rogaland Group is represented by the Balder Formation. It was deposited at the end of Palaeocene and consists of ash-fall deposits within shales distributed over large areas forming a regional marker horizon. The deposition was due to explosive volcanism, believed to be linked to an active rifting phase at the time. It was deposited in a deep marine setting by hemipelagic sedimentation (Isaksen & Tonstad, 1989). The Balder ash fall deposits has been dated from 40Ar-39Ar isotopes to be of early Eocene age (54.5-54.0 Ma) (Berggren et al., 1995) and the Balder formation has thus been included in the early Eocene for the Norlex lithostratigraphy**.** Norlex also includes the siliciclastic Hermod Member to the Sele Formation and the Odin Member to the Balder Formation, in the area east of the North Viking Graben (Gradstein et al., 2010).

2.6.3 The Hordaland Group

The Hordaland Group ranges from Eocene to Early Miocene age. In the northern North Sea the deposits are a couple of hundred metres thick. Marine claystones of brown to light-grey colour are the dominant deposits, with presence of minor sandstones at various levels. The sandstones are generally very fine to medium grained and are often interbedded with claystones. The Hordaland Group is subdivided into the Frigg, Grid, Skade and Vade Formations. The first three formations are sourced from the East Shetland Platform. Within the Norwegian sector they are only recognized in the western parts of the central and southern North Sea. The Vade Formation is only distributed in Quadrant 2, within the Central Graben (Isaksen & Tonstad, 1989). The Norlex division of the Hordaland Group in the area east of the Viking Graben is divided into the Lark and Horda Formations. The Lark formation constitutes two siliciclastic members, the Skade Member and an unnamed member (Gradstein et al., 2010). The Brygge formation makes up the whole Hordaland Group in the Norwegian Sea (Dalland et al., 1988).

2.6.4 The Nordland Group

The Nordland Group is the uppermost and youngest lithostratigraphic group ranging from Middle Miocene to Recent in age. The lower boundary to the underlying Hordaland Group is represented by an unconformity. Shallow marine shelf sandstones of the Utsira Formation overlie the Hordaland Group clays and mark the

base of the Nordland Group. The Utsira Formation sandstones are interbedded with claystones and minor siltstones. The Utsira Formation is the only subdivision defined in the Nordland Group by Isaksen and Tonstad (1989). The succession above the Utsira Formation consists of unconsolidated clays and sands. The uppermost part consists of glacial deposits. The Norlex division of the Nordland Group in the area east of the Viking Graben also includes only one formation, the Kai Formation. Within the Kai Formation is the Utsira Member (Gradstein et al., 2010). On the mid-Norwegian continental shelf Dalland et al. (1988) established the Early Miocene to Late Pliocene Kai Formation and the Late Pliocene-Pleistocene Naust Formation. The corresponding sediments in the North Sea Basin belong to the Nordland Group but have not been divided into specific formations. The Kai Formation is of Early Miocene to Late Pliocene age. It consists of alternating claystone, siltstone and sandstone with limestone stringers. The Naust Formation is of Late Pliocene age. It is laterally continuous along the Mid-Norwegian Shelf. The formation consists of interbedded claystone, siltstone and sand, occasionally with very coarse clastics in the upper part (Dalland et al., 1988).

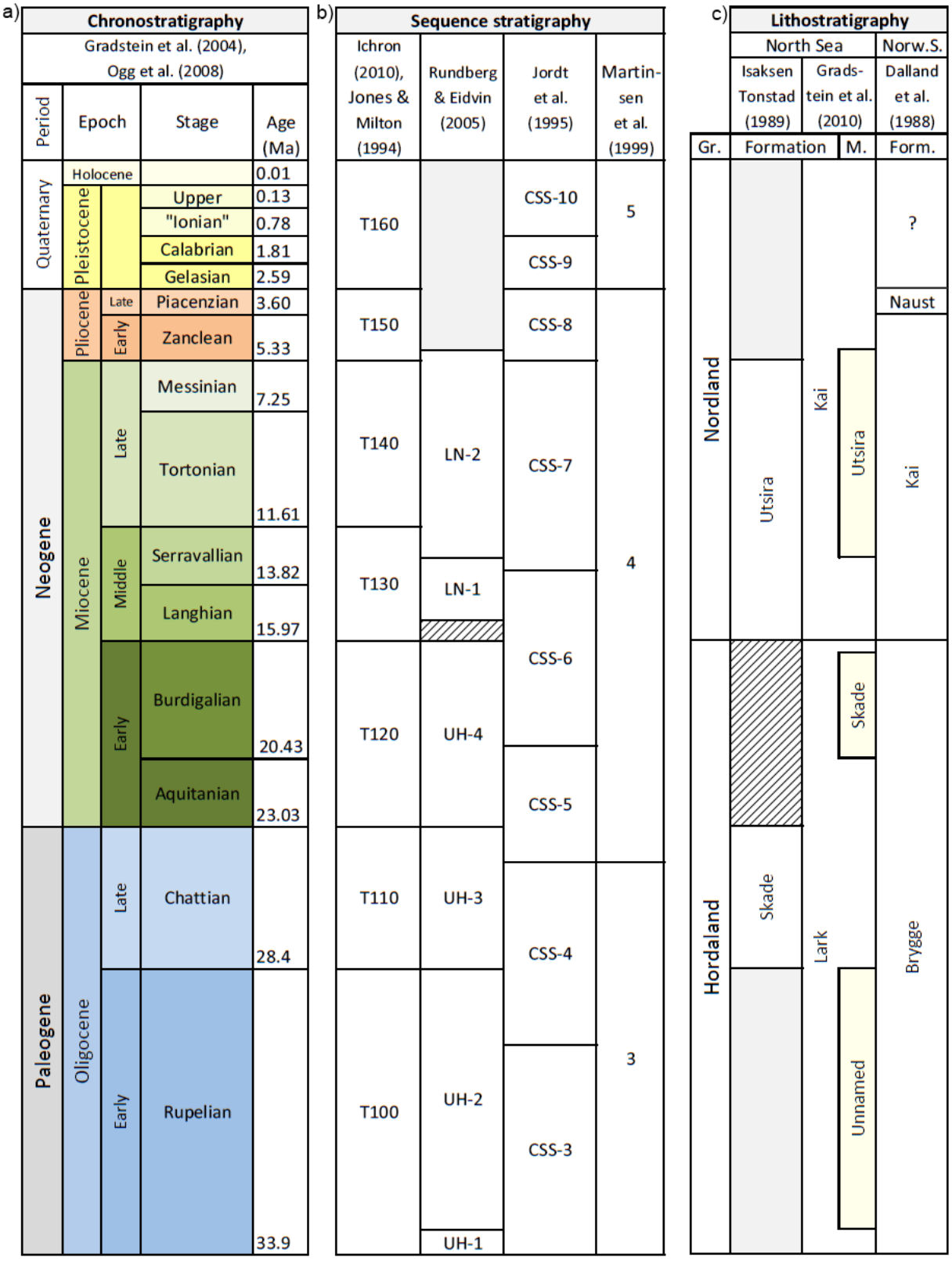
a)
Chronostratigraphy
Gradstein et al. (2004), Ogg et al. (2008)
Period
Epoch
Stage
Age (Ma)
Quaternary
Holocene
0.01
Pleistocene
Upper
0.13
"Ionian"
0.78
Calabrian
1.81
Gelasian
2.59
Neogene
Pliocene
Late
Piacenzian
3.60
Early
Zanclean
5.33
Miocene
Late
Messinian
7.25
Tortonian
11.61
Middle
Serravallian
13.82
Langhian
15.97
Early
Burdigalian
20.43
Aquitanian
23.03
Paleogene
Oligocene
Late
Chattian
28.4
Early
Rupelian
33.9
b)
Sequence stratigraphy
Ichron (2010), Jones & Milton (1994)
Rundberg & Eidvin (2005)
Jordt et al. (1995)
Martin-sen et al. (1999)
T160
CSS-10
5
CSS-9
T150
CSS-8
T140
LN-2
CSS-7
T130
LN-1
4
CSS-6
T120
UH-4
CSS-5
T110
UH-3
CSS-4
T100
UH-2
CSS-3
3
UH-1
c)
Lithostratigraphy
North Sea
Norw.S.
Isaksen Tonstad (1989)
Grads-tein et al. (2010)
Dalland et al. (1988)
Gr.
Formation
M.
Form.
Nordland
Utsira
Kai
Utsira
?
Naust
Kai
Hordaland
Skade
Lark
Skade
Unnamed
Brygge

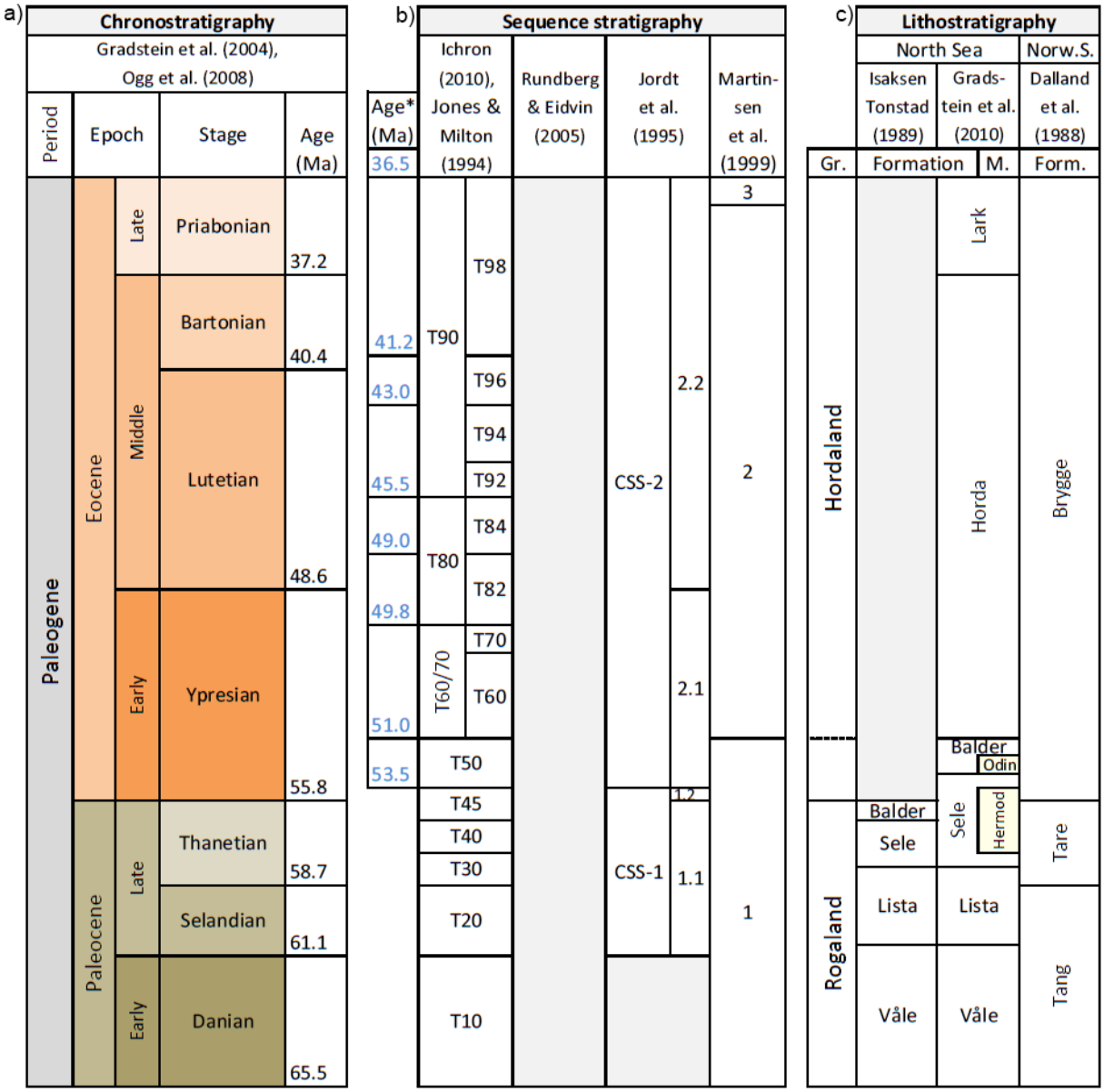

*Figure 9 a) Chronostratigraphic column displaying age division and terminology applied in this thesis. 9 b) Sequence stratigraphic column presenting the sequence stratigraphic division and subdivisions applied. The vertical extent of sequences illustrates their timing of deposition. *Ages presented in blue colour are acquired from dating of high frequency sequences in Figure 15.6 of Jones et al. (2003). 9 c) Lithostratigraphic column presenting the lithostratigraphic schemes mentioned in Chapter 2.6. The vertical extent of the lithostratigraphic units illustrates their timing of deposition. The stippled Rogaland boundary is based on the lithostratigraphic definition from Gradstein et al. (2010), the solid line marks the definition from Isaksen & Tonstad (1989) and Dalland et al. (1988). M = Member.*

2.7 Sequence stratigraphic framework

Basic concepts of sequence stratigraphy are described in chapter 3.2.2. The sequence stratigraphy of the Cenozoic succession in the North Sea has been described by many authors, e. g. Rundberg (1989), Galloway (1993), Jordt et al. (1995), Gregersen et al. (1997), Martinsen et al. (1999) and Rundberg & Eidvin (2005). In addition to the published literature, there are companies in the petroleum industry continuously working on updating their own stratigraphic databases. One of these companies is Ichron Limited. They have developed a sequence stratigraphic scheme for the North Sea based on a 63 well dataset. These high resolution sequences span all the way from Triassic to Cenozoic and are consistent with wells from the Norwegian Sea and West of Shetland areas. Ichron sequences are named with a numbering system, where a letter prefix refers to the geological era of the sequence. Cenozoic sequences have the prefix 'T', as an abbreviation for Tertiary. Cretaceous sequences have the prefix 'K' and Jurassic 'J' (Ichron, 2010). The main sequence stratigraphic scheme applied in this thesis is entitled the "T-sequence" scheme, based on the division and terminology of Ichron Limited. It covers the entire Cenozoic, from Danian to Present. T-sequences of the Palaeocene-Eocene succession are described from Jones & Milton (1994). The T-sequence division of Oligocene-Miocene strongly resembles the division of the Rundberg & Eidvin (2005) scheme. The T-sequences for the Pliocene-Pleistocene succession are divided much like the sequences of Jordt et al. (1995). A description of the Jones & Milton (1994), Jordt et al. (1995) and Rundberg & Eidvin (2005) is presented below. An illustrative comparison of the three divisions can be seen from Figure 9.

2.7.1 T-sequences

Stewart (1987) described the sequence stratigraphy for the Palaeocene-Early Eocene succession based on seismic lines from the Outer Moray Firth Basin. Stewart (1987) completed a division of 10 depositional sequences based on interpreted surfaces of marine onlap and downlap. The sequences were correlatable throughout the basin. With higher quality seismic and updated biostratigraphic information stratigraphers from BP modified the subdivision of Stewart and termed the units by using a 'T' prefix. Jones & Milton (1994) subsequently extended the seismic stratigraphic nomenclature to the Late Eocene.

Sediment accumulation during Palaeocene-Eocene in the North Sea coincided with several episodes of basin uplift. The deposition in the Outer Moray Firth Basin was studied for trends in coastal onlap and relative sea level using seismic data. Two long duration cycles of relative sea-level fall and rise were described along with shorter cycles, associated with the deposition of T-sequences. The first cycle spans from the Palaeocene to the early Eocene. T20 and early T30 are deposited as widespread submarine fan packages. Late T30 consists of a thick package of clinoforms eroded by what is believed to have been a subaerial unconformity surface. During T40 thick packages of clinoforms were deposited and within T45 large packages of basinward prograding clinoforms were deposited. Most of the T45 clinoforms toplap at a level about 600 m below the top of the previously deposited T30 clinoforms. For the T20-T50 sequence coastal onlap moved 80 km landwards indicating a rise in relative sea level. The second cycle spans from mid- to late Eocene. The T84 package displays a basinward shift in coastal onlap of 120 km. A rather steady relative sea level followed, interrupted by minor rise and falls in sea level. During this time a complex package of clinoforms was deposited. Three major units T92, T94 and T96 were deposited and eroded during a successive fall in relative sea level (Jones & Milton, 1994).

2.7.2 Jordt et al. (1995)

Jordt et al. (1995) described the sequence stratigraphy of the entire North Sea. They focused on depositional sequences related to changes in the sediment supply system. The areal extents of the sequences and their main depocentres were presented with a discussion of the sequences' provenance. The Cenozoic succession was subdivided into ten Cenozoic Seismic Sequences (CSS-1-CSS-10).

The oldest sequence is named CSS-1 and is of Late Palaeocene-earliest Eocene age. It was subdivided into two sub-sequences. CSS-1.1 built out by progradation from the east during the Late Palaeocene. The overlying CSS-1.2 aggraded with an even sediment thickness during Palaeocene-lowermost Eocene. CSS-2 makes up the Eocene succession. It is mainly derived from the west and deposited in thick depocentres along the Viking and the Central Grabens. One of the main depocentres is located in the east part of the northern North Sea. A Scandinavian source is suggested for these deposits. The sequence has been subdivided into two sub-

sequences where CSS-2.1 is dominating in the south-east and CSS-2.2 is dominating in the west. CSS-3 is of Early Oligocene age. The CSS-3 sediments are concentrated in the centre of the North Sea basin as the sequence is eroded on the basin flanks. CSS-4 is of late Early-latest Oligocene age. The concentration of CSS-4 sediments is also in the centre of the North Sea basin. The base of CSS-4 marks a mid-Oligocene eustatic sea-level fall. Sediment provenance in northern North Sea is from the East Shetland Platform. CSS-5 is of latest Oligocene-earliest Miocene age and marks the last episode of significant outbuilding from the west into the Central and Viking Grabens. The sequence is absent north and north-west of the Horda Platform.

CSS-6 is of late Early-early Middle Miocene age. CSS-6 is only found in the southern part of the study area and pinches out northwards. CSS-7 is of late Middle-Late Miocene age and is present in the most of the North Sea. North of the Horda Platform sediments are considered to probably have been transported westward from the Scandinavian area directly into the basin. CSS-8 is of Pliocene age. The sediments of the CSS-8 built out westward as prograding clinoforms north of the Viking Graben. CSS-8 is more aggrading further west and truncation along the upper boundary is less pronounced. Jordt et al. (1995) suggest that CSS-8 mainly consists of sediments derived from southern Norway. The sequence is absent in the southern North Sea. CSS-9 is of Early Quaternary age and CSS-10 is of Middle-Late Quaternary age. Jordt et al. (1995) only observed CSS-9 further south than the Viking Graben area, but suggested a thickness below seismic resolution in the northern North Sea. The CSS-10 depocentre built from the east, north of the Horda Platform. The position of this depocentre is suggested to be controlled by faulting along the Øygarden Fault Zone (Jordt et al., 1995).

2.7.3 Rundberg & Eidvin (2005)

The T-sequences spanning from the Early Oligocene to the Late Miocene (T100-T140) are divided into units that strongly resembled the stratigraphic units of Rundberg & Eidvin (2005). The sequences previously established by Jordt et al. (1995) have very a different division (Figure 9). Rundberg & Eidvin (2005) argue for the need for their updated division Oligocene-Miocene based on three problems. Firstly, much of the strata display a poor seismic resolution making them difficult to

interpret. Secondly, the biostratigraphic dating of the Upper Oligocene and Lower Miocene sections were often problematic. This might be caused by different biostratigraphic workers using different index fossils. Thirdly, where the Skade and Utsira formations coexist, the border between them has been poorly defined (Rundberg & Eidvin, 2005).

Rundberg & Eidvin (2005) describe two distinct mega sequences. The base of each megacycle is marked by an unconformity or a regional hiatus. The first unit of Early Oligocene age is called UH-1. UH-1 is wedge-shaped and confined only to the eastern part of the basin. It exists along the Norwegian margin and pinches rapidly out westwards. The Early Oligocene UH-2 corresponds to CSS-3 of Jordt et al. (1995). The lower boundary of the unit is marked by a hiatus. The upper boundary of UH-2 corresponds to a diagenetic horizon characterised by the transition from Opal-A to Opal-CT in Opal rich mudstones. The unit pinches out eastward. Thick sandy intervals have been interpreted within the unit. The UH-3 unit is of Late Oligocene age. The top of the unit is marked by an unconformity north of 60° N. The Early Miocene UH-4 is only present north of 60° N in the central basin and is completely eroded between 61°30 and 62° N. The sandy Skade Formation makes up a large proportion of the unit. The top of the unit is marked by an erosional surface called the mid-Miocene erosional event. The first unit of the second mega sequence is the Middle Miocene LN-1. It forms a basin infilling sequence which onlaps the underlying units. It consists mainly of mudstones with only sparse thin sands present in some wells. The northern extent of the unit is uncertain due to chaotic seismic reflections. The Upper Miocene-Lower Pliocene unit is called LN-2 and comprises the Utsira Formation. It consists of dominantly thick, blocky sands. It is mainly deposited in the centre of the northern North Sea basin (Rundberg & Eidvin, 2005).

2.7.4 Martinsen et al. (1999)

Martinsen et al. (1999) described the Norwegian margin between 60° and 64°N, in terms of five unconformity-bounded megasequences. Lowstand systems dominated in the Møre basin while lowstand, transgressive and highstand systems tract were all interpreted in the North Sea.

The first sequence is bounded by the Base Palaeocene- and the Base Early Eocene unconformities, both surfaces of erosion and hiatus. A Palaeocene lowstand wedge is interpreted base on downlapping nature and sediment distribution before a basinward shift in sedimentation led to the deposition of a localized Eocene highstand progradational wedge. The second sequence is bounded by the Base Early Eocene- and the Intra Oligocene unconformities. The Intra Oligocene unconformity displays no obvious truncation underneath, but a basinward increasing hiatus. Both a lowstand systems tract a highstand systems tract are interpreted related to a fall and subsequent rise in relative sea level.

The third sequence is bounded by the Intra Oligocene and the Base Miocene unconformities. The Base Miocene unconformity is suggested to possibly record subaerial exposure. 2-3 Ma of erosion and 12 Ma of hiatus along the surface is suggested. Solely a lowstand systems tract is interpreted as it onlaps the basin margin while there was significant supply from the west. The fourth sequence is bounded by the Base Miocene and the Base Pleistocene unconformities. The Base Pleistocene unconformity is a prominent erosional surface. The Miocene and Pliocene unit display widely different depositional styles but are interpreted within the same sequence due to the megascale unconformities below the Miocene and above the Pliocene. Within the sequence a maximum transgressive surface called the Base Pliocene is suggested to represent a hiatus with sediment condensation in basinal areas prior to the major clinoform progradation. The Miocene deposits are interpreted as a transgressive systems tract and the Pliocene as a highstand systems tract. The fifth sequence is bounded by the Base Pleistocene unconformity and the seabed. The sequence was not of Martinsen et al. (1999) primary interest and was not discussed in detail.

3. Data and methodology

3.1 Seismic Data

For imaging the subsurface seismic data have been interpreted. Seismic data is acquired offshore by the use of a vessel with acoustic sources. An air canon is commonly used as source and the seismic waves produced by the canon propagate through the Earth's interior. The waves that return to the surface after refraction or reflection at geological boundaries are registered by hydrophones. These hydrophones are laid out on cables, called streamers, pulled behind the moving vessel (Figure 10). When a sound wave hits the hydrophone an electric signal, proportional with the wave's amplitude, is generated and registered. The travel times of the waves are measured as two-way time (TWT). The raw data is subsequently processed before they can be displayed as cross sections for interpretation (Keary & Brooks, 1991; Landrø, 2010).

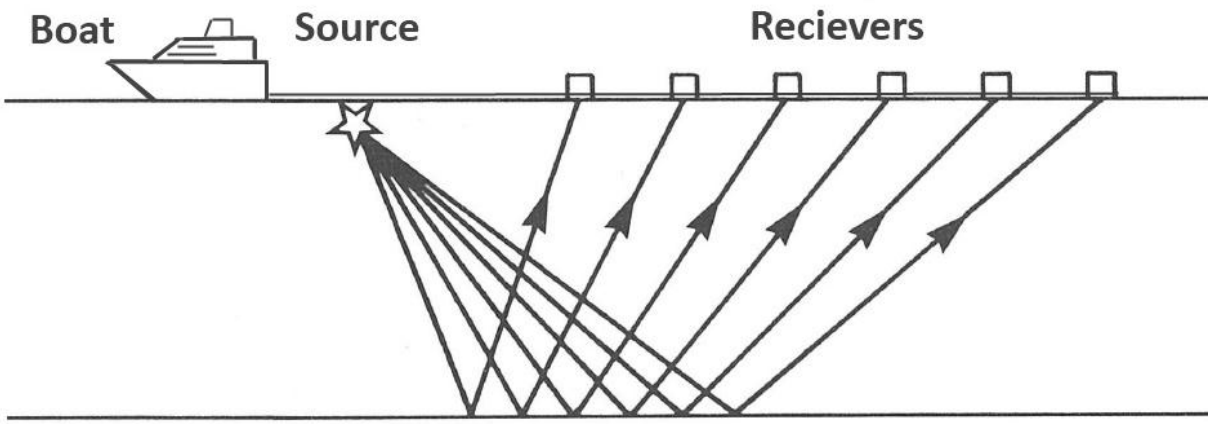

Figure 10. Seismic acquisition offshore. The sound waves are reflected at geological boundaries, such as the seabed in this illustration, the reflected waves are registered by receivers (After Keary & Brooks, 1991)

Traditionally, seismic acquisition was performed by pulling one cable with hydrophones behind the vessel, creating two-dimensional profiles. The resolution of the subsurface imaging was depending on the density of 2D lines acquired. Orienting 2D lines in a grid created cross points which improved the quality control of seismic interpretation. Modern 3D surveying is performed by vessels that can pull up to 20 parallel cables. Subsequently refractions and reflections from the subsurface can be

registered by the hydrophones in all three dimensions. The resulting data set can be displayed in any direction. This improves both the imaging resolution and the quality control. Original seismic lines are called inlines and lines displayed perpendiculars to the inlines are called crosslines (Landrø, 2010).

3.1.1 Seismic processing

When seismic data are collected they are organised as traces corresponding to each shot. Geophysical processing often starts with removing noise from the data. Noise may be sourced from waves, the seismic vessel itself or other vessels and human activity in the area. Noise is reduced by removing unwanted spikes and filtering out known frequencies such as swell-noise frequencies. A Common MidPoint gather is performed by sorting the data to a common midpoint so that these traces represent the same location. In a 3D seismic survey shot-receiver pairs are sorted into cells, called bins. Normal MoveOut correction compensates for the effects of the separation between the seismic source and each of the receivers on the cables. In the case of a horizontal reflector the hyperbolic shape (due to the time delay) will be flattened after correction. When NMO corrections have been performed, the traces are added to each other, in a process called stacking. This is an important seismic processing tool as it improves the signal-to-noise ratio. The traces in each CMP gather are summed and then the traces can be imaged as a function of travel time. Inclined reflectors will however not be correctly displayed without a migration process. As can be seen from Figure 11 unmigrated data plot reflectors at the CMP location and need to be moved to its correct position (Keary & Brooks, 1991; Landrø, 2010).

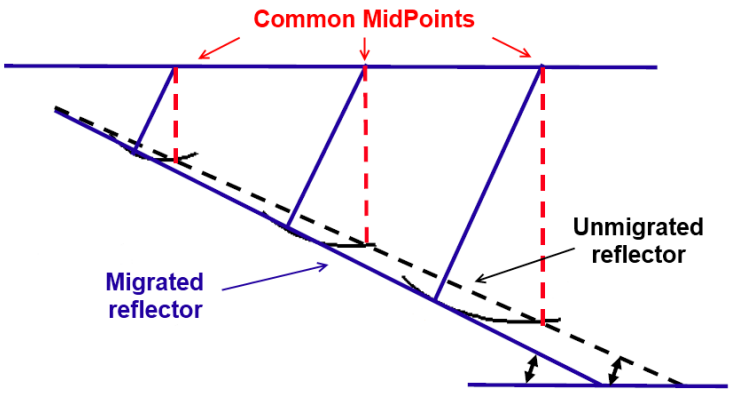

Figure 11. Illustration of unmigrated post-stack seismic data versus migrated post stack seismic data (After Landrø, 2010).

3.1.2 Seismic survey CS02

The seismic utilised in this thesis is an extensive three dimensional cube called CS02 v.04. The survey consists of 43 individual 3D surveys, which are merged together. Merging of several neighbouring 3D cubes has made it possible to do large regional interpretations in three dimensions. The individual 3D cubes are based on released public data. According to the Norwegian Petroleum Directorate regulations, data can only be kept confidential for a maximum period of 10 years prior to becoming public (NPD, 2012). Therefore most data included in CS02 is 10 years or older. In some cases the data is more recent, if production licences have been relinquished. The survey covers an area of 22500 km^2 in the northern part of the North Sea (Figure 12). The survey area lies between latitudes 60° to 62° N, within the Norwegian sector. As the merged survey is of such an extensive size, with an irregular shape, a reduction of the survey has been made for use in interpretation. The crop still covers the whole width of the Northern North Sea within the Norwegian sector. The area of interest was limited to the northern section of the Viking Graben after studying time slices. From 0-1000 ms the reflector patterns on time slices indicated a continuous progradational system in this area.

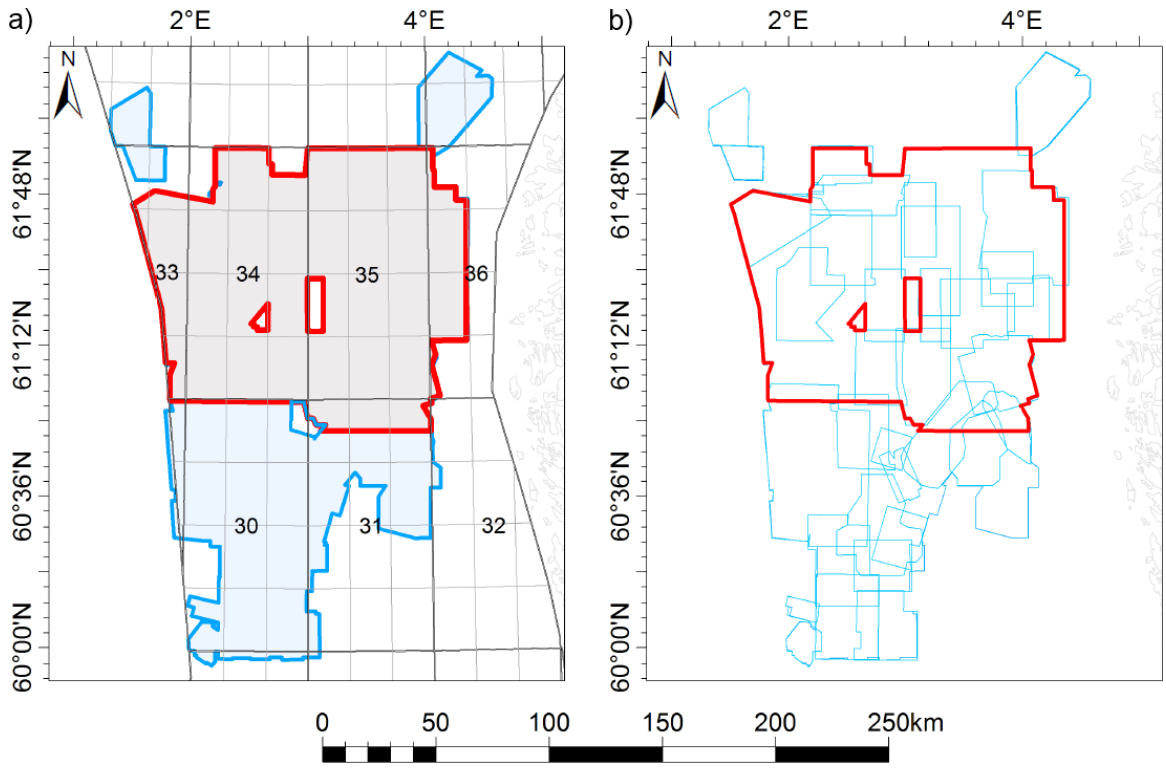

Figure 12 a) The extent of survey CS02 v.04 is marked in blue and the crop is marked in red. 12 b) An illustration of how different surveys are included in CS02 v.04.

Information about the survey CS02 v.04		
Geodetic datum	ED50	
Elipsoid	International 1924	
Projection	UTM 31N	
Format	SEG-Y, 32 bit float point	
Polarity	European GDF Zerophase	
First sample	0 ms	
Last sample	7000 ms	
Sample rate	4 ms	
Spacing between inlines	25 m	
Spacing between crosslines	25 m	
Bin size	25x25 m	
Inline direction	0 Degrees	
Crossline direction	90 Degrees	
Vendor	Carmot Seismic AS	
Processer	Geokinetics UK	
Size of survey	Original	Crop
Inline range	10300-17200	10700-16600
Crossline range	10060-21100	14300-19300
Length N-S	271 km	125 km
Width W-S	168,6 km	147,5 km

Table 2. Information about the seismic survey CS02.

Surveys included in CS02 v.04			
BPN9301	NH8902R97	NVG2000	ST9703
EL8807	NH9111R98M98	NVG96	ST97M3
MC3D-35-7	NH9204	NX0701	ST98M1
MC3D-Q34	NH9304	PC07N023	ST98M5
MN9401	NH9401	SG9202	ST98M6
MN9601M	NH9402	SG9603MR99	ST98M7
MS97M	NH9405	SG9701M	ST98M8
NH0301	NH9801	SH9004	STNH98M
NH0402	NH9802PGS	ST0503	TNE01
NH0712	NH9802R04	ST8513R92	TQ-3412
NH8502R93	NH9805R99	ST9303	

Table 3. Seismic surveys included in the merged survey CS02 v.04. Letters denote abbreviation of operator or multiclient. The first two digits of the survey name indicate year of acquisition or in some cases the Quadrant where the survey is located.

The merging of CS02 has been done by processing individual surveys of different vintages based on final filtered or raw migration stack versions of the original data. Prior to merging, the surveys are standardised as much as possible to ensure continuity in events across survey boundaries. Inlines are oriented towards the north for all surveys (Carmot, 2010). Traces have been included where there is a lack of data to maintain an inline and crossline increment that is consistent (Carmot, 2012).

3.1.3 Artefacts in seismic survey CS02

The presence of artefacts in the seismic data needs to be distinguished from actual data during seismic interpretation. Obvious artefacts in the seismic survey are documented. Pull-ups are an artefact caused by velocity aberrations that can produce false highs, or even obscure true highs due to an overlying thick zone of high velocity material (Etris et al., 2001). In Figure 13 a) false highs are produced for the normally horizontal strata directly underneath an incised valley. Pull-ups appear on all interpreted surfaces directly underneath the incised valleys interpreted on the Top T110 horizon. Artefacts due to the merging of several 3D cubes of different vintages are visible. Linear features in both cross section and on time slices are observed. The differences between surveys are often observable as an abrupt shift in all reflector amplitudes along a vertical trend. In worst cases, as seen from Figure 13 b), reflector continuity may even become inconsistent.

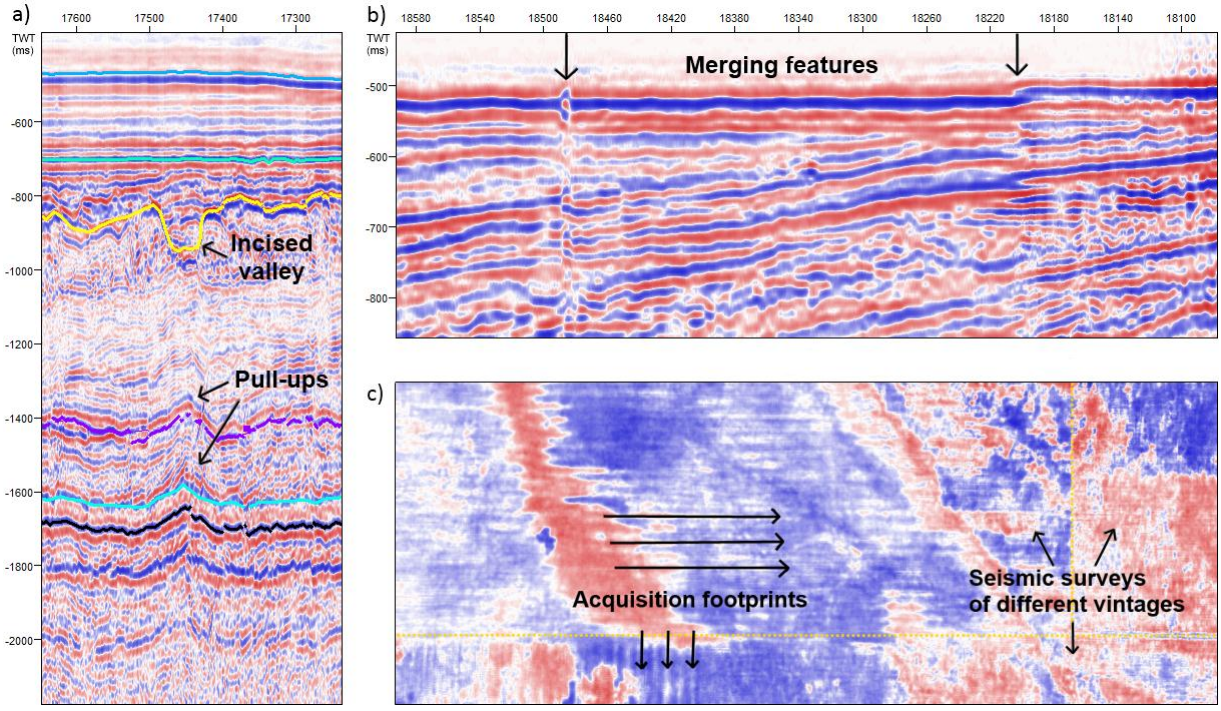

Figure 13 a) Pull-ups below incised valley (Inline 15100). 13 b) Merging features (Inline 12400). 13 c) Acquisition footprints on seismic surveys of different vintages, time slice at 300ms.

Acquisition footprints generate artefacts in a linear spatial grid pattern along the direction of inlines. On the merged 3D seismic survey CS02 acquisition footprints are observable on shallow time slices and interpreted horizons. Acquisition footprints tend to mirror parts of the acquisition geometry used for acquiring the seismic survey (Chopra & Larsen, 2000). A faulty geometry of the streamers and guns may have caused the artefacts (Marfurt et al., 1998). The artefact appears as linear striations masking geological features down to about 800 ms in some areas. As CS02 is a merged survey, the occurrence of acquisition footprints varies both in orientation and magnitude. On Figure 13 c) seismic surveys of three different vintages are cut in a time slice. Even though processing is designed to correct for systematic errors and noise, some artificial features have passed uncorrected through the processing. These artefacts are observable on most surveys of CS02, but are in most cases very subtle and do not significantly disturb the interpretation.

3.1.4 Visualisation and seismic attribute tools

Data can be visualized in several ways. Surfaces can be displayed in 2D and 3D using a variety of colour-scales to highlight geological features of the data. Seismic attributes can be displayed on surfaces, time-slices, random intersections and as volume renders, with a seismic colour scale. According to Barnes (2007) many attributes produce very similar results and their redundancy was discussed. For that reason only a limited selection of available attributes has been used in this thesis. The following seismic attribute descriptions are based on Daber et al. (2008).

Structural smoothing

Data conditioning before performing automatic interpretation is performed to produce more complete areal coverage and improved the picking stability. Petrel's smoothing operator is Gaussian, and is supposed to reduce noise without degrading the structural expression. Mathematically it is expressed as:

$$hG(k) = \frac{1}{\sqrt{2\pi\sigma}} exp(-\frac{1}{2}\frac{k^2}{\sigma^2})$$

Variance (Edge method)

Variance is Schlumberger's patented method for imaging discontinuities in the horizontal continuity of amplitudes. It is used to isolate edges from the input data set. It is most often used to isolate faults but can also be used for bringing out stratigraphic features. The method computes a normalized population with an optional weighted vertical smoothing. The normalized variance algorithm mathematically given as:

$$\sigma_t^2 = \frac{\sum_{j=t-L/2}^{j=t+L/2} w_{j-t} \sum_{i=1}^{j} (x_{ij} - x_j)^2}{\sum_{j=t-L/2}^{j=t+L/2} w_{j-t} \sum_{i=1}^{j} (x_{ij})^2}$$

where x_{ij} is the sample value at horizontal position, i, and vertical sample, j, and w_{j-t} is the vertical smoothing term over a window of length, L.

Extract value

The Extract value utility is used for extracting values from a seismic volume close to or at the level of a chosen surface. This utility allows the user to produce Surface attribute maps from seismic volumes already created as Volume attributes. The Variance (Edge) attribute volume can be extracted along an interpreted seismic horizon.

Mean amplitude

The Mean amplitude attribute is an arithmetic mean of the amplitude and is a measure of trace bias. Either positive or negative bias may be an indication of the presence of bright spots, which can indicate hydrocarbons. Mean Amplitude is computed using the following formula:

$$\frac{(\sum_{i}^{n} \mathrm{amp})}{k}$$

Where k is the number of live samples.

Maximum magnitude

The Maximum magnitude attribute measures reflectivity within a time or depth window. The output is mapping of the greatest reflectivity value found within the analysis window, whether positive or negative. This attribute may be used to map the strongest direct hydrocarbon indicator within a zone.

RMS Amplitude

RMS Amplitude is the square root of the sum of the squared amplitudes, divided by the number of samples. RMS amplitude maps geologic features which are isolated from background features by amplitude response. Mathematically, it is given as:

$$\sqrt{\frac{(\sum_{i}^{n} amp^{2})}{k}}$$

Where k is the number of live samples.

Isochron thickness

Isochron thickness is defined as the time difference between two horizons. For this thesis the input horizons have been in the depth domain measuring vertical thickness between depth converted surfaces.

Volumes

The volume between two surfaces may be calculated using the Volume operation. The operation also calculates the area where the volume is. The area of volume calculation can be limited by implementing a boundary polygon.

Dip angle

The Dip angle operation calculates the dip angle at each node in the grid and locates the steepest angle between the surface and the horizontal plane. The output of the operation can be displayed as a polygon.

3.1.5 Calculation of accumulation rates

The average accumulation rate is calculated mathematically from the formula:

$$SR_{Av.} = \frac{V}{\Delta t} * A$$

Where V is the volume (cm^3), Δt is the age interval of deposition (ka) and A is the area extent of the unit ($cm^{2)}$.

The maximum accumulation rate is defined at the point of the unit's greatest thickness, at the depocentre. The maximum accumulation rate is calculated from the formula:

$$SR_{Max} = \frac{h}{\Delta t}$$

Where h is the maximum thickness (cm) and Δt is the age interval of deposition (ka).

3.1.6 Depth conversion

The subsurface exists in the depth domain. Seismic reflection data however portrays the subsurface in recorded two-way time (TWT). An accurate depth conversion is therefore necessary to improve the realism of the subsurface imaging. An accurate depth conversion should use existing wells and tie these to the seismic. A reliable depth conversion should also be able to accurately predict depths for new wells as well. Depth conversion requires actual vertical propagation velocity. This is often called “True velocity” and is best obtained from vertical seismic profiles, check shot surveys, or calibrated sonic logs. Depth conversion can be done by using a wide range of existing methods. Two broad categories of methods can be defined. The first category is direct time-depth conversion. This method uses only known depths and seismic times at well points. Velocity information from the seismic is not taken into use. Depth conversion by the use of a velocity model will include all available velocity data. A velocity model aims to having more likelihood of working adequately also in between known depth points. Velocity models require sufficient computing resources, modelling expertise, and time to develop the model. Most seismic interpretation is done in the time domain rather than the depth domain. The advantage of interpreting in the time domain comes to show if additional well data is acquired. The velocity model will most likely be updated and time domain interpretations can easily be depth converted to fit with the new data (Etris et al., 2001). Depth conversion of each surface in this thesis is done by applying the velocity model in the form of a 3D cube data volume called ‘Vstack_NNS_Calibrated_V4_ June9th_2010’. The model is made by using available stacking velocity data from the surveys in the merged dataset. High frequency noise and spikes in the velocity data from all the surveys are removed and the data sets are harmonised. Check shot data from the wells has been used. At well locations a 100% match between well and survey has been made to calibrate the stacking velocities (Carmot, 2010).

3.2 Seismic Interpretation

The seismic interpretation was performed using the Schlumberger software Petrel 2011.2 on a Windows 7, 64 bit workstation. Extensive continuous reflectors, displaying local amplitude maxima, were picked first and interpreted. On the colour template for this thesis peak events, representing an increase in acoustic impedance, are represented by blue seismic reflections. Trough events, representing a decrease in acoustic impedance with depth, are represented by red seismic reflections. In order to obtain a geological control of the interpretation, existing boreholes displaying tops of stratigraphic units are overlain the seismic section. When the interpreted horizons are traced to the borehole, appropriate stratigraphic indicators can be used (Kearey & Brooks 1991).

Interpreting horizons in Petrel was performed using three basic methods:

1. Manual interpretation: In between the manually picked points Petrel interpolates linearly.
2. Seeded 2D Autotracking: As points are picked they will be tracked along a reflection in the 2D intersection window until it comes to a discontinuity and does not fulfil the constraints specified in the autotracking parameters.
3. Seeded 3D Autotracking: As points are picked they will be tracked outwards in all directions to get a 3D view of a distinct reflection. It will stop interpreting when it comes to a discontinuity and does not fulfil the constraints specified in the autotracking parameters.

In order to keep a good quality control of the interpretation a combination of manual interpretation, 2D seeded autotracking and 3D seeded autotracking was utilized. The continuity of reflections was decisive to which method was applied. In areas of very poor seismic quality and reflector continuity manual interpretation was applied. In areas of very good reflector continuity 3D seeded autotracking was used. As 3D seeded autotracking interprets both along and into the intersection window visible on screen making it challenging to ensure quality control. Therefore 2D seeded autotracking interpreting every 100^{th} inline and crossline has for some horizons been the most common method applied.

3.2.1 Seismic stratigraphy

Seismic stratigraphy is the study of stratigraphy and depositional facies, using seismic data. Seismic reflection terminations and configurations are used for recognizing and correlating depositional sequences. Seismic units can be interpreted as packages where concordant reflections are separated by discontinuity surfaces. A package is interpreted as consisting of genetically related strata, bounded at their top and base by unconformities or their correlative conformities. Discontinuities are defined by reflection terminations (Figure 14). When a reflector termination is described as onlapping, initially horizontal strata terminate against an initially inclined surface. If a termination is downlapping, initially inclined strata terminate down dip against an initially inclined or horizontal surface. Apparent downlap may occur when units of inclined strata flatten and has a continuation that is thinner than the vertical resolution of the seismic. Reflector terminations terminating up dip at the top of the unit are described as either toplapping or erosionally truncated. Toplap against the overlying surface is a result of non-deposition and only minor erosion. Erosional truncation is the result of sediments removed along an unconformity surface. Sometimes erosional surfaces produce seismic reflections themselves. If not the systematic terminations of underlying reflections can define the surface. If an erosional surface shows strong reflection a “follow cycle” may mask underlying reflections. In these cases only onlap by the overlying sequence will show the correct position of the unconformity. Unconformities that are non-angular can be traced from areas where the unconformity shows angularity.

When the seismic section has been subdivided into packages of concordant reflections the continuity, configuration and amplitudes can be analysed. If the internal reflections of a package show great continuity it suggests a widespread, uniformly stratified deposition. Seismic reflection configurations may be even or wavy, parallel to sub-parallel. A divergent configuration can be observed on wedge shaped units where the thickening of the unit is accomplished by thickening of the individual reflections rather than by reflection terminations. It suggests lateral variations in rate of deposition or a progressive tilting of the depositional surface. A chaotic reflection configuration shows discontinuous and discordant reflections. The configuration may be due to deposition in a high energy setting or post depositional

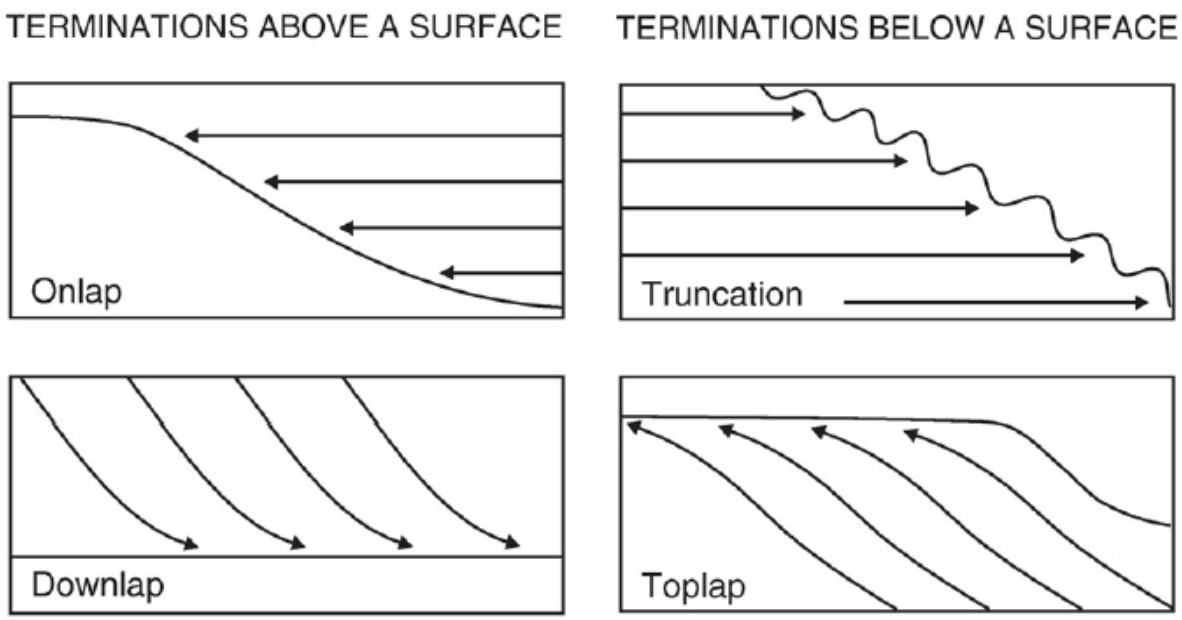

Figure 14. Reflector terminations above and below a stratigraphic surface (After Mitchum and Vail, 1977).

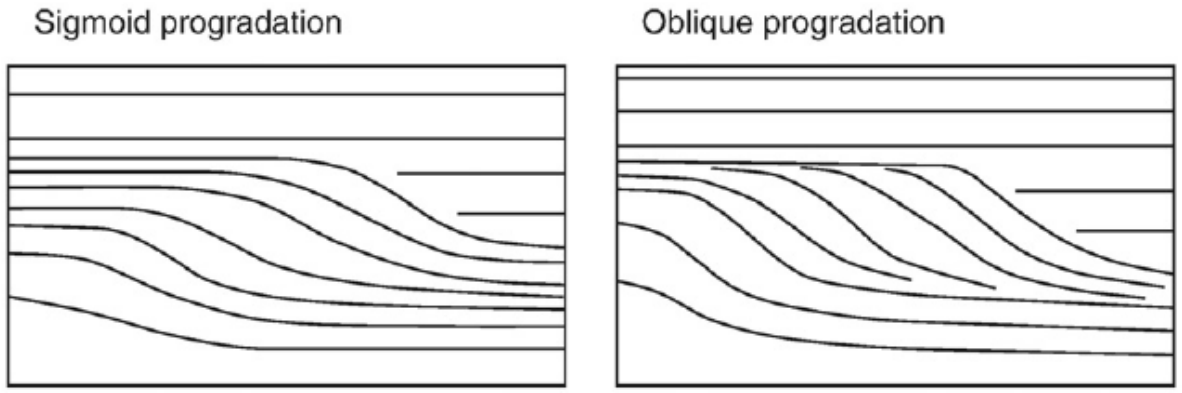

Figure 15. Reflector geometries associated with a prograding shelf-slope system (Mitchum & Vail, 1977).

deformation. Packages that show a reflection-free configuration may be so due to homogeneous, non-stratified or steeply dipping geological units. Examples of such units are igneous masses, salt features or thick homogeneous packages of sediments. Packages of prograding clinoforms can be described based on their configurations. A prograding unit may have sigmoid, oblique, complex sigmoid-oblique, shingled and hummocky clinoform configuration. Sigmoid and oblique configurations are most commonly observed. Sigmoid clinoforms display gently

dipping upper and lower segments, and a thicker, steeper, lens shaped middle segment on cross sections (Figure 15). The depositional angle is usually less than 1°. A distinctive feature of the sigmoid shape is the continued upbuilding of the topset. The sigmoid configuration implies relatively low sediment supply and an increasing relative sea level. Oblique shaped clinoforms consist of steeply dipping strata which terminate updip by toplap at a nearly flat upper surface. The depositional angle may reach as much as 10°. The internal shape of an oblique clinoform may show parallel reflectors downlapping onto the depositional surface. Commonly the internal reflectors gradually turn concave upwards in the lower portions before terminating by either real or apparent downlap. Oblique clinoform shape implies relatively high sediment supply and a stillstand of relative sea level (Mitchum et al. 1977)

3.2.2 Sequence stratigraphy

Sequence stratigraphy is a method used to determine the order of deposition and erosional events in a basin (Catuneanu et al., 2009). The main tool of sequence stratigraphy is to analyse the stacking pattern of strata and the key surfaces that bound successions (Catuneanu et al., 2011). Several models of sequence stratigraphic analysis have been described in the literature. Catuneanu et al. (2009) examined the points of agreement and the differences between existing models and provided some guidelines for a standard workflow. Sequence stratigraphy is described in this thesis based on the nomenclature and definitions suggested by Catuneanu et al. (2009). Stratigraphic sequences records a succession of strata deposited during a full cycle of change in accommodation or sediment supply. Accommodation is created and destroyed by rise and fall in base level. In an open marine setting base level is commonly approximated as the sea level. Stratigraphic sequences are defined from bounding surfaces and systems tracts. Systems tracts are based on genetic types of deposits. These genetic types of deposits and their bounding surfaces are core concepts that are independent of the sequence stratigraphic model applied. The genetic types of deposits and the bounding surfaces are described below:

- A forced regression is driven by a base level fall and results in a progradational and downstepping stacking pattern (Systems tracts: *early lowstand, late highstand, forced regressive wedge* and *falling-stage*).
- Normal regression is driven by sediment supply outpacing the rate of new accommodation during a time of base level rise or stillstand.
    - Lowstand normal regression follows the onset of a base-level rise after a period of base-level fall (Systems tracts: *late lowstand* and *lowstand*)
    - Highstand normal regression at the late stage of base-level rise (Systems tracts: *highstand* or *early highstand*)
- Transgression is driven by a rise in base-level at rates higher than the sedimentation rates. Transgressive deposits display retrogradational stacking patterns (Systems tract: *transgressive systems tract*)

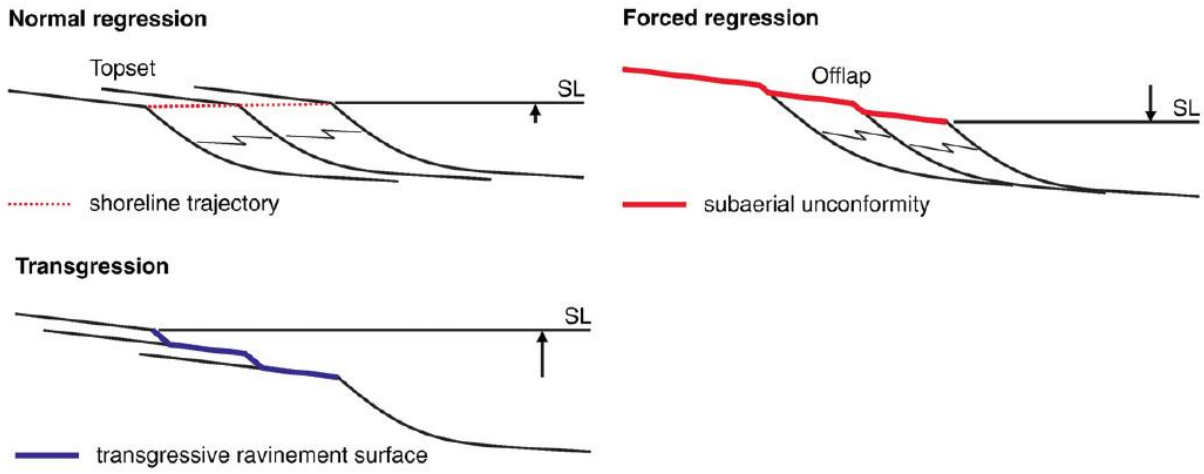

Figure 16. Genetic types of deposits: Normal regressive, Forced regressive and Transgressive (Modified from Catuneanu et al., 2009).

Sequence stratigraphic bounding surfaces, identified by the use of reflector terminations and stacking patterns:

- *Subaerial unconformity* is an unconformity that forms under subaerial conditions, as a result of fluvial erosion or bypass, pedogenesis, wind degradation or dissolution.
- *Correlative conformity* is a stratigraphic surface that marks the change in stacking patterns from highstand normal regression to forced regression, or from forced regression to lowstand normal regression.
- *Regressive surface of marine erosion* is a subaqueous erosional surface that forms from waves scouring in a regressive, wave-dominated setting.
- *Maximum regressive surface* is a surface that marks a change from lowstand normal regression to transgression.
- *Maximum flooding surface* is a surface that marks a change from transgression to highstand normal regression. It is commonly a downlap surface in shallow-water settings.
- *Transgressive ravinement surface* is an erosional surface that forms by wave or tidal scouring during a transgression.

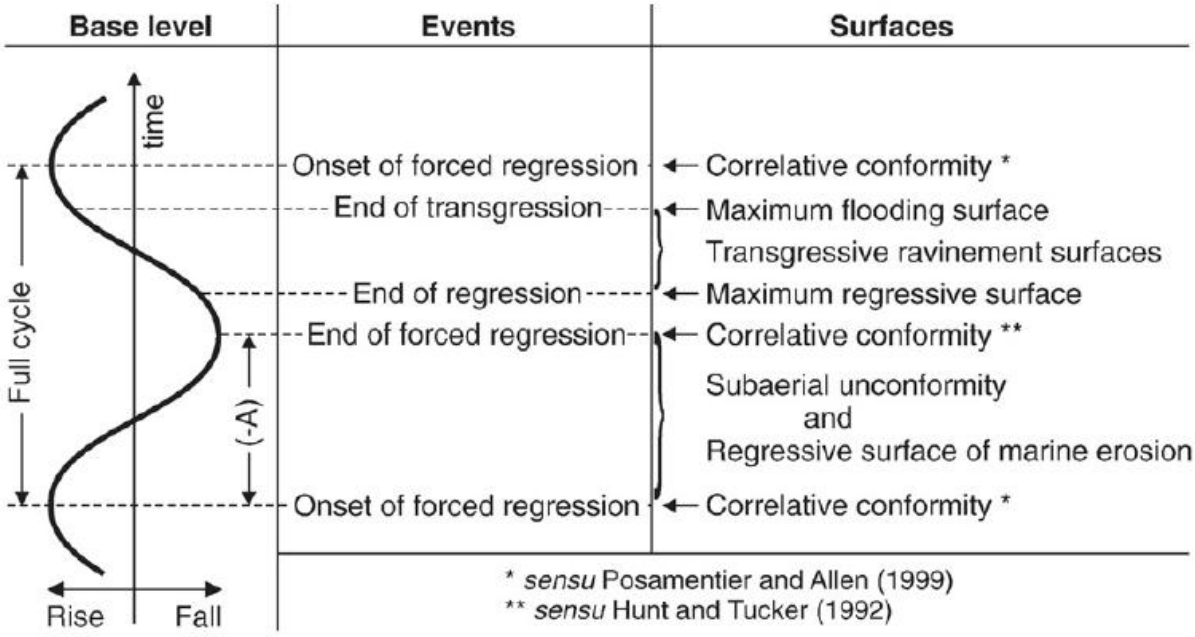

Figure 17. Timing of seven sequence stratigraphic surfaces relative to events and base level changes (Catuneanu et al., 2009)

3.2.3 Shoreline and shelf-edge trajectories

Shoreline and shelf-edge trajectories describe the sedimentary systems lateral and vertical migration through time (Helland-Hansen & Hampson, 2009). With sufficient sediment supply and water depths, the basinward progradation of coastal prisms and clastic wedges will result in the deposition of clinoforms (Steel & Olsen, 2002). The geomorphological breaks in slope of clinoforms mark the points that the trajectory path follows (Helland-Hansen & Hampson, 2009). To analyse the successive position of the points a profile orientated parallel to the depositional-dip direction of the clinoform is necessary (Bullimore et al., 2006). Analysis of trajectories visualizes even subtle changes of each genetically related advance or retreat of a shoreline or shelf edge. Shelf clinoforms record the advance of a shelf margin. They can typically be several hundred metres high. In modern systems shelf clinoforms are recorded in water depths of 20-200 m. Shoreline clinoforms are normally a few tens of meters high. They are located close to the shoreline and are produced by progradation of deltas, barrier island shorelines and strandplains (Helland-Hansen & Hampson, 2009). Helland-Hansen & Hampson (2009) subdivide the shelf-edge trajectories as either ascending, descending of non-migratory and the shoreline trajectories as either ascending regressive, descending regressive, transgressive or nonmigratory. Bullimore et al. (2006) divide the shelf-edge trajectories as low or high angle positive, low or high angle negative or flat (Figure 18). Positive trajectories display strongly progradational clinoforms where the break in slope is positioned above and more basinward than the previous one. This configuration is interpreted as regressive during a rising relative sea-level. Negative trajectories display clinoform tops that are planed off by erosion. The configuration is interpreted as a forced regressive progradation during falling stage systems tract or a lowstand wedge systems tract. Slope failure (slumping) is commonly observed on low angle positive and low angle negative shelf edge trajectories (Bullimore et al., 2006).

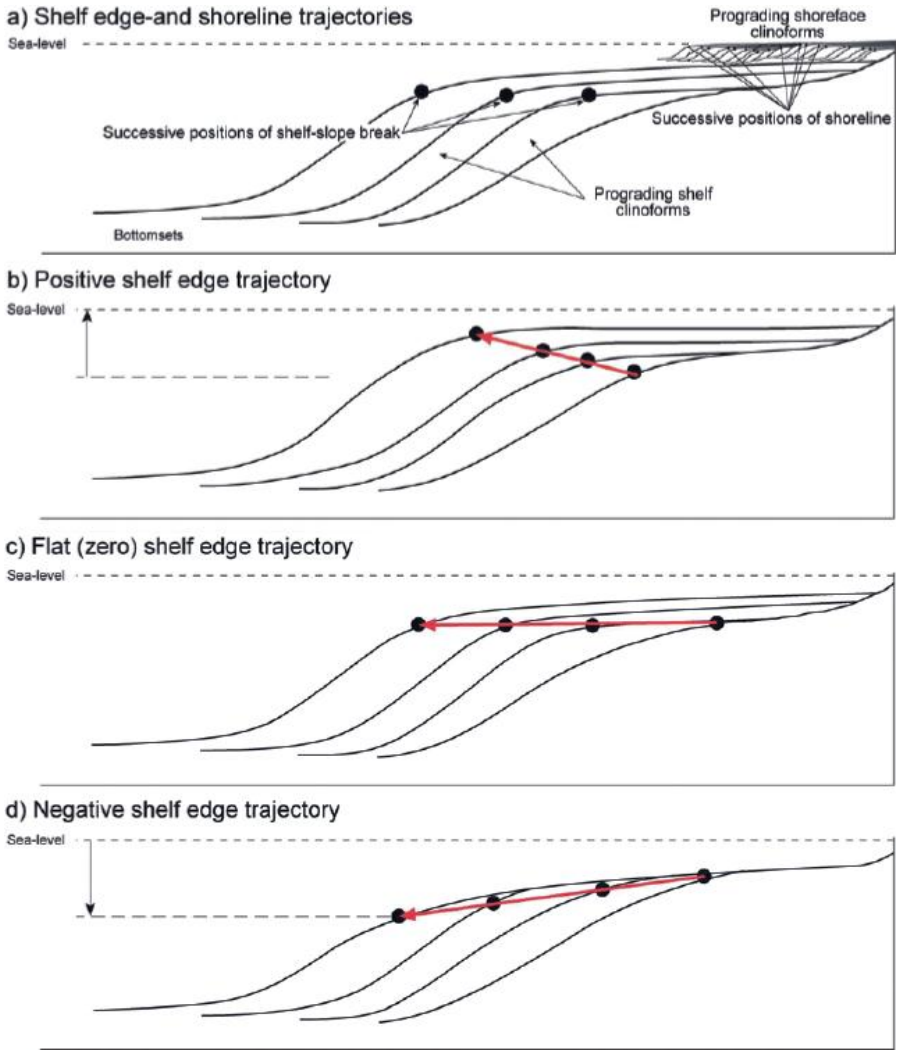

Figure 18 Shelf edge- and shoreline trajectories in dip-oriented cross sections.18 a) The successive positions of the shelf edge or shoreline allows for the identification of trajectories. The scale of shoreline vs. shelf edge clinoforms is illustrated. 18 b) Regressive high angle positive trend. 18 c) Regressive flat trend. 18 d) Forced regressive negative trend (Modified from Steel & Olsen, 2002).

3.3 Well Data

Biostratigraphic analyses, based on cuttings from wells, are implemented in this thesis in order to obtain dating of the interpreted seismic horizons. Geophysical well logs are used for interpreting lithology.

3.3.1 Well data for seismic interpretation

While performing the interpretation well tops displaying stratigraphic units were displayed over the seismic in Petrel. The well top depth information is based on released data by the Norwegian Petroleum Directorate (NPD). The well tops have

been correlated to be displayed correctly on the seismic intersections by using check shot and vertical seismic profiling (VSP) data. In the area of interest many wells have been drilled. However, not all of these wells contain available stratigraphic information. Many of the wells also lack check shot data. Wells containing check shots and stratigraphic information were used during the interpretation. In certain areas it is often challenging to pick the correct seismic reflector, due to poor reflector consistency and continuity. Stratigraphic information while interpreting ensures a better quality control.

3.3.2 Dating of interpreted horizons

Released data on stratigraphy from NPD has been available and possible to display over the seismic. The intervals dated are often sparse and constrained to the end of geological epochs. Data provided from a proprietary study by multiclient Ichron Limited have therefore been implemented. Ichron data contains specific dating (in Ma) and often provides more information at shallow depths. NPD chronostratigraphic data are based on information provided by the exploration companies. The biostratigraphic analysis has been performed by different companies using different biostratigraphic markers. Ichron Limited has done the biostratigraphic analysis on all wells using the same palynological, micropalaeontological and nannopalaeontological marker events. The marker events have also been calibrated to wireline and measure while drilling (MWD) log data (Ichron, 2010).

3.3.3 Well data from well completion reports

The biostratigraphic dating of strata at shallow depths is sparse. Several of the post Oligocene horizons remained undated with the data provided by NPD and Ichron. Well reports from completed wells in the area were therefore investigated. The goal was to acquire biostratigraphic dating with depth information in the Miocene-Pleistocene succession. Six well reports contained additional information at shallow depths. Four of the well reports contained depth information for the top of the Late Miocene (34/7-6, 34/7-1, 34/7-8, 34/10-30). Five of the well reports contained information for the top of the Late Pliocene (35/2-1, 35/2-2, 34/4-6, 34/7-1, 34/7-8). In the results chapter well data from completion reports of three wells are displayed in Figure 35 and 36 (34/4-6, 35/3-1, 35/8-2). The depth information was implemented in Petrel and displayed over the seismic.

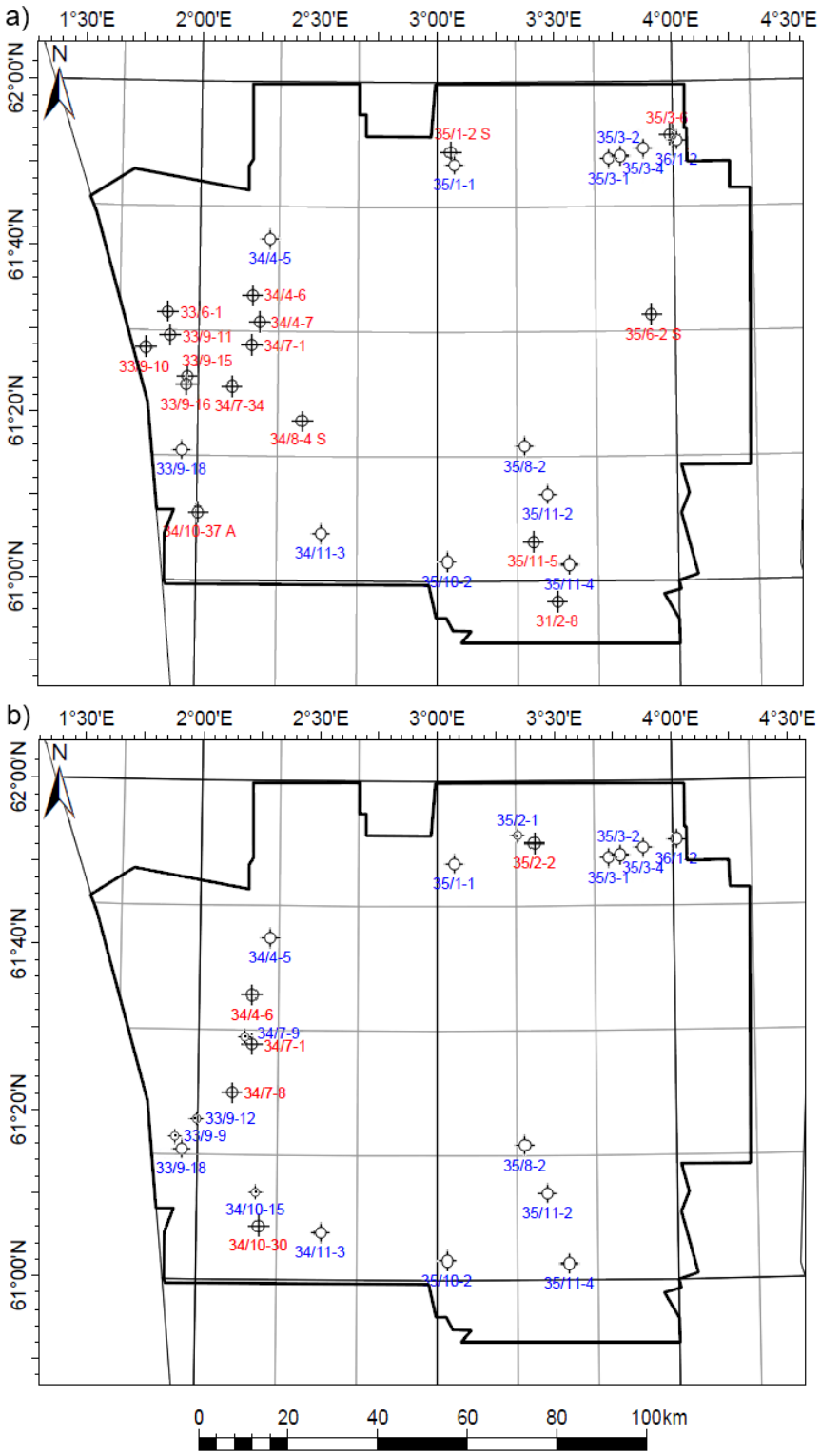

Figure 19. Maps showing the location of wells used. Figure 19 a) displays the wells with well top information provided by NPD. Wells marked in blue also contain data from Ichron. Figure 19 b) displays the wells with data provided from Ichron (blue) and wells with additional information from well reports (red).

3.3.4 Well selection process

In order to secure the quality of the interpretation and the dating a well selection process was performed. Wells that did not display properly on the seismic were not included. Many of the wells in the northern North Sea area did not contain well top information provided from neither NPD nor Ichron. These wells were also discarded. Some of the wells containing stratigraphic information did however lack check shot data and had to be discarded as well. As the stratigraphy of interest is found at shallow depths only wells containing data at shallow depth were chosen. To ensure that the data at shallow depth was correct all the check shot data sets were investigated. In a function window in Petrel all the Seabed tops provided by the NPD were displayed. Each well's check shot data was subsequently displayed in the same function window to ensure that the check shot data had a span all the way from the seabed to the total depth of the well (TD). Wells that did not contain any check shot data along the seabed depth curve were discarded.

Some uncertainties exist when dating stratigraphy at shallow depths. In the oil industry it is not common to have cuttings from shallow depths returned to the surface. When initiating drilling the cuttings are returned to the seabed. In some frontier areas the returns to seabed are however picked up by using a remotely operated underwater vehicle (ROV) and are investigated. On some rare occasions the upper sections are drilled by using riserless mud returns (RMR), which brings cuttings to the surface. The shallowest sequence registered is not necessarily the top of a sequence rather than the depth at which the first cuttings have been transported to the surface and investigated. Wells containing sequence well tops in the Miocene-Pleistocene stratigraphy have been looked up in the Ichron report. In the reports appendix stratigraphical summary charts for each well can be studied. On these charts all biostratigraphical markers observed are displayed at the depth discovered. In some wells only a few sparse markers are observed making these wells more uncertain for dating than a well containing many markers. It is also possible to see whether the top of the sequence is placed at the same depth as the first returns to the surface.

Wells with NPD tops						
31/2-8	33/6-1	33/9-10	33/9-11	33/9-15	33/9-16	34/10-37
34/10-37 A	34/4-6	34/4-7	34/7-1	34/7-34	34/8-4 S	35/11-5
35/1-2 S	35/3-6	35/6-2 S				
Wells with NPD & Ichron tops						
33/9-18	34/11-3	34/4-5	35/10-2	35/1-1	35/11-2	35/11-4
35/3-1	35/3-2	35/3-4	35/8-2	36/1-2		
Wells with Ichron tops						
33/9-12	33/9-9	34/10-15	34/7-9	35/2-1		
Wells with additional information from well reports						
34/4-6	34/7-1	34/7-8	34/10-30	35/2-1	35/2-2	35/3-1
35/8-2						

Table 4. The selected wells used for interpretation and dating. Additional well information is available in Appendix C.

4. Results

The results chapter starts off with a presentation of the seismic interpretation. In section 4.1 the interpreted horizons are dated and subsequently given appropriate names. In section 4.2 the horizon identification is presented, based on seismic stratigraphic principles. Section 4.3 contains a description of reflection patterns, observed features and cross section illustrations of the units. Units that display similar characteristics are described together. Section 4.4 contains a sequence stratigraphic analysis and the last section (4.5) describes the thickness, distribution and accumulation rates of the units. Additional horizon surface maps, unit thickness maps and amplitude maps are enclosed in Appendix A.

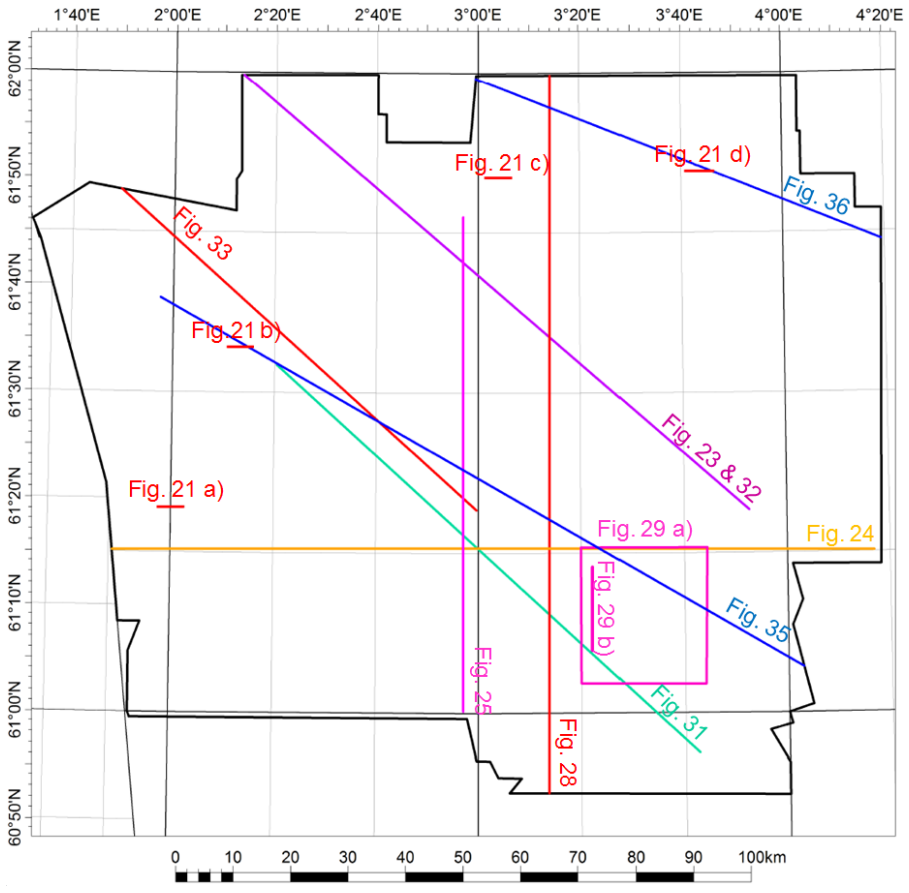

Figure 20. Map displaying the location of the figures presented in the result chapter.

4.1 Dating of horizons

21 horizons have been interpreted in 3D. For the sequence stratigraphic analysis 3 additional horizons have been interpreted in 2D. The horizons have been given names referring to the T-sequence they belong to. The horizons that mark the top of a T-sequence are entitled “Top” and horizons within T-sequences are entitled “Intra”. The horizons were dated by overlying well top data over the seismic displayed in cross sections. 22 wells were used for dating (Table 4 & Figure 19). 16 wells contained biostratigraphic dating (Ichron, 2010) and 6 additional wells contained biostratigraphic dating from Statoil, Hydro, Saga or Robertson Research. A variety of well sections is presented in Figure 21. Figure 22 illustrated how a well match for several wells along a surface can ensure the quality control of the interpretation.

For horizons interpreted in Palaeogene stratigraphy the data quantity was very good. Top K10-J110, -K120, -T10, -T50 and -T110 were dated with high confidence. The Top T50 horizon was identified as the top of the Balder Formation in the Ypresian stage, for a more specific dating the youngest age of the Balder ash from Berggren et al. (1995) is used. The Intra T100 horizon occasionally coincided with the well top location of T100, but was most commonly observed at deeper levels. In the Neogene stratigraphy data quantity was lower. The two wells displayed in Figure 21 c) and d) provided dating for Top T130 and T140. The T150 well tops often displayed the depths of first returns to the surface. The location did not mark a transition from T150 to T160. Thus, they were not the location of sequence tops. The well section in Figure 21 b) contains information from a biostratigraphic report. The ‘Late Miocene’, ‘Pliocene’ and ‘Pleistocene’ well tops are chronostratigraphic equivalents of the Top T140, T150 and T160 sequences, respectively. The Top T140 horizon was dated from well reports in four wells.

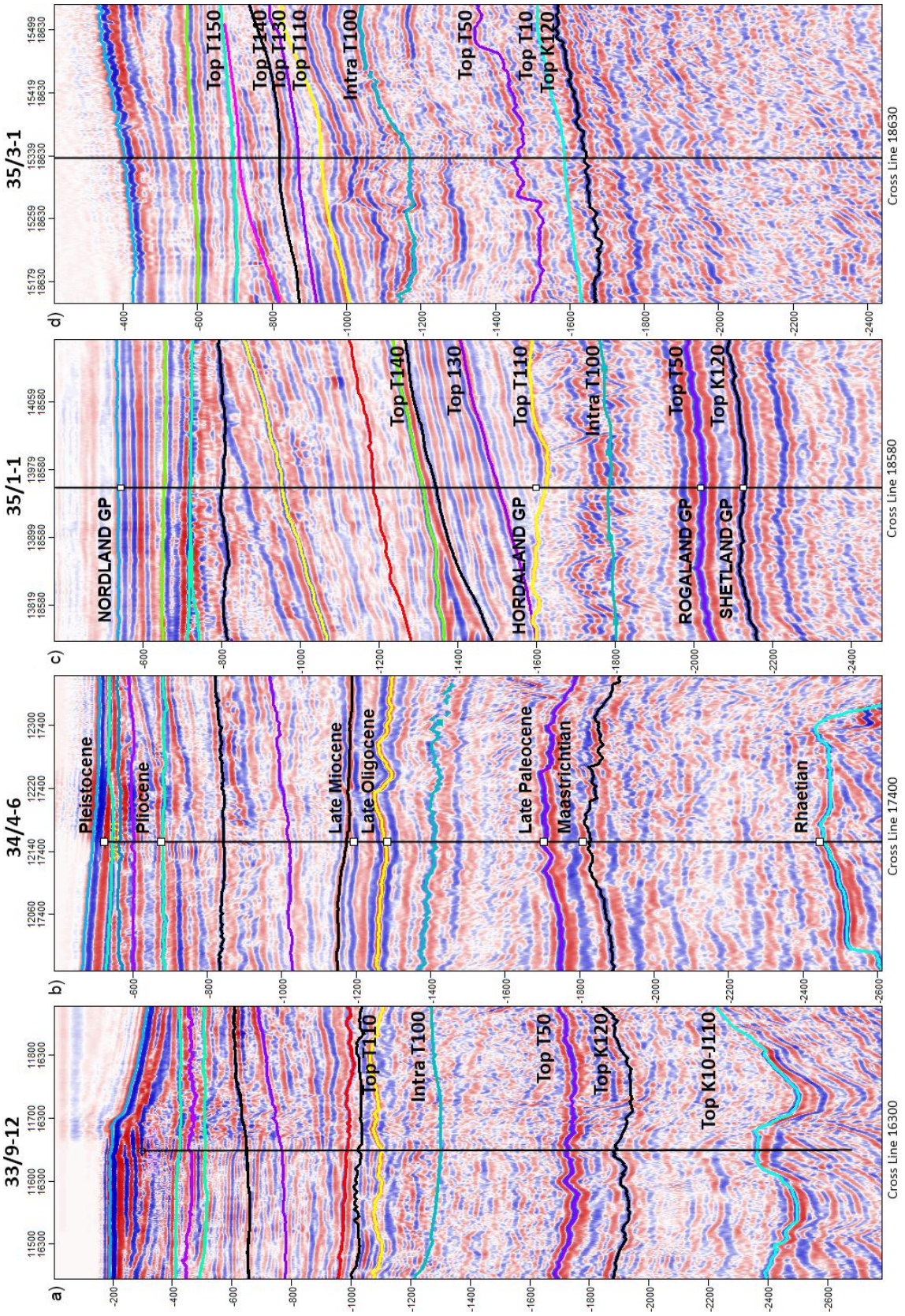

Figure 21. Four wells displayed over seismic cross sections. Figure 21 a), c) and d) contain Ichron well tops that are not shown due to confidentiality (Chapter 1.1), the dated horizons are shown by name. Figure 21 b) displays well top information acquired from the well report for 34/4-6 (Saga, 1987). Figure 21 c) displays well tops from NPD based on Isaksen & Tonstad (1989).

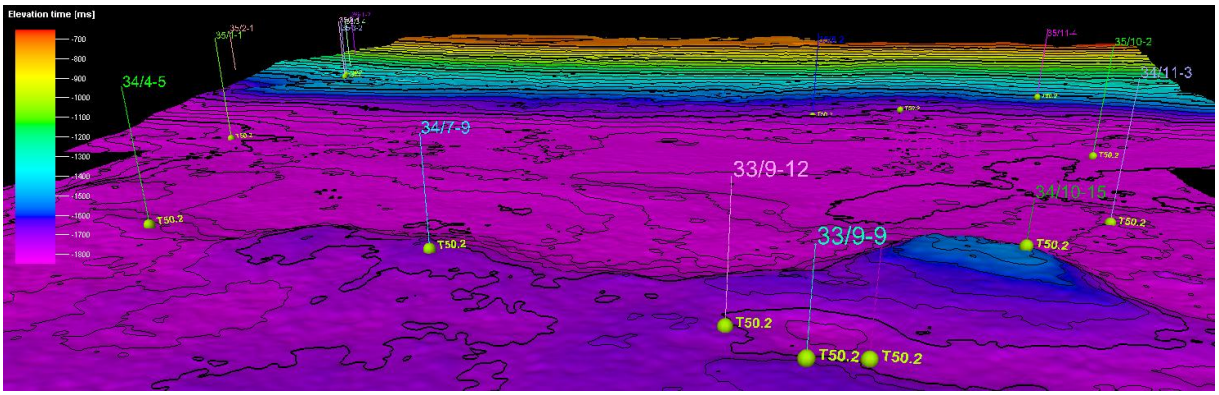

Figure 22. The dating of the Top T20-T50 horizon quality checked by displaying multiple T20-T50 well tops.

The Pliocene-Pleistocene transition was investigated in the Peon discovery wells 35/2-1 and 35/2-2. The regional angular unconformity interpreted as Top T150 horizon is dated from underlying Pliocene sediments separated from the overlying Early to Middle Pleistocene sediments in the well report for 35/2-1 (Hydro, 2006). In the well report for 35/2-2 the sediments overlying the unconformity are dated Early Pleistocene. However, it is stated in the report that the age datings of the Pleistocene sediments were difficult due to uncertainty of reworking (Statoil, 2010).

A Pliocene-Pleistocene transition is also suggested by three other older well reports. They all displayed a very good match with one of the interpreted clinoform horizons. All three wells were drilled by Saga in the mid-80s, with biostratigraphic analysis done in cooperation with Robertson Research International. For 34/7-8, drilled in 1984, the biostratigraphic dating is well documented in the available biostratigraphic report. For 34/4-6 and 34/7-1, drilled in 1986, less documentation is available. The dating at shallow depths has been performed using cuttings taken at 10 m intervals. 34/7-8 and 34/4-6 has a record of 10 and 20 metres of Pleistocene stratigraphy. Consequently only one or two samples have been available for dating in these wells. However, in well 34/7-1 a record of 135 metres of Pleistocene stratigraphy is dated. Only the completion report from this well has been available. It is however likely that the dating is performed based on the same microfossils as in well 34/7-8, as the same companies have performed both datings (Saga, 1985, 1987; Jolley et al., 1987). The seabed is the top of Pleistocene succession and is entitled as Top T160.

Horizons	Epoch	Stage	Age (Ma)	Dated in wells	Lithostratigraphy from NPD well tops	
					Group	Formation
Top T160					Top Nordland	
Intra T160 E	Middle Pleistocene	?Calabrian	?0,78	35/2-2*		
Intra T160 A-D						
Top T150	Late Pliocene	Piacenzian	2,59	35/2-1, 35/2-2*, 34/4-6*, 34/7-1*, 34/7-8*		
Intra T150 A-G						
Top T140	Late Miocene	Messinian	5,33	34/4-6*, 34/7-1*, 34/7-8*,		Top Utsira
				34/10-30*, 35/1-1, 35/3-1		
Top T130	Middle Miocene	Serravallian	11,61	35/1-1, 35/3-1		
Top T110	Late Oligocene	Chattian	23,03	33/9-12, 33/9-18, 34/7-9, 34/11-4, 35/1-1, 35/10-2, 35/11-3	Top Hordaland	
Intra T100	Late Eocene - Early Oligocene	Priabonian - Rupelian	28,4-33,9-	33/9-12, 33/9-18, 34/7-9, 34/11-3, 35/10-2, 35/11-2, 35/11-4		
Top T50	Early Eocene	Ypresian	54,0	33/9-12, 34/10-15, 35/1-1, 35/8-2, 35/10-2, 35/11-3, 35/11-4	Top Rogaland	Top Balder
Top T10	Early Palaeocene	Danian	61,1	35/8-2, 35/10-2, 35/11-2, 35/11-4		Top Våle
Top K120	Late Cretaceous	Late Maastrichtian	65,5	33/9-12, 33/9-18, 34/4-5, 34/7-9, 34/10-15, 34/11-3, 35/1-1, 35/8-2, 34/7-9, 35/8-2	Top Shetland	Top Jorsalfare
Top K10-J110	Late Jurassic - Early Cretaceous	Volgian - Ryazanian	140,2-150,8	33/9-12, 34/11-3, 35/10-2, 35/11-2		

*Table 5. Overview of interpreted horizons with dating, and the wells they have been dated from. Exact dating of the Intra T100 has not been possible, the age span of the T100 sequence is listed instead. *Data based on information from final well reports.*

4.2 Horizon identification

Seismic horizons are picked from reflectors that display surfaces of discontinuity. They are defined by surrounding reflection terminations. The area of interest is large so reflectors with a widespread distribution are preferred.

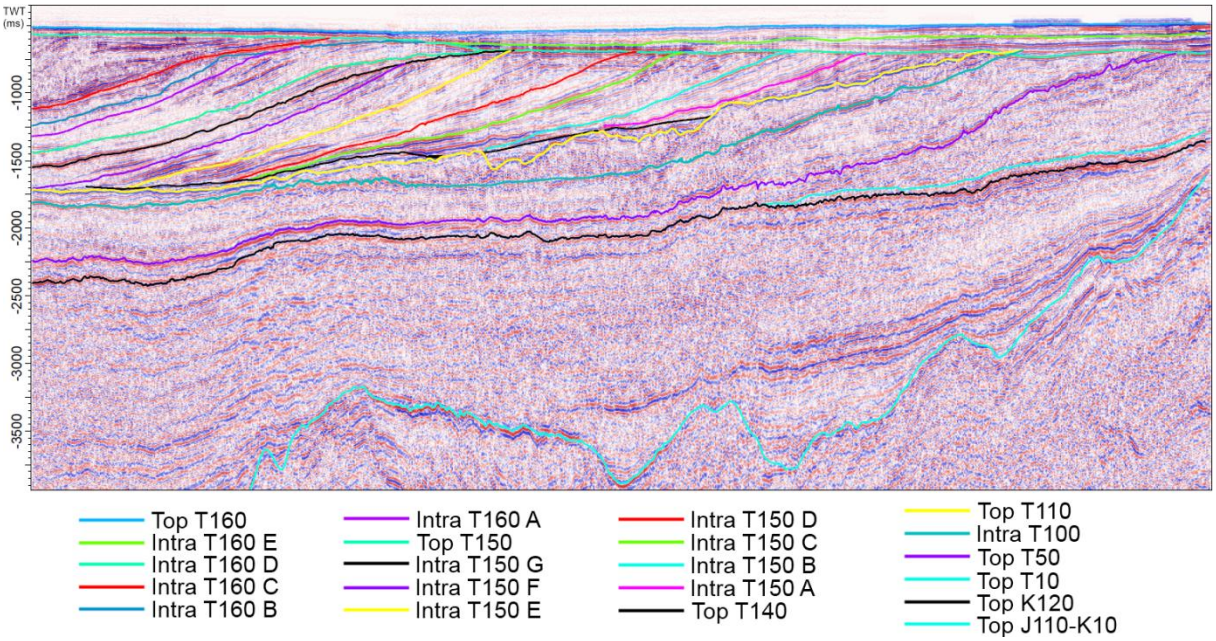

Figure 23. Cross section displaying all the 21 regionally interpreted horizons. The cross section location is displayed in Figure 20.

Top K10-J110 is identified by the terminations of reflectors above and below the surface. The reflectors below the surface are erosionally truncated. The reflectors above Top K10-J110 are onlapping onto the surface. Reflectors above tend to bend upwards towards the topographic highs. Top K10-J110 is the Base Cretaceous Unconformity (BCU). It is dated much older than the stratigraphy of main interest in this thesis; it was interpreted in order to observe possible effects on overlying post-rift sediments.

Top K120 is identified near the Norwegian coast to the east by reflectors below the surface that terminate against Top K120 by erosional truncation. Reflectors above the horizon are onlapping towards Top K120 near the Norwegian coast and downlaps onto it from about 4° - 3°20'E. From 3°20'E and westward reflector

terminations above and below Top K120 are not observed. Top K120 is assigned as the top of the Shetland Group.

Top T10 is identified near the Norwegian coast within Quadrant 36 by reflectors above terminating against the surface by onlap. The interpreted Top T10 horizon display reflector terminations as well. In the SE corner of 36/7 it onlaps the underlying K10-K120 unit. In the NE corner of 36/4 it is erosionally truncated by the Top T150 horizon. The horizon also shows termination to the south and west, by downlapping the Top K120 horizon. Well tops indicate the presence of the T10 sequence also further west, but below seismic resolution, just above the Top K120 horizon. Top T10 is assigned as the top of the Våle Formation.

Top T50 is identified near the Norwegian coast by the reflectors above onlapping onto it. From longitude 3°15’ and westwards reflector terminations are hard to define as overlying reflectors display a chaotic reflection pattern. The Top T50 horizon itself is erosionally truncated by the Top T150 horizon in the east. Top T50 is assigned as the top of the Rogaland Group.

Intra T100 is defined in the same manner as Rundberg & Eidvin (2005) defined the top of their UH-2 unit. Intra T100 corresponds to a diagenetic horizon, characterised by the transition from Opal-A to Opal-CT in Opal rich mudstones. The Intra T100 is interpreted due to being the reflector displaying the strongest amplitude between Top T50 and Top T110. The strongest amplitudes are displayed close to the Norwegian coast and along a NW-SE trend in the basin. In terms of reflector terminations it is definable near the Norwegian coast by overlying reflectors terminating against it by onlap. It often marks a base of the stratigraphy most heavily affected by polygonal faulting and the top of stratigraphy with more moderate polygonal faulting density. In some areas the horizon is very difficult to interpret due to chaotic reflection patterns and a lack of lateral continuity of the strong amplitude horizon. The Intra T100 horizon is erosionally truncated by the Top T150 horizon in the east.

Top T110 is defined by reflectors terminating against it above and below. Reflectors below the horizon terminate by truncation, from 3°10’E and eastwards towards the Norwegian coast, in the southern half of the study area. In the northern half of the study area truncation is observed as far west as 2°50’E. Incisions truncate the underlying reflectors in the NE quarter of the study area. The reflectors below display

chaotic patterns which makes reflector termination identification difficult. This is normally the case in the western half of the study area. Top T110 is interpreted as the top of the chaotic reflection pattern. Reflector terminations within the incised valleys are onlapping the valley edges. Above the Top T110 horizon reflectors terminate by onlap along the Norwegian coast. In the middle of the study area some reflectors are observed downlapping westwards onto the surface. Downlapping reflectors are also seen on either side of incised valleys and in the NW corner of the study area. Some mounds are interpreted along the Top T110 horizon. Overlying reflectors onlap the interpreted mounds. The Top T110 horizon is erosionally truncated by the Top T150 horizon in the east. Top T110 is assigned as the top of the Hordaland Group.

Top T130 is only interpreted in the north-east corner of the study area. Reflectors rarely terminate against it, only one overlying reflector is observed onlapping the Top T130 horizon. The Top T130 horizon itself terminates against Top T110 by downlap towards the west and onlap towards the south and east. Its northern extent is not known.

Top T140 was initially interpreted as two separate horizons. Due to simultaneous well dating, the horizons have subsequently been merged. The prominent incised valley of seen in Figure 30 accounted for the separate interpretations. Top T140 is identified by overlying downlapping reflectors. Top T140 itself is interpreted as erosionally truncated by the Top T150 horizon in the south-east corner of the study area. Further north the Top T140 horizon onlaps the underlying Top T110 horizon to the east. Towards the north and in the north-west corner of the area of study the horizon downlaps onto the underlying T110 horizon. Along the incised valleys Top T140 appears to be terminating by downlap. This is most likely an erosional feature created by incision. The Top T140 horizon frequently coincides with NPD well tops entitling it as the top of the Utsira Formation.

Intra T150 A-H are identified as clinoform surfaces that downlap Top T140 and are erosionally truncated by Top T150. Intra T150 F is an exception as it is erosionally truncated by Intra T150 G and not Top T150.

Top 150 is defined by the underlying reflectors terminating by erosional truncation. This is widely observed in the study area. Reflectors also terminate above the

horizon by onlap in a westerly direction of the slightly inclined Top T150 horizon. In the NW corner of the study area the horizon deepens to a level where reflection terminations against it are not observed.

Intra T160 A-E are identified in the same manner as the Intra T150 A-H horizons. They are clinoform surfaces that downlap the Top T140 horizon, or in the NW where Top T140 is not interpreted they downlap the Top T110 horizon. Intra T160 A-C are erosionally truncated by the Intra T160 D horizon. Intra T160 E does not display reflectors terminating against it. The Intra T160 horizon itself terminates by onlapping the underlying Top T150 horizon towards the west, in the middle of the study area.

Top T160 represents the present day seabed. Some reflectors beneath the horizon are erosionally truncated. The Top T160 marks the top of the Nordland Group.

4.3 Unit description

The seismic units' interpretation is presented in this chapter and illustrated by examples of interpreted seismic cross sections. For the T150 and T160 units NW-SE dip-oriented seismic cross sections are presented. Much of the Cretaceous-Palaeogene strata display a poor seismic resolution due chaotic seismic reflection pattern in large parts of the area.

Unit T10 is very thin and the reflectors within the unit are discontinuous and chaotic.

Unit T20-T50 is thin in the majority of the area and displays a wavy parallel internal reflection pattern. However the reflectors are seldom continuous, they are frequently disrupted. Towards the east the T20-T50 unit is much thicker than anywhere else. The reflection pattern is still chaotic with disrupted reflectors. The parallel reflectors seen to the west continue along the Top K120 horizon. The internal reflection pattern of the wedge resembles a divergent configuration.

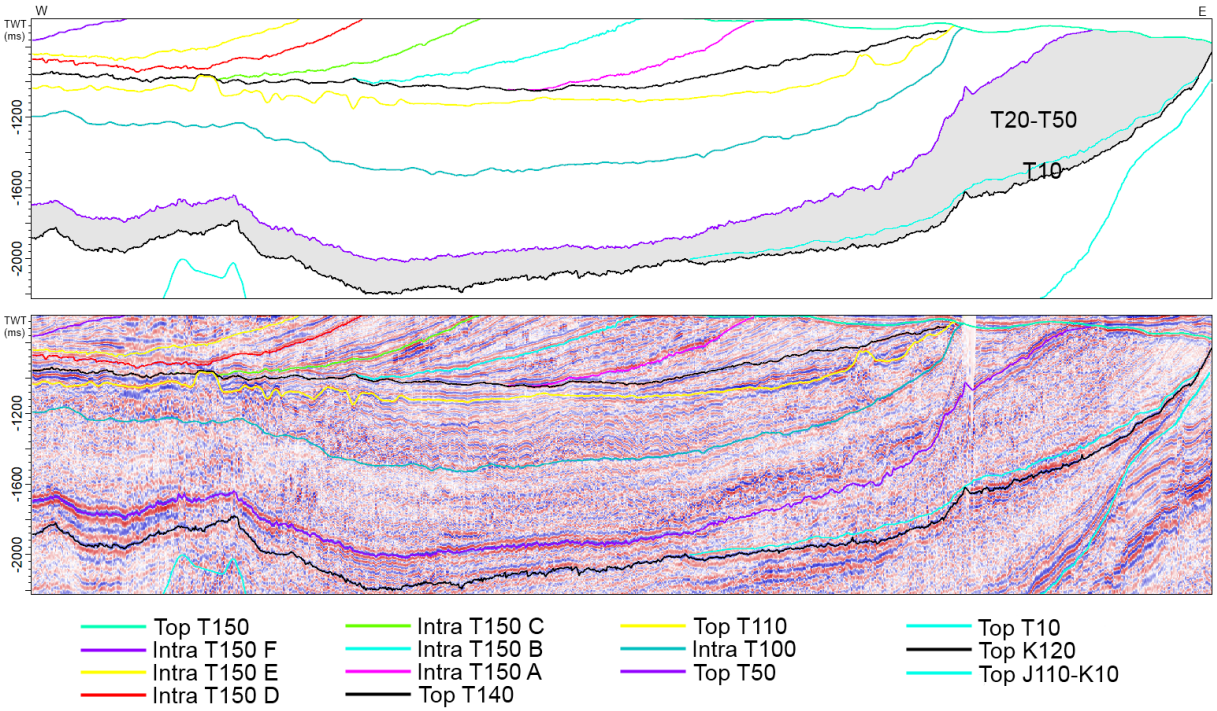

Figure 24. Cross section with and without the seismic displayed. Units T10 and T20-T50 are marked by a grey area in the top section.

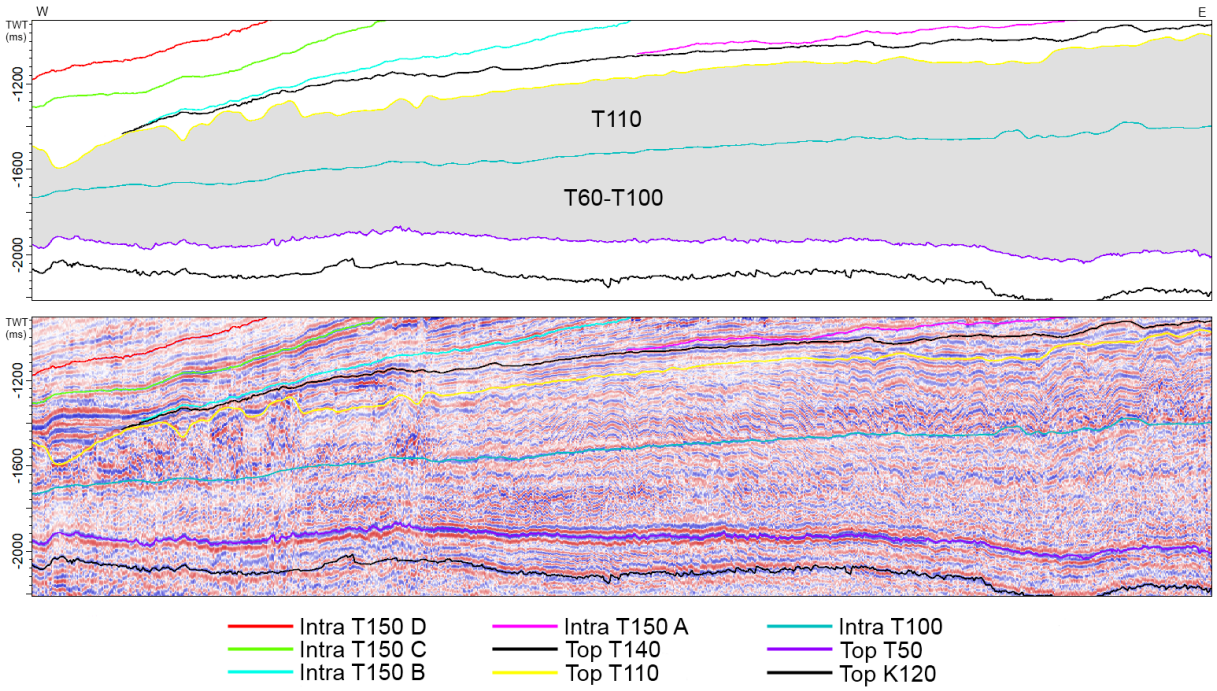

Figure 25. Cross section with and without the seismic displayed. Units T60-T100 and T110 are marked by a grey area in the top section.

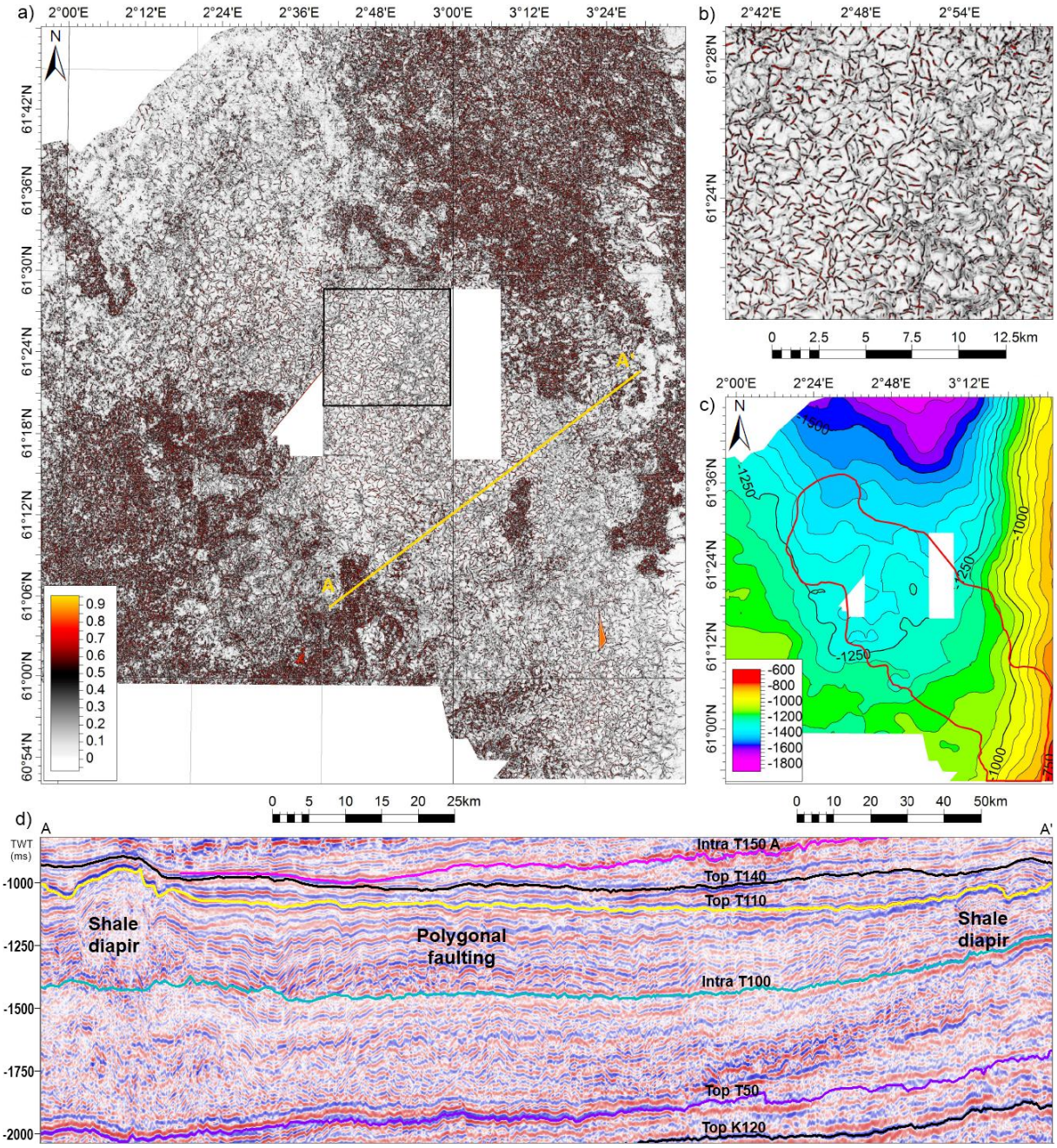

Figure 26 a) Polygonal faulting illustrated on seismic cube processes with structural smoothing and variance (edge) method. The surface illustrated is taken between the Intra T100 and Top T110 horizons. No dominant fault orientation is observed. Figure 26 b) enlarged view of the surface. Figure 26 c) Topography of the surface displayed in depth with area of the highest density of polygonal faulting marked in red. Figure 26 d) displays a cross section perpendicular to the NW-SE orientation of the polygonal faulting. Polygonal faulting is observable from the Top T110 horizon down to below the Top T50 horizon. Polygonal faulting is most frequent in the stratigraphy between Top T110 and Intra T100.To the left and right of the cross section shale diapirs are visible below the bulges in the Top T110 horizon.

Units T60-T100 and T110 displays a chaotic pattern much like the underlying units. Some features are however identifiable. The otherwise initially horizontal, parallel reflectors of units T60-T100 and T110 are frequently disrupted by numerous small scale faults. The faulting is observable in both units, but is most characteristic within T110 where the reflectivity is the strongest and the fault through appears to be the largest. The feature is known as polygonal faulting where the numerous faults display varying strike. In the area studied the polygonal faulting does not display a dominant strike orientation, as can be seen from Figure 26. The fault throws are estimated to be in the order of 10-50 m. The area affected by polygonal faulting is observed along a NW-SE orientation. In the NW the T60-T100 and T110 units becomes thinner. The Top T110 horizon displays an irregular surface. Mounds have been interpreted as shale diapirs moving into the overlying T140 unit. The diapirs are located in a pattern that resembles the NW-SE orientation of the polygonal faulting (Figure 27). The diapirs are also visible on Figure 26 a) and d) on each sides of the polygonal faulting area. One diapir is centred in the area of polygonal faulting. The shale diapirs are commonly observed up to the level of the Top T140 horizon with reflectors within the T140 unit onlapping the sides.

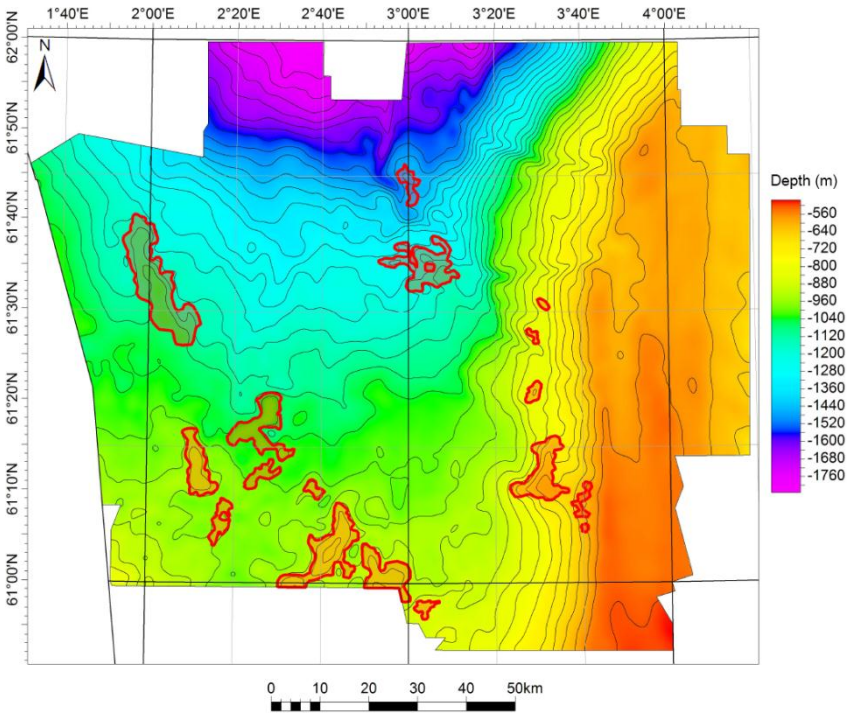

Figure 27. Shale diapirs forming mounds on the Top T110 map. The diapir circumference is marked in red. The diapirs are distributed along the sides of the NW-SE orientation of polygonal faulting. A cross section with shale diapirs is shown in Figure 26 d).

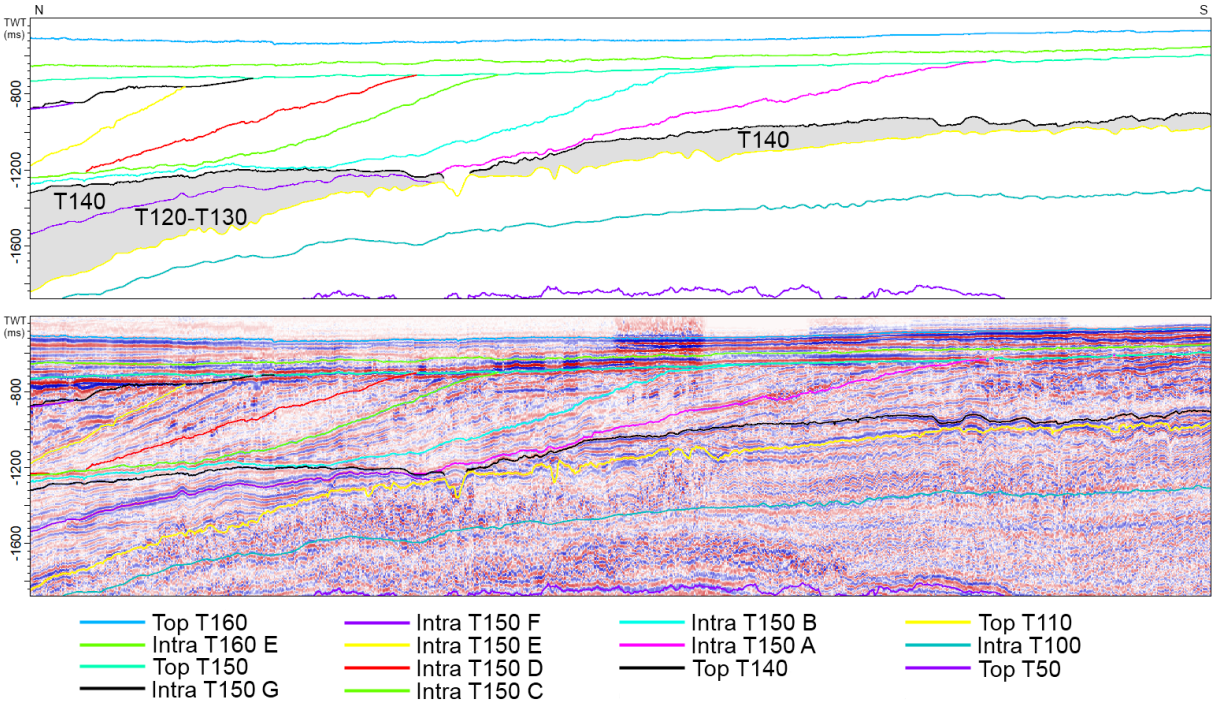

Figure 28. Cross section with and without the seismic displayed. Units T120-T130 and T140 are marked by a grey area in the top section. T120-T130 is only dated and interpreted in the NE parts of the area studied. T140 is interpreted over large parts of the area studied and is locally very thin.

Unit T120-T130 has only been interpreted in the north-eastern part of the study area. Dating of the horizon was only available in this area; possible southern and western continuations of the reflector are disrupted by incisions. T120-T130 has a prismatic shape with inclined parallel internal reflectors along inlines. The bottom reflectors of the unit onlap the Top T110 horizon towards the south. On seismic cross sections displayed NE-SW the internal reflectors are clearly downlapping the Top T110 horizon towards the south-west. The internal reflection pattern and thickness map indicate that the sediments are sourced from north-east of the area studied.

Unit T140 is interpreted as widespread. In the north-eastern corner of the area studied the internal reflection pattern resembles that of the T120-T130 unit. The internal reflectors are however onlapping the Top T120-T130 horizon towards the east instead of the Top T110 horizon. The internal reflectors of T140 are erosionally truncated where the unit thins near the incised valley (Figure 30 c). The north-eastern part of T140 also appear to be sourced from north-east of the area studied. In central

parts of the area of study the unit is thinner and fewer characteristics are identifiable. Some internal reflectors are observed downlapping westwards onto the Top T110 horizon indicating it may consist of several internal units. Where shale diapirs have been interpreted the internal reflectors of T140 are onlapping their sides.

About 70-100 ms above the Top T110 horizon, in the south-east corner of the area studied, multiple small scale channels are observed. The channels are a few hundred metres wide and probably no deeper than a couple of tens metres (Figure 29 b). The channels are located on a gently westward dipping slope and display a gentle sinuosity. The channels diminish westward and are truncated in the east by the Top T150 horizon. Figure 29 b) displays the channels on a seismic cross section. The channel system is much clearer from a map perspective. A surface extraction from a seismic cube processed with the variance (edge) volume attribute is displayed in Figure 29 a).

In the north eastern part of the study area two much larger incision features are observed. Two incisions form up 1-4 km wide and 100-200 m deep valleys. The incisions are interpreted along the seismic horizon Top T110. They divide and carve into and the Top T140 horizon as well (Figure 30). The incised valleys cut into the steep basin margin from the west and subsequently propagate northwards along the north-south basin axis into the deeper Møre Basin. The incisions display a gentle sinuosity. For the southern incision several valley are joined together into branches. Both systems are divided in two before extending outside of the area studied. As can be seen from Figure 30 b) the northernmost incision is much less well defined on the seismic attribute surface west of 3°28’E. The continued path west of 3°28’ should therefore be considered as solely a suggested path.

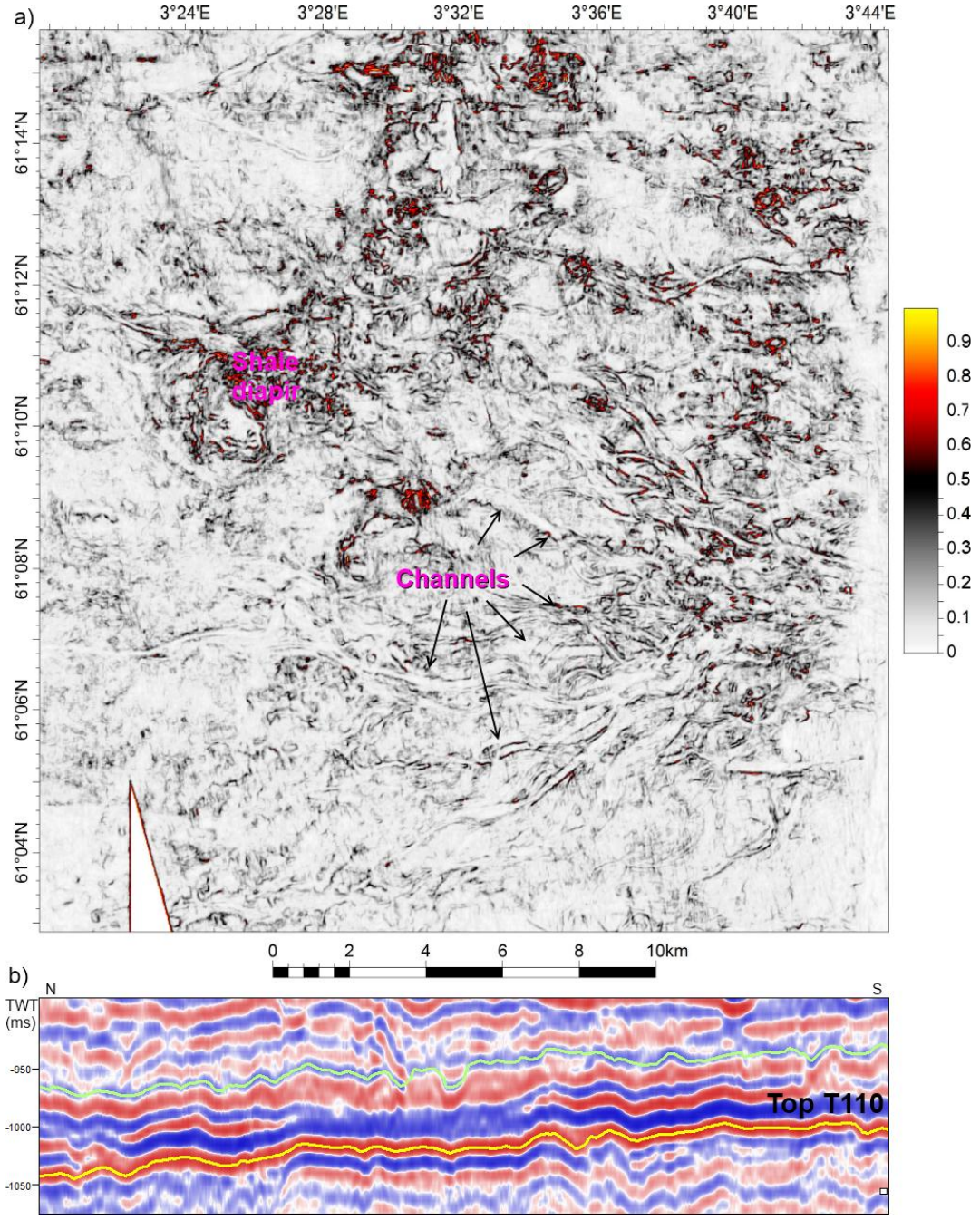

Figure 29. Small channel features observed ca. 70-100 ms over the Top T110 horizon. The location of the figure can be seen from Figure 20. 29 a) Multiple channels illustrated on seismic cube processed with variance (edge) method. 29 b) Seismic section (inline 14600) displaying the surface illustrated in a) as a green horizon ca. 70-100 ms above the Top T110 horizons.

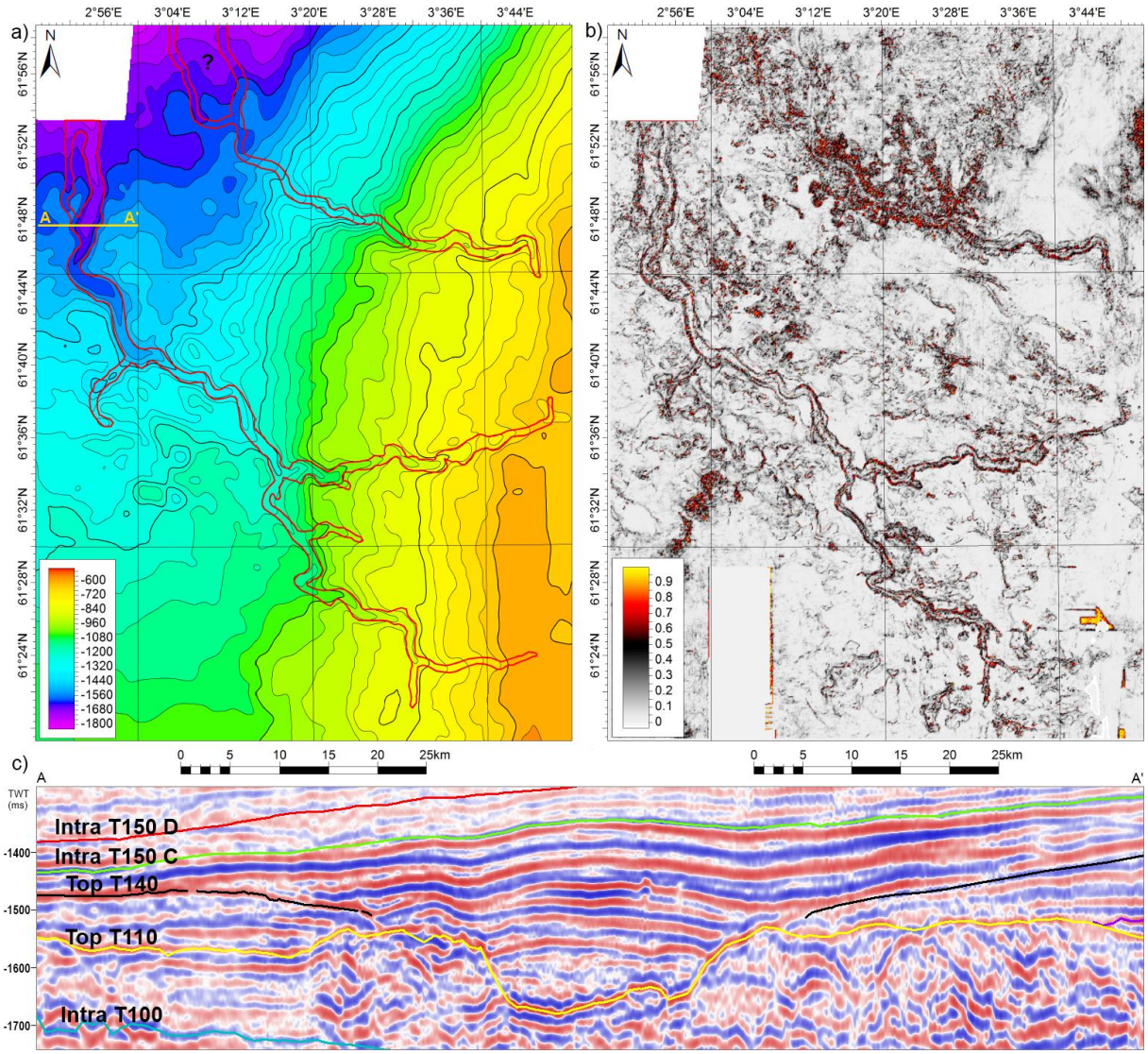

Figure 30 a) Topographic map of the Top T110 horizon in the NE corner of the study area. Interpreted channels marked with red, yellow line marks location of Figure 30 c). Figure 30 b) displays the same channels on a surface with extracted values from the variance (edge) volume attribute. The surface is taken 25 ms below the Top T110 horizon. Figure 30 c) displays the most prominent channel in cross section, cross line 18400.

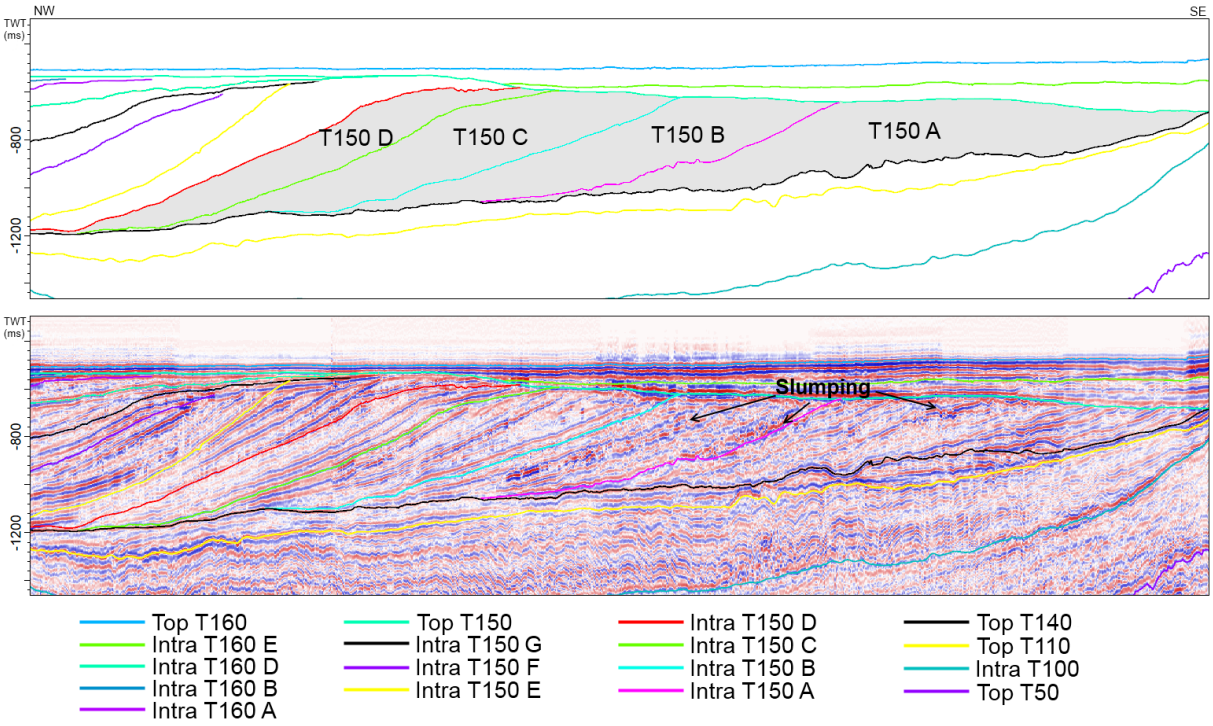

Figure 31. Cross section parallel to depositional strike, with and without the seismic displayed. Units T150 A-D are marked by a grey area in the top section.

Units T150 A-D are the lowermost and oldest units within the T150 Pliocene succession. All units are bounded by a regional downlap surface at the base and an upper regional unconformity at the top. The T150 units are separated by inclined unconformity clinoform surfaces. In Figure 31 the top of unit T150 D is defined by an unconformity clinoform surface, while in Figure 32 the top is defined by the upper regional unconformity. The regional downlap surface's present day position is at a lower level towards NW than in the SE. This affects the shape and thickness of the units. T150 A displays the thinnest vertical thickness, but a great stratigraphical thickness. The internal reflectors of the units are parallel with the inclined unconformity clinoform surfaces. From unit A to D the inclination of the internal reflections gradually becomes steeper. The inclination decreases from the top of the units and down towards the downlap surface for all units. The clinoforms are interpreted as having an oblique configuration. Within units B and C some levels of irregular reflectors are visible. They may be indications of clinoform surfaces with slump deposits.

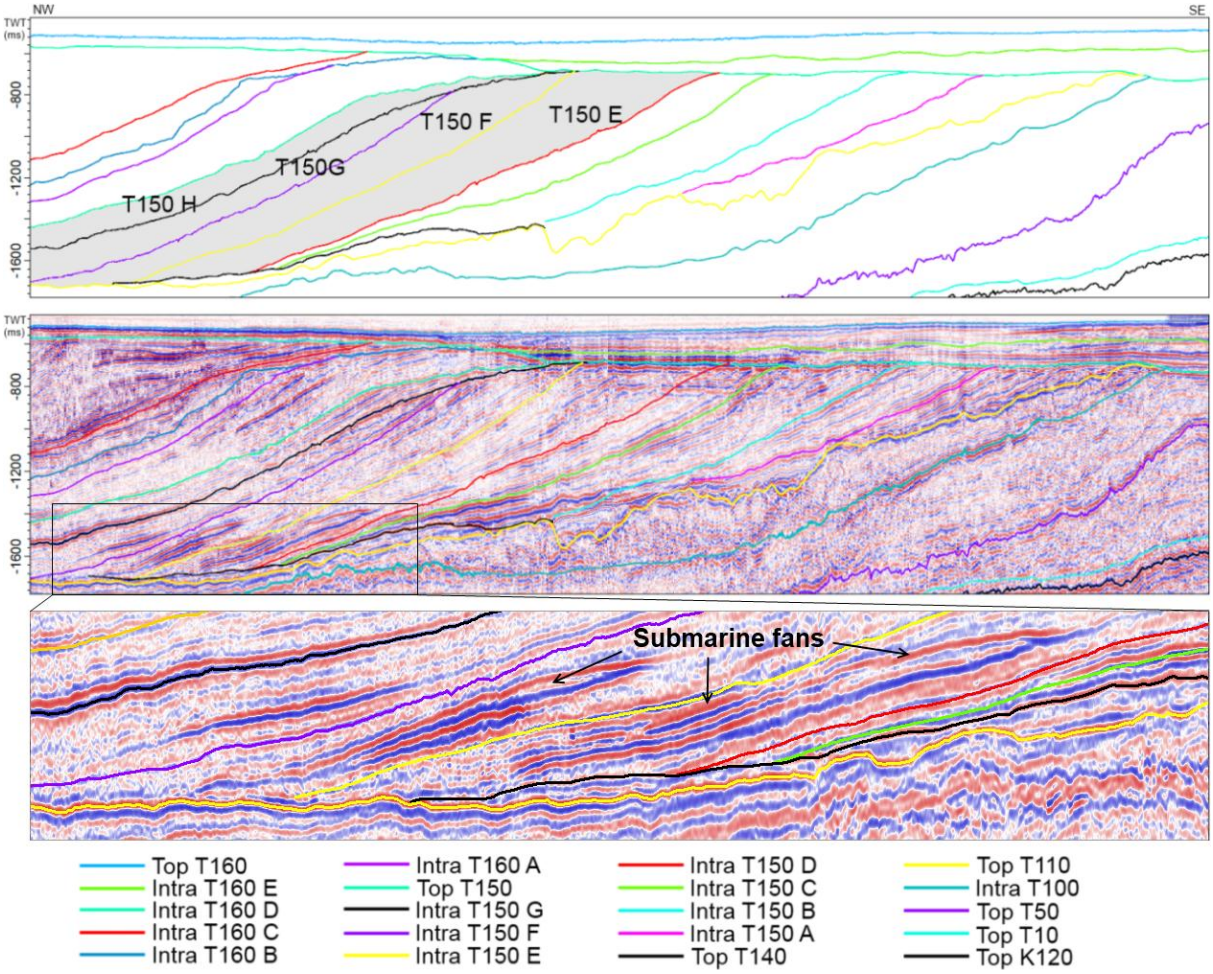

Figure 32. Cross section parallel to depositional strike, with and without the seismic displayed. Units T150 E-F are marked by a grey area in the top section. The lowest section displays a zoom in on the submarine fans at the clinoform toes.

Units T150 E-H are bound by unconformity clinoform surfaces between every unit and a regional downlap surface at the base. The upper boundaries of units T150 E-H vary throughout the area studied. The internal reflectors of T150 E downlap onto the regional downlap surface. In the north of the area studied T150 E is erosionally truncated by the upper regional unconformity surface. Further south the unit is also erosionally truncated by the Intra T150 G horizon. The internal reflections of unit T150 E are more parallel to the Intra 150 D horizon than the Intra T150 E horizon. Internal reflectors of unit T150 G downlap onto the regional downlap surface in south, but extends outside the study window in the north. Unit T150 H lower termination only extends outside the study window. The top of the units F-H are erosionally truncated by the Top T150 clinoform surface. The internal reflectors in the units T150 F-H are parallel with the inclined unconformity clinoform surfaces at the base. From unit E to

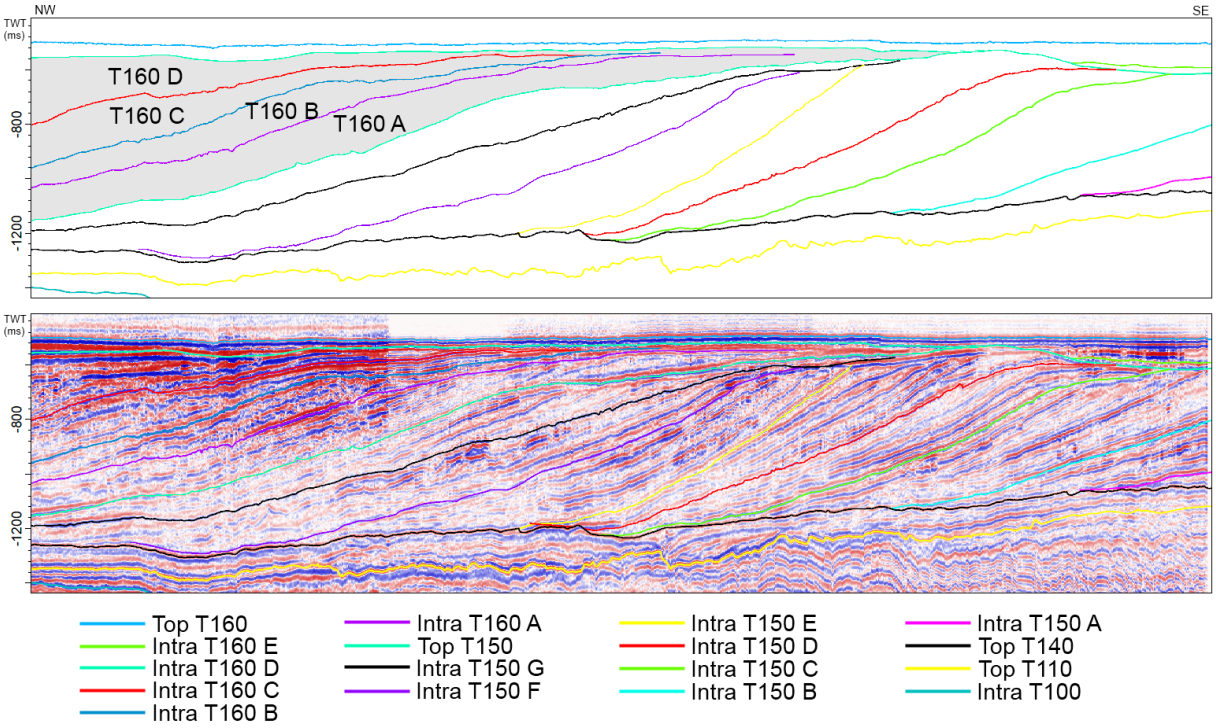

Figure 33. Cross section parallel to depositional strike, with and without the seismic displayed. Units T160 A-D are marked by a grey area in the top section.

H the inclination of the internal reflections gradually becomes steeper. The inclination decreases from the top of the units and down towards the downlap surface for all units. At the bottom of the units a series of small fans are visible. They are elongated and display progradation towards the north-west (Figure 32).

Unit T160 A-D all extend outside the study window. All units are erosionally truncated by an upper regional unconformity. In the northern parts of the area studied the upper boundary of unit B is the Intra 160 B horizon and the T160 A is also erosionally truncated by the Intra T160 B horizon. The internal reflectors of units T160 A-D do not display the parallelism of units T150 A-H, but a more chaotic pattern. The horizons separating the units are however more clearly defined.

Unit T160 E & F are the uppermost units interpreted. The internal reflection configuration is highly parallel. Some wavy reflectors forming wide and shallow incisions are observed. Reflector terminations are truncated against these incisions. Reflectors also terminate against the seabed by truncation and against the underlying regional unconformity by onlap.

The **Seabed** displays a striking feature on cross sections is the Norwegian Channel Ice Stream (NCIS). It forms an N-NW trending incision into the seabed. With reference to the area of flat seabed at a depth of about 130 metres in the SW corner, the NCIS has made an incision of 290 metres down to a maximum of 420 metres at the deepest. Within the NCIS many plough marks are observable, having mainly the same orientation as the incision itself.

When studying the autotracked seabed surface numerous pockmarks are observable. The pockmarks have been regionally mapped at seabed level over the whole area of interest (Figure 34 a). All the pockmarks observed are located within the vicinity of the NCIS. On the SW flank of the NCIS no pockmarks are observable due to seismic artefacts. The NE flank of the NCIS has a high frequency of iceberg plough marks possibly overprinting visible pockmarks. Pockmarks are observable over most parts of the NCIS. The highest density is seen in the SE corner of the area of study. Within the circle in Figure 34 b) a pockmark is easily observable on the surface, but is difficult to identify on a seismic section

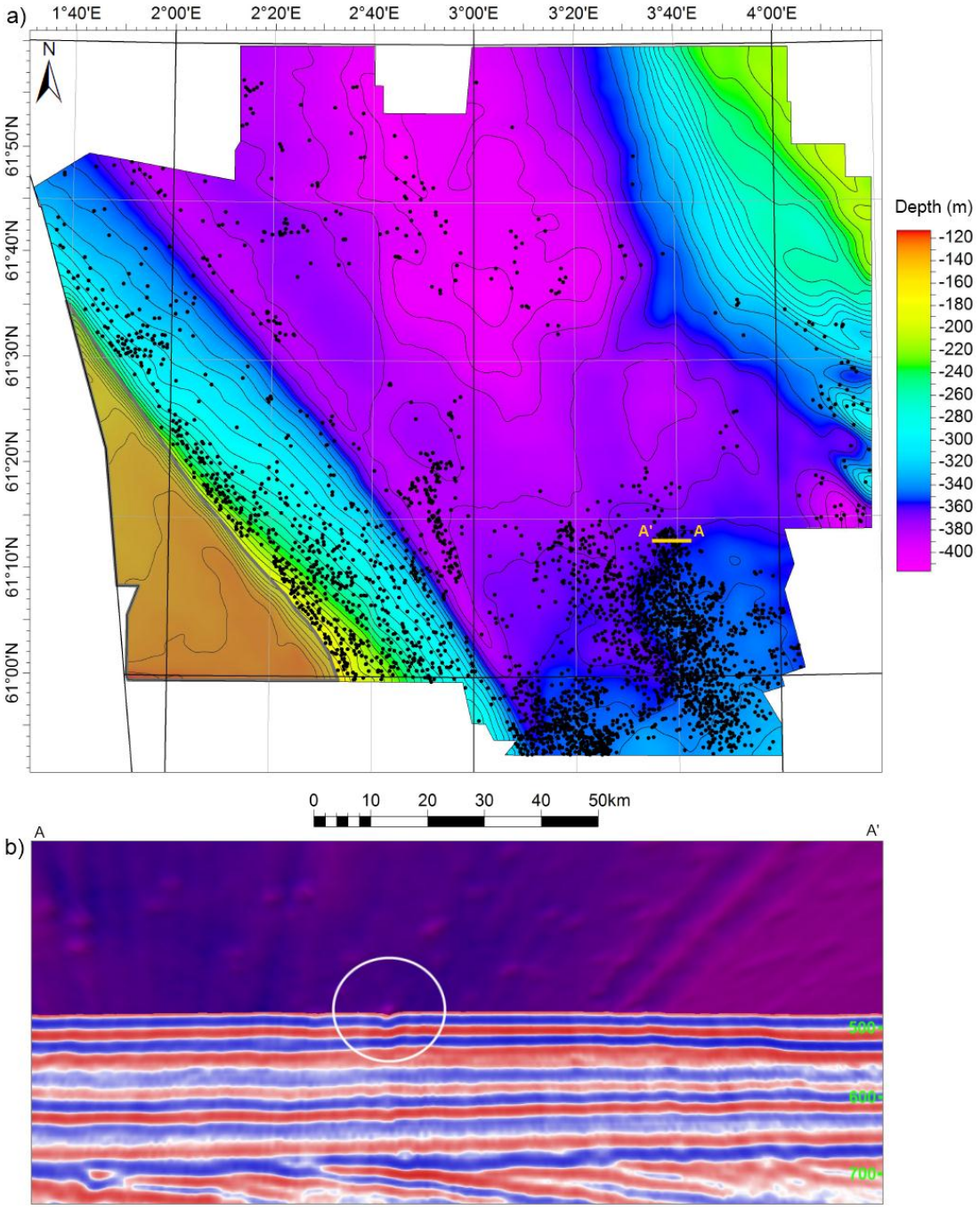

Figure 34 a) Map of the seabed with observed pockmarks marked by black spots. Most pockmarks are observed in the SE corner of the area studied. No pockmarks are identified in the SW corner marked in grey due to overprinting by seismic artefacts. 34 b) Screenshot of a seismic section put together with the seabed surface. Within the circle a pockmark is easily observable on the surface, but is harder to identify on a seismic section.

.

4.4 Sequence stratigraphy

For the sequence stratigraphic analysis two cross sections are presented (Figure 35 & 36). Dip-oriented cross sections are favourable as well as the presences of a well tie. Best effort was made to combine these preferences. The well tops in Figures 35 & 36 are taken from well reports. To improve the foundation for analysis three additional horizons were interpreted within the mostly chaotic T20-T50 and T60-T100 units. Within the T20-T50 unit a horizon was picked based on overlying downlapping reflectors. A proper well tie for the horizon is not displayed in any of the figures, but a Thanetian age was indicated by correlation to the nearby 35/11-4 and 36/1-2 wells. Within the T60-T100 unit a reflector defined by overlying downlapping reflectors in the eastern half was interpreted. It was dated by 35/8-2 and 35/3-1 as the top of the Ypresian stage. Another reflector within T60-T100 was interpreted based on a few overlying reflectors onlapping it towards the east. It was dated as the top of the Priabonian stage in wells 35/3-1 and 35/8-2 (Ichron, 2010).

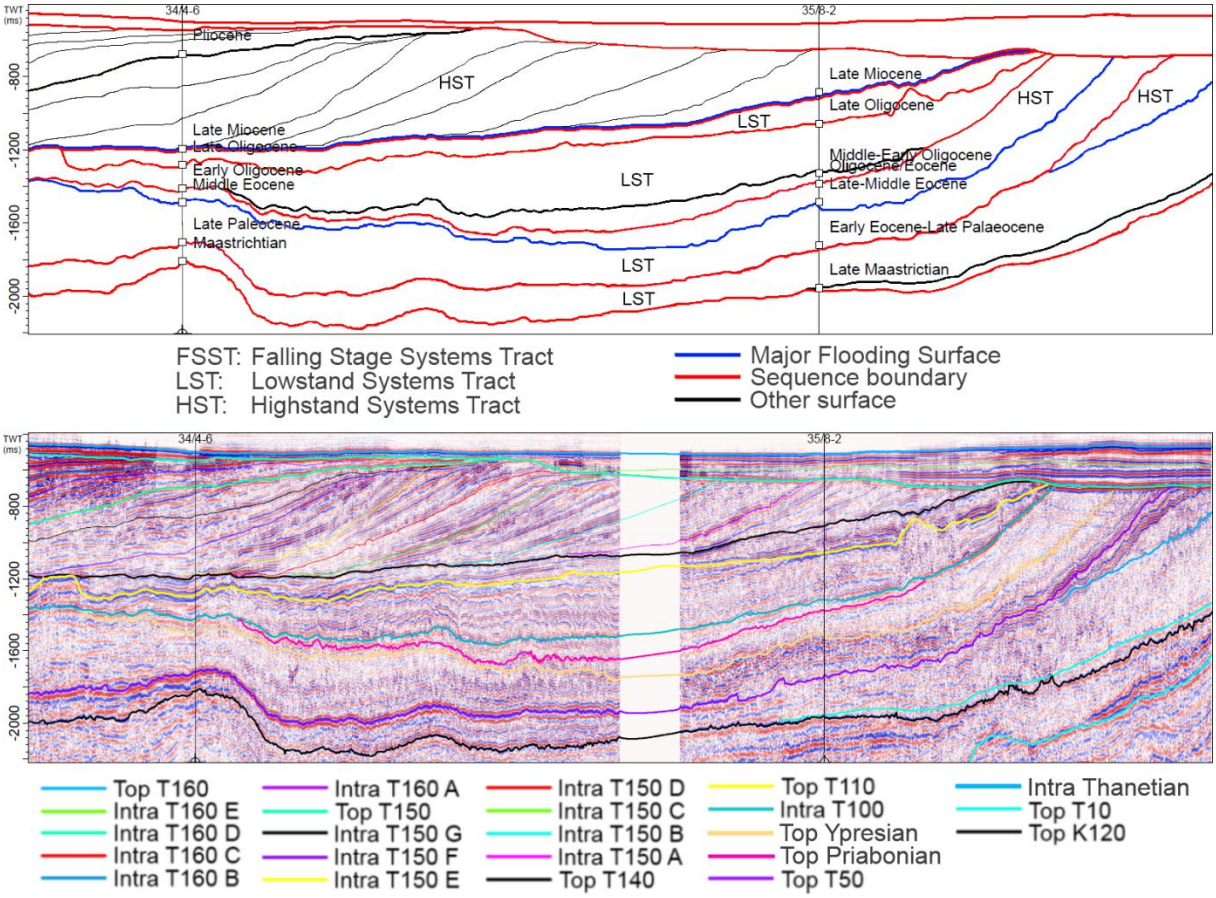

Figure 35. Interpretive sequence stratigraphic model of the Cenozoic based on seismic cross sections. The well tops displayed are taken from the well reports of 34/4-6 and 35/8-2 (Saga, 1977, 1987).

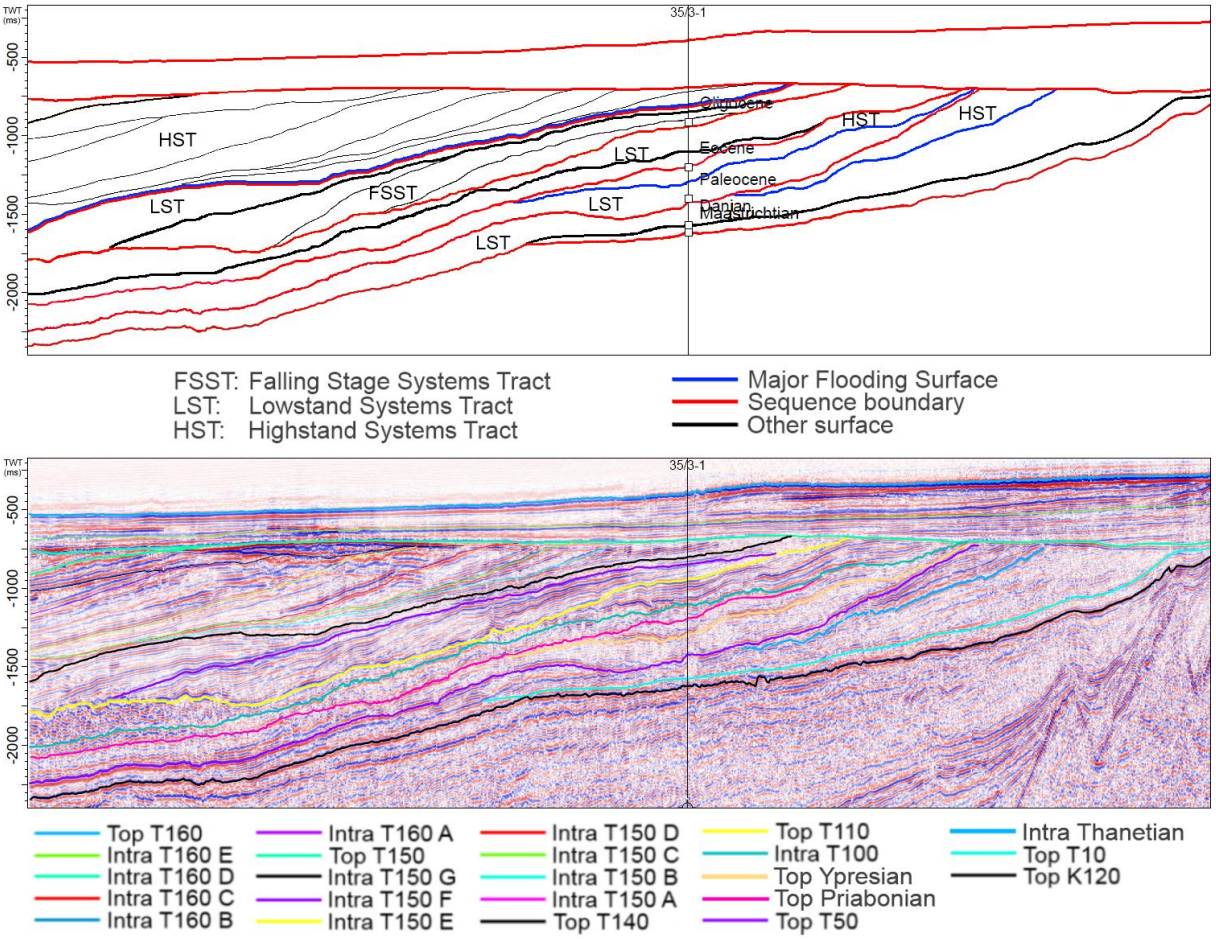

Figure 36. Interpretive sequence stratigraphic model of the Cenozoic based on seismic cross sections. The well tops displayed are taken from the well report of 35/3-1 (Gulf, 1982).

Six sequences have been defined. The bounding surfaces are picked based on erosional events and breaks in sedimentation. The surfaces are the Top K120, -T50, -Priabonian, -T110, -T140, -T150 and -T160 horizons. Erosional surfaces, identified by reflector truncations, are the Top K120, -T50, -T110 and -T150 horizons. Truncations of reflectors underneath the Top Priabonian horizons are hard to identify, due to a chaotic seismic pattern, but a marked shift in sedimentation is clear at the eastern basin margin. Obvious truncations beneath the Top T140 horizon are also hard to identify, but in the north-east of the study area two large valley incisions are formed along the horizon. Top T160 marks the end of deposition as the present day seabed.

The first sequence (K120-T50) consists of a lowstand systems tract (LST) and a highstand systems tract (HST). The LST consists of a thin unit deposited along the basin margin followed by a thicker unit with downlapping reflectors and basinal deposition. A prograding wedge is interpreted as a HST as the previous system was abandoned and followed by a transgression and a period of renewed sediment supply higher up at the basin margin.

The second sequence (T60-Priabonian) also consists of a lowstand systems tract and a highstand systems tract. The LST consists of some turbidity deposits overlying the Top T50 horizon in parts of the eastern basin margin. The sediments within the LST are mainly sourced from the west and onlap toward the east. Minor input was also sourced from the east. The HST is interpreted as deposition along the eastern basin margin after a transgression.

The third sequence (Priabonian-T110) consists of only a lowstand systems tract. The upper parts of the sequence have been completely removed. A basinward increase of sedimentation following the previous HST is interpreted.

The fourth sequence (T120-T140) consists of a falling stage systems tract (FSST) and a lowstand systems tract. In the north-east the sequence forms downlapping wedges along the basin margin. The T120 and T130 make up the FSST that gradually prograde and downsteps into the basin. The T140 sediments are mainly positioned in the centre of the basin and make up the LST. Incisions have removed parts of the sequence.

The fifth sequence (T150-T160 D) consists of a highstand systems tract (HST). The regressive succession of clinoforms built out from a more landward position, at a much higher level than the T140 LST. A major flooding surface (MFS) is interpreted at the base of the sequence. The sixth sequence (T160 E-F) is deposited mainly by glacial processes (Sejrup et al., 2000).

4.4.1 Shelf edge trajectories

The shelf edge trajectory polygons are extracted by measuring the maximum rate of inclination using an algorithm in Petrel (Section 3.1.4). The shelf edges are picked for the T150 and T160 units where the steepest angle between the clinoform surface and the horizontal plane is located. The extracted polygons are displayed in a map view in Figure 37 a). The polygons illustrate the basinward progradation during Pliocene and Pleistocene. In the south-western corner no steep angles were recorded between the clinoform surfaces and the horizontal plane. The dip angle operation located and displayed a channel feature on the Intra T160 B horizon (Figure 37 b). The shelf edge trajectory polygons are displayed as points in cross sections. Two dip-oriented cross sections displaying surfaces in the depth domain are chosen for the trajectory analysis (Figure 38). The units closest the eastern basin margin have had their upper parts truncated. Younger surfaces than Intra T150 C in Figure 38 a) and younger surfaces than Intra T150 E in Figure 38 b) have more of the upper parts preserved. In Figure 38 c) the two trajectories are placed together. Changes in the trajectory paths are evident and the two cross sections display similarities. A flat shelf edge trajectory is evident in the south-east where the erosion has been most severe. From T150 C to E a low andgle positive shelf edge trajectory is displayed. A negative trajectory follows T150 E before a transgression. The T150 G horizon has eroded into the underlying T150 H, which is visible in Figure 38 as the T150 G and H polygons are crossing. A succession of negative, positive and negative trajectories follows for the T160 horizons displaying variations in the relative sea level.

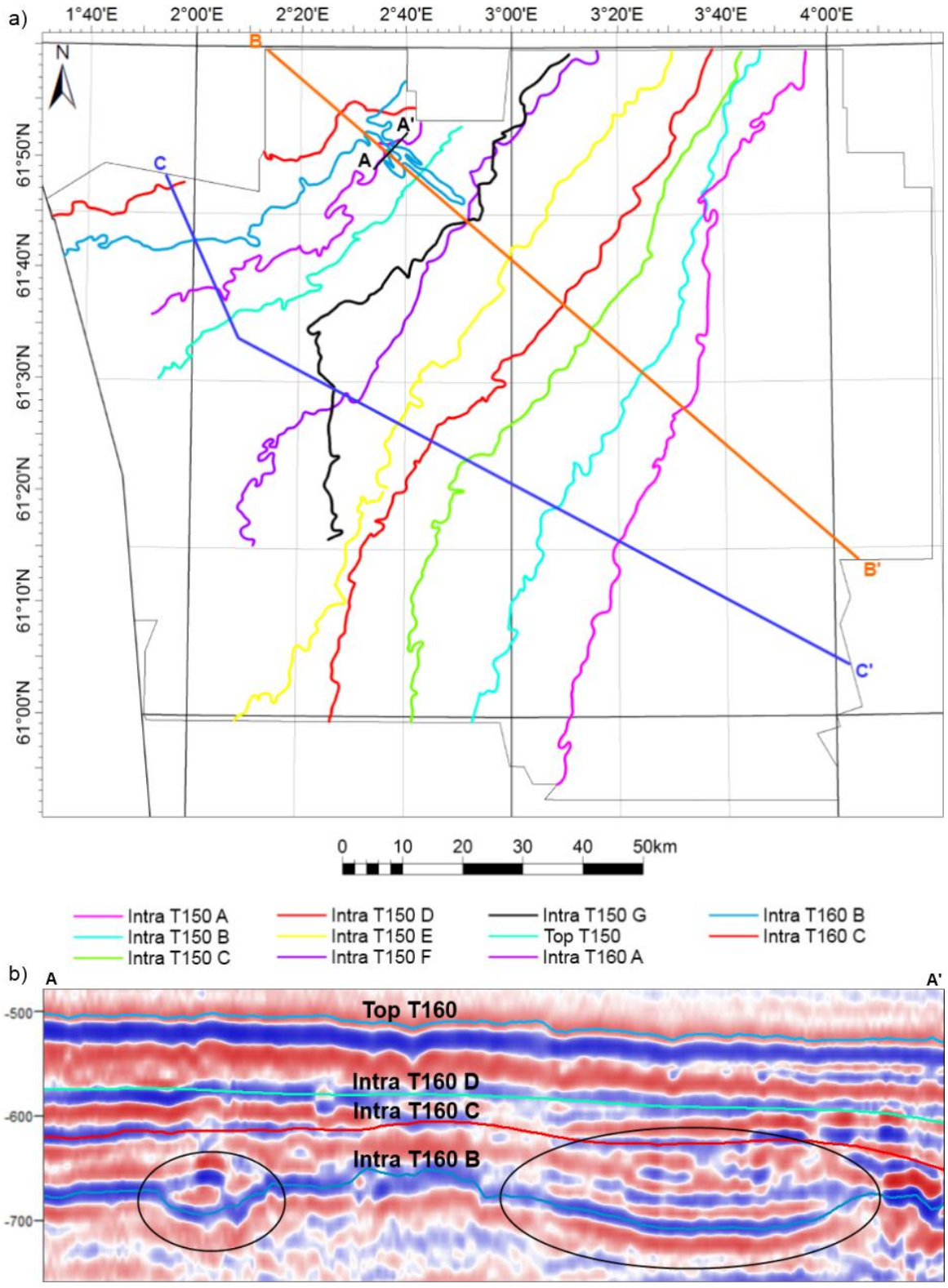

Figure 37 a) Map view of the shelf edge trajectory polygons of the horizons Intra T150 A-F, Top T150 and Intra T160 A-C. Intra T150 G crosses the Intra T150 F polygon. T150 G is an erosional surface. The dip angle calculation performed for extracting the polygons encountered a channel feature along the Intra T160 B horizon. 37 b) Cross section with the channels along the Intra T160 B horizon.

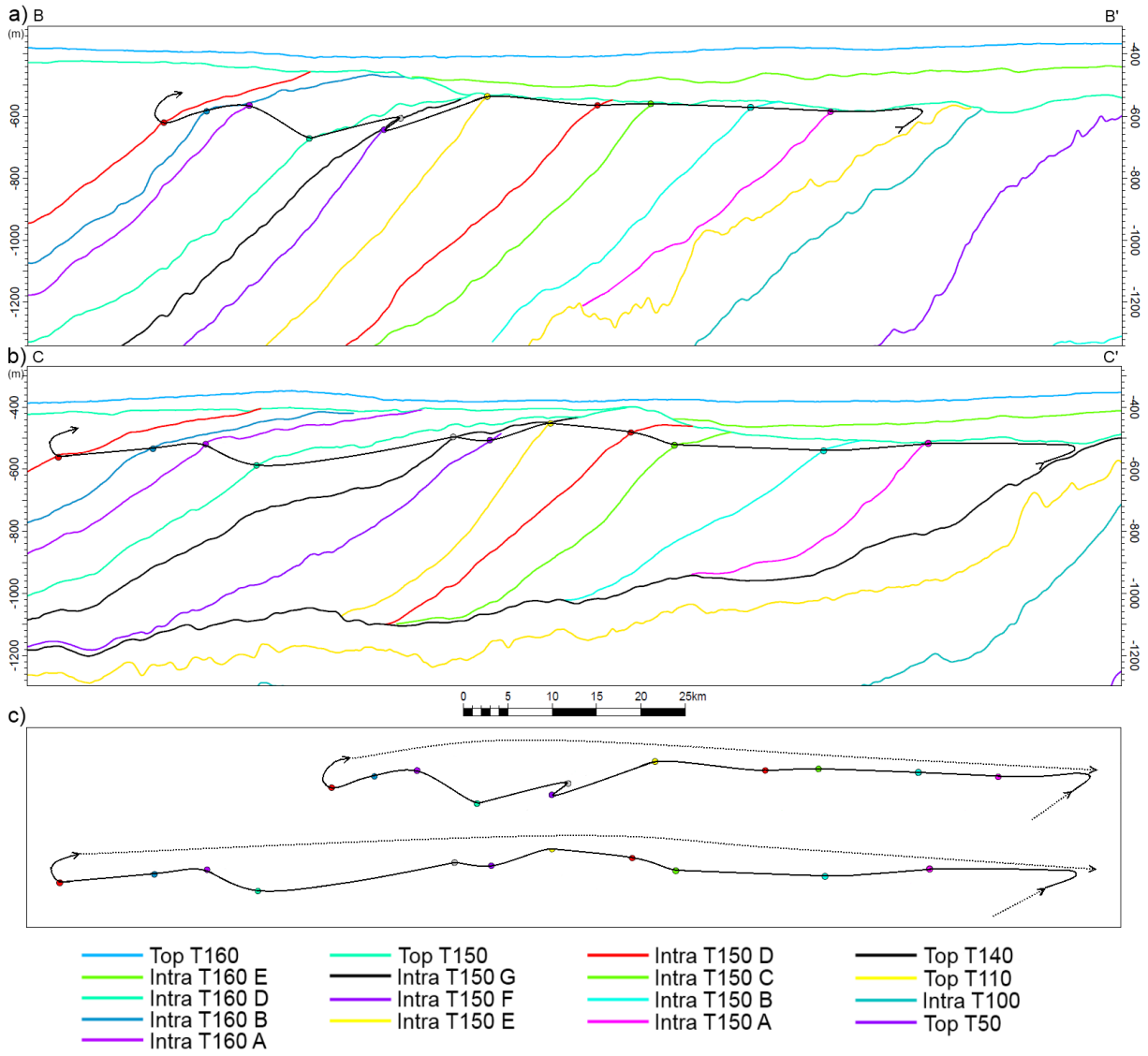

Figure 38. Shelf edge trajectory in two dip-oriented cross sections. The vertical scaling, in the depth domain, is the same for both cross sections. For location of cross section see Figure 37 a).

4.5 Thickness, distribution and accumulation rates

The unit thicknesses and volumes have been calculated and are presented in Table 6, 7 and 8. A variety of thickness maps are presented in Figure 40 and 41. The thickness maps of all units are enclosed in Appendix A. The maximum and average accumulation rates have been calculated, using input values enclosed in Appendix B. The graphs in Figure 39 display a dramatic increase in accumulation rates towards the end of the Cenozoic. The accumulation rates were also relatively high in the Palaeocene and Late Oligocene. The maximum accumulation rates are calculated at the unit's depocentre.

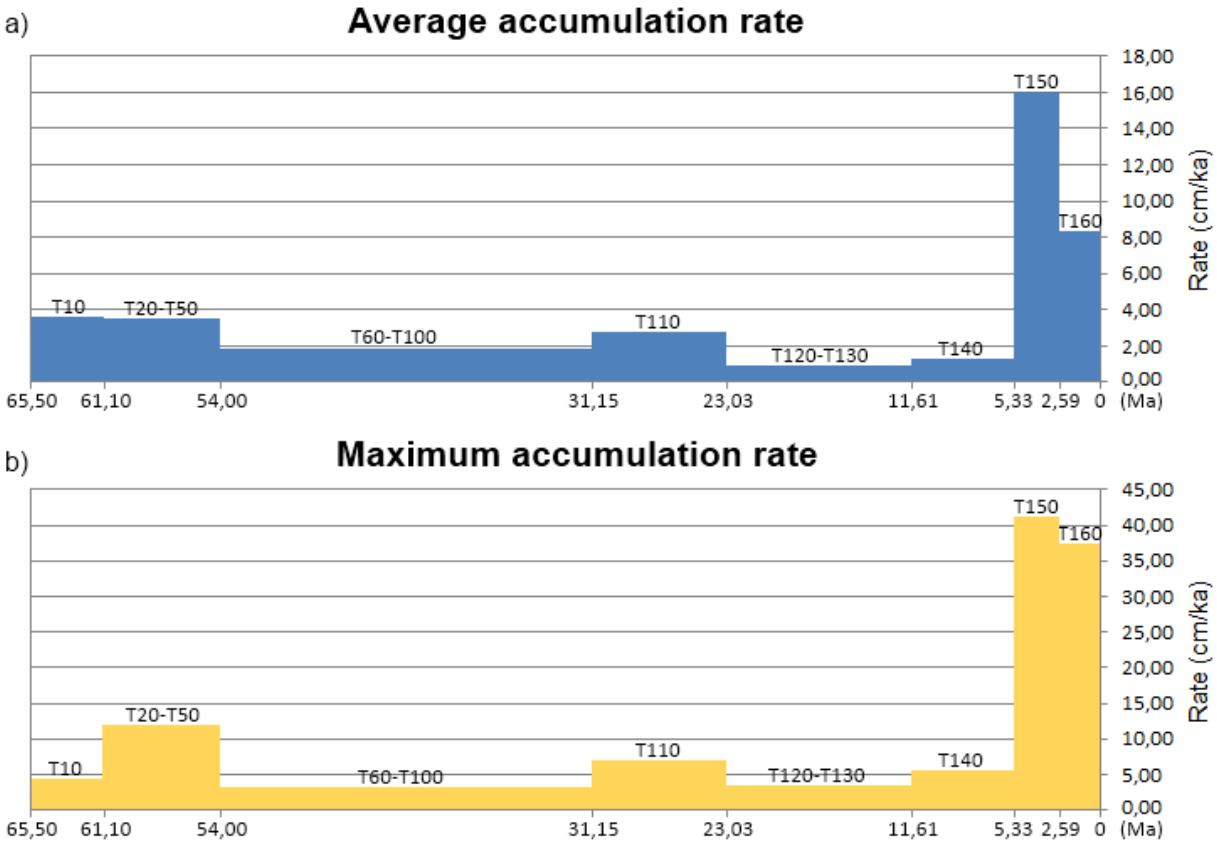

Figure 39 a) Graph displaying the average accumulation rate of all units. 39 b) Graph displaying the maximum accumulation rate of all units.

Units	Maximum thickness (m)	Average thickness (m)	Volume (km3)	Maximum accumulation rate (cm/ka)	Average accumulation rate (cm/ka)
T160	966,3	218,5	3204	37,31	8,34
T150	1126,4	359,6	5275	41,11	16,01
T140	328,9	83,3	987	5,51	1,33
T120-T130	340,2	81,1	247	3,56	0,91
T110	573,8	227,2	2815	7,07	2,80
T60-T100	751,3	442,9	5692	3,29	1,85
T20-T50	851,7	252,5	3688	12,00	3,50
T10	192,3	80,3	417	4,37	3,71
K10-K120	6651,2	2020,2	28933	8,31	2,44

Table 6. The maximum and average vertical thicknesses of all units, the sediment volumes of each unit and the maximum and average accumulation rates.

Unit K10-K120 is thick and covers the complete Cretaceous sediment record. The largest sediment thickness is located in the northern part of the area studied, within the Sogn Graben and the Marulk Basin (Figure 40 a). The unit is also thick in the southern parts of the study area, within the Viking Graben. The Sogn Graben rift topography is completely diminished by the infill of the K10-K120 deposits. The Viking Graben topography towards the south is nearly diminished, but the Marulk Basin is not filled to the same level as the grabens. The basin location is recognizable on the T10 base map (Appendix A) as a 500 m deepening towards the north-west. Unit K10-K120 is thin towards the east and over the Horda Platform and the Tampen Spur area.

Unit T10 has only been mapped in the eastern part of the study area (Figure 40 b). The unit is probably present within the rest of the area of study as a very thin unit. The thickness is greatest near the Norwegian coast where it locally as much as 190 m thick. The unit thins closer to zero towards the west and south. Unit T10 has a lobe that extends in an SW direction with sediments filling a topographic low.

Unit T20-T50 is very thick in the east, near the Norwegian coast (Figure 40 c). It is the thickest in the south-east where a vertical thickness of 850 m of sediments are preserved. Another peak of 690 m is located just north of it. Unit T20-T50 displays an even thickness distribution west of 3°30’E with thicknesses varying from 100 to 230 m.

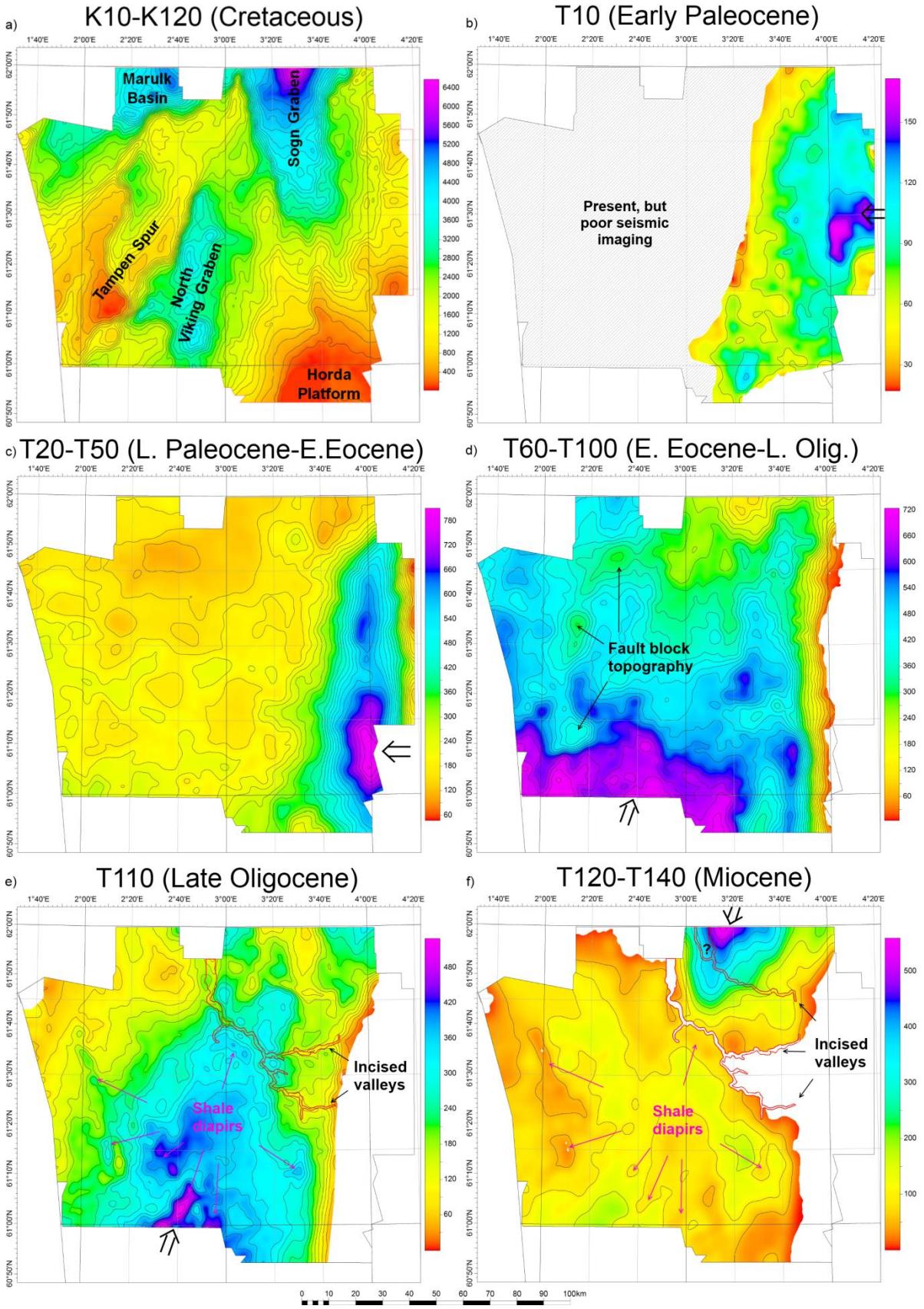

Figure 40. 6 thickness maps (m). Arrows symbolise the main sediment input 40 a) Unit K10-K120. 40 b) Unit T10. 40 c) Unit T20-T50. 40 d) Unit T60-T100. 40 e) Unit T110. 40 f) Units T120-130 and T140 combined.

Unit T60-T100 thickness varies within the study area (Figure 40 d). The unit is much thicker in the SW than towards the north-east. In the south-west the unit is up to 750 m thick while in the north it thins down to locally only 100 m. Several peaks of both thickening and thinning are observed. The thinning features in the western half of the area studied are located above elevated fault block topography.

Unit T110 is thickest in the southern half of the area (Figure 40 e). The unit thins towards the west, north and east. The unit is eroded close to the Norwegian coast. T110 is also very thin in the north-western corner. Local peaks are visible on the thickness map. Most of the local thinning peaks in the north-east corner are caused by incisions into the Top T110 horizon. Most of the local thickening is related to mud diapirs.

Unit T110 is thickest in the southern half of the area (Figure 40 e). The unit thins towards the west, north and east. The unit is eroded close to the Norwegian coast. T110 is also very thin in the north-western corner. Local peaks are visible on the thickness map. Most of the local thinning peaks in the north-east corner are caused by incisions into the Top T110 horizon. Most of the local thickening is related to mud diapirs.

Unit T120-T130 is limited to the north-east corner of the studied area. The unit thins out to zero thickness towards the west, east and south. In the north of the north-east corner the unit is the thickest with a local maximum of 340 metres. **Unit T140** is less than 200 metres thick in most of the studied area. Only in the northern part it has a thick local maximum of 330 metres. Variability in the units' thickness is affected by the underlying incisions and mud diapirs. The unit thins out towards the east and the north-west. A combined thickness map of unit T120-T130 and T140 is seen from Figure 40 f). T120-T130 and T140 represent the preserved Miocene sedimentary record.

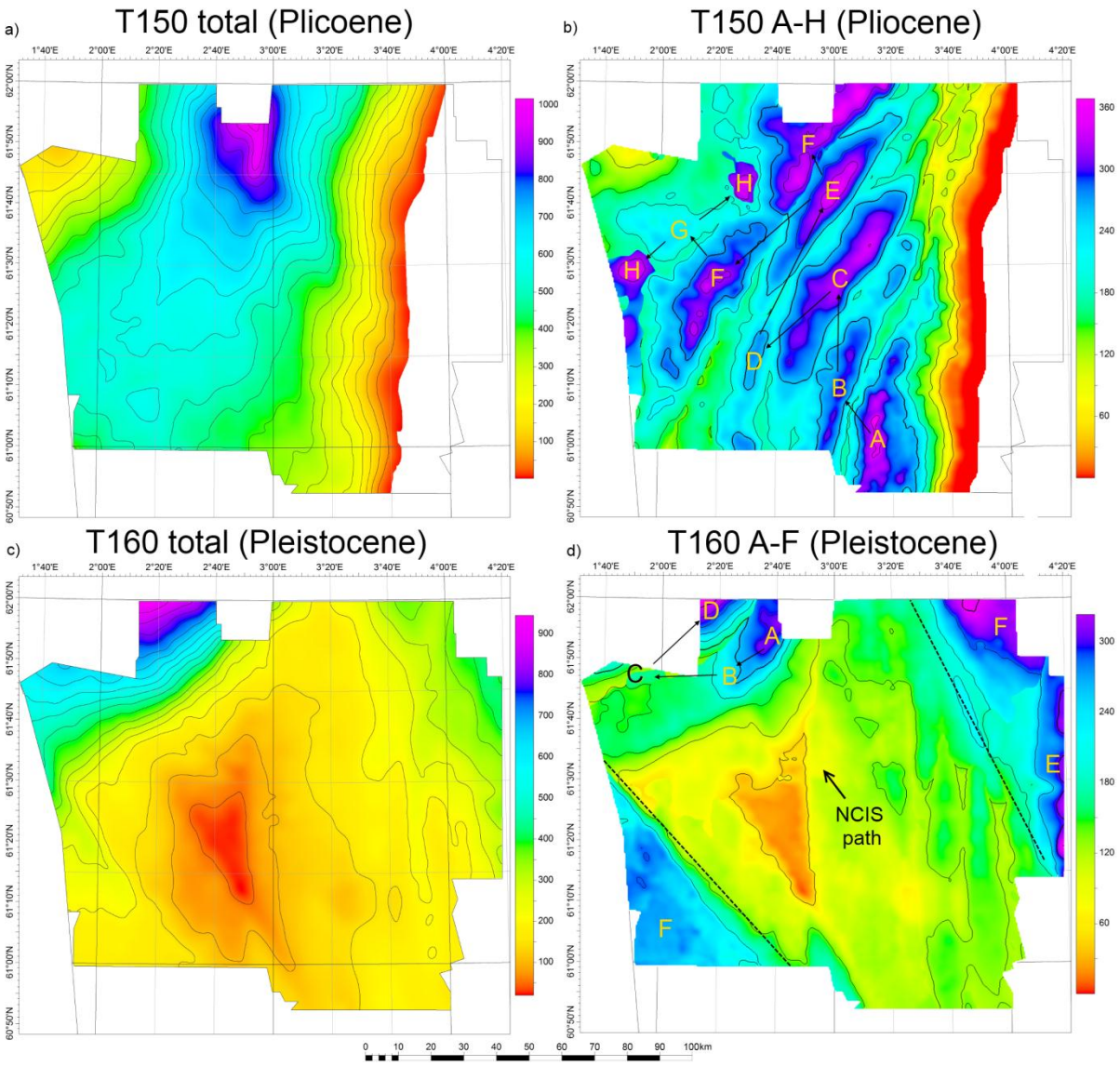

Figure 41. 4 thickness maps (m). 41 a) Displays the combined T150 units, the complete Pliocene deposits. 41 b) Displays the thickness maps of all T150 A-H units in one window. The clinoform depocentre movement progrades as local maxima from the south-east corner of the area of study north- and westwards (arrows). All units have one depocentre. T150 F and H display two depocentres each. 41 c) Displays the combined T160 units, the complete Pleistocene deposits. 41 d) Displays the thickness maps of all T160 A-F units in one window. The depocentres seen as local maxima in the north-western corner of the area of study are deposited before the local maxima in the east and south-west. The depocentres of T160 B and C are very thin. The subsequent erosive path of the NCIS is recognizable in the area between the dashed lines.

Units	Maximum thickness (m)	Average thickness (m)	Volume (km3)
T150 (total)	1126,4	359,6	5275
A	369,0	100,0	532
B	334,8	116,4	536
C	391,4	130,4	780
D	330,0	119,7	664
E	399,3	143,2	785
F	359,6	155,5	862
G	441,8	137,0	522
H	237,8	102,8	594

Table 7. The maximum and average thicknesses of the T150 units. To the right the sediment volumes of each unit.

Unit T150 A-H units are clinoforms. T150 A-E all have lower terminations against the T140 unit while T150 F-H have terminations that extend outside the area of study. The clinoforms are elongated in the north-north-east direction and are prograding towards the west-north-west. The clinoforms deposited first are oriented north-south and prograde westwards, while subsequent clinoforms are oriented more to the north-east and prograde in a north-westward direction (Figure 41 b). All the T150 units combined have an average thickness of 360 m and a maximum vertical thickness of 1126 m (Figure 41 a). T150 A and B are the first interpreted clinoforms and show the greatest thickness in the southern half of the area. Both units are much thinner towards the north. T150 C has a maximum thickness centred in the middle of the area studied and it is also very thin northwards. T150 D clinoform has an even distribution of about 200 metres along its extension. It is however the thickest in the south. T150 E is the first clinoform to have its thickest section in the northern half of the study area. T150 F has two thickness maxima. One is located in the southern half and the thickest in the northernmost part. T150 G and H are much thinner than previous clinoforms. T150 G has one local maximum whereas T150 H has two local maxima. The progradational pattern of depocentres is not linear and depocentres tend to move north- and southward (Figure 41 b).

Units	Maximum thickness (m)	Average thickness (m)	Volume (km3)
T160 (total)	966,3	218,5	3204
A	341,7	103,9	529
B	175,3	63,0	184
C	187,8	65,7	159
D	537,0	115,2	246
E	325,7	92,0	766
F	333,9	90,4	1320

Table 8. The maximum and average thicknesses of the T160 units. To the right the sediment volumes of each unit.

Unit T160 constitutes of four clinoform units (A-D) and two units deposited above the clinoforms (E-F). The four clinoform units are located in the north-west of the area studied and are seen as local thickness maxima in Figure 41 d). All the T160 units combined have an average thickness of 218 m and a maximum vertical thickness of 966 m (Figure 41 a). T160 A displays a local maximum in the north of the study area. T160 is a thin package that displays a very local thickness maximum at the NW edge of the study area. T160 C is a very thin unit of only about 40 m until it abruptly thickens towards the north-west. T160 D is wedge shaped with a gradually increasing thickness from 0 in the south-east to 520 metres in the north. T160 E is only present in the eastern half of the study area. It covers Quadrants 35 and 36 but only barely enters Quadrant 34. It is thickest along the Norwegian coast. T160 F is interpreted to cover the whole of the studied area. It is however very thin at some locations within Quadrant 34 where the path of the NCIS is recognisable (Figure 41 d).

5. Discussion

5.1 Sedimentary processes

The observed depositional processes for the Neogene comprise background sedimentation, delta deposition, shelf and slope processes with submarine fan deposition. The underlying Palaeogene has been affected by post depositional deformation of polygonal faulting and shale diapirism.

5.1.1 Depositional processes

Background sedimentation

Prior to the deposition of the Utsira Formation the Miocene epoch was dominated by slow accumulation of silt and clay (Gregersen et al., 1997). After the deposition of the Utsira Formation a 'Shale Drape unit' covered the Miocene sands (Gregersen & Johannessen, 2007). Shale drapes are deposited from pelagic sedimentation generated in the open sea. The deposits consist of more than 75 % biogenic material. The area of study is located on a continental margin, where the clastic supply is higher than in the open sea. The deposition was most likely hemipelagic, which means that there is a higher fraction of terrigenous clay and silt. Hemipelagic sedimentation is a slow and steady fallout process where the debris is generated at shallow water depths and settles at the bottom by gravitational force. It is an ongoing process and may be the dominant depositional process at highstand conditions. Hemipelagic sedimentation is also referred to as background sedimentation (Stow et al., 1996). In the northern North Sea hemipelagic sedimentation is likely to have dominated at the highstand conditions following the deposition of the Utsira Formation, and prior to the progradation of the Pliocene clinoforms.

Miocene delta deposition

A channel system has been interpreted in the south-eastern part of the area of study (Figure 29). The channels are located 70-100 ms (TWT) above the base of the Late Miocene T140 unit. The T140 unit comprise the sandy Utsira Formation (Isaksen & Tonstad, 1989) along with subunits that have been defined by various authors. These subunits include the silty 'Lower Miocene unit' (Eidvin & Rundberg, 2001), the 'Utsira Sand East unit' (Gregersen & Johannessen, 2007), the 'Glauconitic Sand unit', the

‘Basal Upper Pliocene unit’ of ice-rafted pebbles (Eidvin & Rundberg, 2001), and the ‘Shale Drape unit’ (Gregersen & Johannessen, 2007). Detailed interpretation and identification of all these units have not been performed, due their thinness and a lack of detailed well control. The sands of the Utsira Formation have been suggested as dominantly supplied from both from the eastern- (Rundberg, 1989; Gregersen et al., 1997) and the western margin (Galloway, 2002). Gregersen & Johannessen (2007) pointed out that the preserved evidence of westward progradation were sparse. The thickness of the ‘Utsira Sand East unit’ and some north-westward running incisions (Gregersen, 1998) pointed towards and eastern source. The channel system is located along the eastern basin margin within the ‘Utsira Sand East unit’. The channels are interpreted as the basinward portion of a delta where the upper fluvial segment has been completely removed by Pleistocene erosion. The channels are located on a gently dipping slope, and display low sinuosity. From the morphology the delta is classified as river dominated with sediment dispersal at the delta front. Shallow distributary channels are related to sand deposition, while clay, silt and finer sand may have been deposited between the channels (Reading & Collinson, 1996). The ‘Utsira Sand East unit’ has been suggested to be either time equivalent (Gregersen & Johannessen, 2007) or younger (Martinsen et al., 1999) than the main Utsira Formation sand body. The early phase of the Utsira Formation deposition can thus be related to delta environments on the Norwegian basin margin.

Shelf and slope processes

The Pliocene-Pleistocene prograding complex (T150-T160) display large clinoforms that, due to their great heights (200-500 m), are interpreted as progradation shelf deposits (Helland-Hansen & Hampson, 2009). The clinoforms are to a great extent mud prone (e.g. Isaksen & Tonstad, 1989; Gregersen & Johannessen, 2007; Saga 1977, 1985, 1987). Fine-grained sediments are dominantly transported to the shelves in suspension from land (Johnson & Baldwin, 1996). Sediments are transported from land to the shelf by one of three methods; (1) by river mouth bypassing from deltas, especially during flooding; (2) By estuary mouth bypassing during ebb tide, or; (3) by shoreface bypassing, where shoreface sediment are eroded by storm and wave processes (Reading & Collinson, 1996). Astonishing amounts of fine grained sediment can be fed from drainage systems onto shelves (Johnson & Baldwin, 1996) and it is within these deposits the greatest accumulation rates are recorded. For the

Pliocene and Pleistocene the average accumulation rates are 16,01 and 8,34 cm/ka respectively.

Resedimentation processes are the main processes for transporting large volumes of sediments from an originally shallow water setting into deeper water. Remobilised deposits have been interpreted within several of the T150 units (Figure 31). They are deposited by either slumping or debris flow processes. These processes are driven by gravity and transport the sediments in a mixture with water. The process can be triggered by high slope gradients, high sedimentation rates, a seismic shock or storm and wave action. Within fine grained sediments slumping can occur even at low gradients. Slumping involves plastic deformation, and the movement freezes when the applied shear falls below a critical value. Debris flows move with plastic flow of a sediment and water mixture. They are divided into non-cohesive or cohesive. Non-cohesive debris flows sustain their mobility due to intergranular collisions of well sorted sand or gravel. Cohesive debris flows have high mud content and may sustain mobile longer and transport sediments over larger distances. Very turbulent cohesive debris flows may even become turbidity currents (Stow et al., 1996). The high mud content on the shelf makes non-cohesive debris flow less likely than cohesive debris flow. However the slope deposits observed within the T150 units have not been transported far. They are generally observed high up on the slope. Slope deposition by slumping is most likely although some deposits may be the result of short transported debris flows.

Submarine fan deposition

Submarine fans are observed in the northern parts of the area of study. Such fans develop on the sea floor seaward of a major sediment point source. The fan morphology is considered to reflect the lithological composition. Sand-rich submarine fans systems typically display a moderate size and a radial shape. The sands are derived from sand-rich shelves, transported into the basin via canyons. Submarine fans containing both mud and sand typically display a more moderate size and lobate morphology. They receive their sediments from mixed delta, coastlines or shelves that are cut by canyons. Mud-rich submarine fan systems display large, elongated, major deep-sea fans. They are typically fed by far travelling, low density turbidity currents. These currents transport sediments by fluid turbulence and the sediments

are kept in suspension by the upwards components of fluid motion (Stow et al., 1996). Submarine fan development may occur at any time during a sequence cycle. The volumes of clastic sediments delivered to a basin for fan development is however considered higher at periods of relative sea level fall. Thus, submarine fans have often been related to base level falls (Emery & Myers, 1996). Submarine fans are only observed in the northern parts of the area studied (blocks 34/1, 34/2, 34/3). They extend outside the area of study, which makes it difficult to study their morphology. However, they appear to be elongated along a SW-NE trend. Further to the east falling stage and lowstand systems tract Miocene deposits have been interpreted. They are suggested to be sourced from the north-east. The submarine fans may have been formed in relation to these deposits, sourced from the north-east. The strong amplitudes displayed may be an indication of sand content. Sand dominated fan systems are normally fed by canyons (Stow et al., 1996). Two large incised valleys have been interpreted (Figure 30). The southernmost of these extends out of the area of study not far from the submarine fans. The incision is, however, observed to cut into deeper levels than that of the submarine fans deposits. The incised valley may be considered as a potential feeder channel for the submarine fans at an earlier stage, before it cut into greater depths. This was probably a long lived channel. No other canyon or feeder system has been observed. The fans are located at the base of the Pliocene prograding complex. Thus, there is the possibility that the observations are mass flow deposits sourced by the Pliocene progradation. The SW-NE trend matches the orientation of the shelf edge trajectory (Figure 37 a). This possibility was also suggested by Gregersen & Johannessen (2007).

5.1.2 Post depositional processes

Shale diapirism

Shale diapirs have been mapped along the Mid-Miocene unconformity at depths of 600-1200 m (Figure 27). Diapirism is generated by buoyancy forces resulting from a density contrast between low density sediments moving vertically into higher density sediments. Remobilised shales of the Hordaland Group have moved upwards into the Utsira Formation sands. Løseth et al. (2003) described massive diapirs (40-100 km) which are a magnitude larger than those observed in this thesis (largest: 10-40

km). The size difference is likely due to their usage of a 2D seismic grid with only minor 3D data coverage. Løseth et al. (2003) related the generating mechanism to fluid injections and proposed that the fluids were sourced from overpressured Jurassic reservoirs. The injection formed a low-density mixture and a density contrast large enough for diapirism. The varying distribution of mud diapirs were explained by underlying Cretaceous and Palaeocene sand bodies that transported the gas and fluids laterally. The area of diapirs makes up less than 5% of the area where the Hordaland Group is deposited. This explanation would thus imply unlikely large sand bodies within the Cretaceous and Palaeocene in the northern North Sea. Rundberg et al. (1989) related the shale diapirism to differential compaction, but the distribution does not display any relation to the underlying BCU topography. There is however a slight resemblance to the path of the Pleistocene formed NCIS (Figure 42). Jordt (1996) proposed that rapid deposition of Miocene sands caused the deformation. Gregersen et al. (1998) related the diapirism to localised deposition of the Utsira Formation sand bodies. The relationship between shale diapirism and the distribution of the Utsira Formation (Eidvin, 2009) is evident from Figure 42. The interpreted Miocene delta is collocated with some of the mud diapirs. There is a known relationship between diapiric activity and distributary mouth sedimentation in delta environments (Reading & Collinson, 1996). Thus some of these diapirs may have started to form during an early stage of Utsira Formation deposition.

The diapirs in the area of study are commonly observed up to the level of the base of Pliocene deposits (Top T140). The reflectors within the Late Miocene strata (T140) typically onlap the sides of the diapirs. The distribution of the Utsira Formation in the Tampen Spur area was investigated following an oil spill incident in 2008. Oil containing water, produced from the Tordis field, was supposed to be injected and stored in an aquifer in the Utsira Formation sands, but were instead injected into shales (Eidvin & Øverland, 2009). The subsequent stratigraphic investigation of sidewall- and conventional well cores of wells 34/7-12 and 34/7-R-1 H revealed that the Utsira Formation was not present where the injection well for Tordis had been drilled. Upper Pliocene deposits were discovered conformably overlying the Oligocene shales. About 3,6 km to the north, in well 34/7-2, the Utsira Formation was present as a 10 m thick sand unit (Eidvin, 2009). The well locations of 34/7-12 and 34/7-R-1 H both coincide with one of the mapped shale diapirs. Along with the

onlapping reflectors this indicated that the diapirism occurred syn-depositional with the Utsira Formation. None of the shale diapirs have move up into the Pliocene sediments (T150) which gives a strong indication that the diapirism was completed prior to the deposition of major clinoforms.

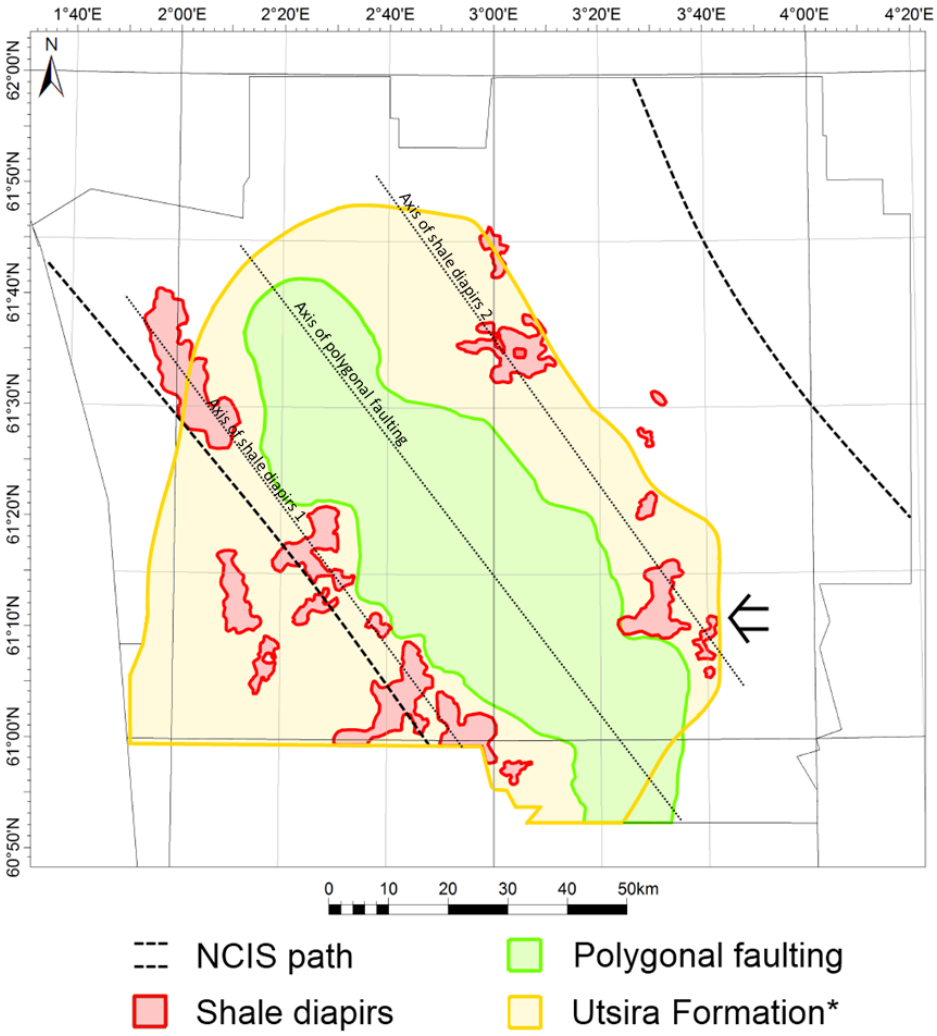

*Figure 42. Map with the observed post depositional processes polygonal faulting and shale diapirism along with the path of the NCIS and distribution of Utsira sands. The arrow marks the sediment input at the location of the interpreted delta. *Distribution based on Eidvin (2009).*

Polygonal faulting

The distribution of a polygonal fault system has been interpreted (Figure 26). These systems consist of intraformational faults that exhibit a polygonal pattern in a map view. Polygonal faults are typically developed in fine-grained sediments. Their generating mechanism is not yet well understood, but the faulting is generally

believed to be related to post depositional processes, independent of external tectonic processes. Polygonal faults are considered as important pathways for fluid flow through low permeability sediments (Van Rensbergen, 2003). Polygonal fault systems have been recognised in over 50 basins worldwide (Cartwright et al., 2003). The generating mechanisms are not fully understood. These issues will not be resolved in this thesis as it requires specialized competence within geomechanics and clay diagenesis. A summary of possible generating mechanisms are presented by Cartwright et al. (2003) as gravity collapse, density inversion, syneresis or compactional loading.

Rundberg (1989) described Cenozoic extensional faulting in the Norwegian sector of the northern North Sea which he regarded as soft sediment deformation and suggested that they were triggered by seismic activity along the Øygarden Fault Zone. The classification of polygonal faults as non-tectonic was established along with the entry of 3D seismic data. In the Eocene-Lower Miocene succession in the southern and central North Sea Cartwright (1994) documented extensive polygonal faulting. Cartwright (1994) noted that the polygonal faulting was concentrated along the basin axis, where the deepest depositional environment had prevailed and clay dominated. Along the basin margins dominated by sediment progradation polygonal faulting was not observed. Clausen et al. (1999) investigated intraformational faults on the Horda Platform for an area between 60° and 61°N. A strongly dominant strike of NW-SE trend was revealed within the Late Oligocene sequence. To reason for the dominant strike trend the effects of downslope gravity sliding and possible regional tectonic stresses were included as contributing generating factors, in addition to an anomalously high fluid pressure. The polygonal faults in the area of study do not display any dominant strike trend. They are not formed on a slope so that gravity sliding is not a likely affecting factor. To determine the timing of the faulting Clausen et al. (1999) modelled the development of fluid pressure. The timing of maximum fluid overpressure was suggested at the Early-Late Miocene boundary with a majority of faulting and pressure release in the Late Miocene. The loading of the Pliocene sediments was suggested to have built up the fluid pressure again, but not to the same magnitude as in Late Miocene. Berndt et al. (2003) interpreted polygonal faulting in the Miocene sediments of the Kai Formation in the Ormen Lange Dome. They declared that polygonal faulting exists in substantial parts of the outer Vøring

and Møre margins. They suggested that the de-watering and development of polygonal faults commenced shortly after burial due to the observation of polygonal faults offsetting the seabed. The distribution of polygonal faulting in the area of study resembles the distribution of the Late Miocene Utsira Formation (Figure 42). Sparse polygonal faulting is visible at the depth of Eocene sediments. The density of polygonal faulting is increase upwards into the Late Oligocene sediments. They have barely offset the Mid-Miocene unconformity (Top T110), but no faulting is evident in overlying sediments. It is suggested that the deposition of the large Pliocene-Pleistocene prograding complex may have contributed to additional deformation, due to the extensive loading. However, polygonal faulting has been observed to commence shortly after deposition (Berndt et al., 2003). The distribution of polygonal faulting suggests that they may have been affected by the deposition of the Utsira Formation.

Pockmarks

By studying vertical pipes they related to fluid expulsion Berndt et al. (2003) discovered that they were going from the level of polygonal faulting and up to terminate at different stratigraphic levels where some terminated at the seabed surface in circular pockmarks. Thus, they suggested that the development of the polygonal fault system may have been active until present. Similar fluid expulsion pipes have not been recognised on the seismic data of this thesis. Pockmarks on the seabed have been mapped (Figure 34 a) and their minimal effect on the seismic is seen from Figure 35 b). The area of highest pockmark density is located above polygonal faults. However, the north-westward extent of polygonal faulting area is not located below areas of high pockmark density. Pockmarks have also been related to other overpressured gas and fluid expulsions (Hovland et al., 2002). Pockmarks are known to occur in abundance above several hydrocarbon fields, e.g. the Troll Field in the North Sea (Hovland, 1981). Within the path of the NCIS pockmarks are likely to have been formed by fluid expulsions from overconsolidated Quaternary deposits within the Norwegian Trench (Nygård et al., 2007). However, more research is needed to establish this link.

Relationship between post-depositional processes

The post depositional processes of polygonal faulting, shale diapirism and pockmark formation appear to have occurred as unrelated events. The pockmarks have probably been formed in the Quarternary and the shale diapirs in the Miocene. The polygonal faulting may have started as early as in the Eocene-Late Oligocene, shortly after deposition. A possible link between the processes could be that fluid expulsions from polygonal faulting have contributed to fluid overpressure in certain areas, which may have triggering the shale diapirism. The axes along the polygonal faulting and shale diapirism display a similar orientation. This may be caused be the north-western orientation of the average maximum horizontal stress regime in the north-western Europe (Zanella & Coward, 2003).

5.2 Tectonostratigraphy

5.2.1 Erosion

Several stratigraphic breaks have been interpreted from seismic stratigraphic principles of reflector terminations. Unconformities are interpreted at the base of the Palaeocene, Oligocene, Miocene, Pliocene and Pleistocene and in the Early Eocene. Truncations are most commonly observed along the basin margin for the base Palaeocene, Oligocene, Miocene and in the Early Eocene. The basinward reflector continuations are commonly correlative conformities. Time-stratigraphic breaks may be the result of erosion or a hiatus. During a hiatus there is non-deposition (Wheeler, 1958). The base of the Palaeocene deposits (Top K120) is reported as an erosional surface in well reports (e.g. Saga, 1985, 1986, 1987, 1988, 1991; Statoil, 1989). However, the Early Eocene (Top T50) and the base Oligocene unconformities are not reported as erosional (Saga, 1986, 1988, 1991). Commonly, in well reports the Early Eocene unconformity is placed at the Palaeocene-Eocene boundary. This is due to earlier dating of the Balder Formation regional marker horizon (Deegan & Scull, 1977; Isaksen & Tonstad, 1989). The formation has been more accurately dated to be of Early Eocene age (e.g. Berggren et al., 1995).

The Mid-Miocene unconformity (Top T110) (e.g. Jordt et al., 1995, 2000; Eidvin, 2000; Rundberg & Eidvin, 2005) is observed to truncate reflectors in the basin as well

as on the basin margins. The surface is reported as erosional (e.g. Saga, 1985, 1986, 1987, 1988, 1991; Gulf, 1982; Statoil, 1989). Martinsen et al. (1999) suggested that the Mid-Miocene unconformity displays a break in sedimentation of 14-15 Ma, where 2-3 Ma are attributed to erosion and the remaining 12 Ma to a hiatus. The unconformity has also been suggested to have lasted longer. Rundberg & Eidvin (2005) suggested a stratigraphic break of 15-20 Ma in the northern North Sea. The break in sedimentation thus extends from the latest Oligocene into the Late Miocene. In the northern North Sea Late Miocene deposits (T140) are directly overlying the Late Oligocene deposits (T110), and where the T140 unit has not been interpreted; the Oligocene deposits are overlain by the Pliocene prograding complex (T150). On the Norwegian Sea margin the Mid-Miocene unconformity has been regarded as a hiatus (Eidvin et al., 2007), with erosion on structural highs (Henriksen & Vorren, 1995). In the southern North Sea Early-Middle Miocene deposits have been interpreted (Jordt et al., 1995). The erosional event has been the most severe in the northern North Sea.

The base Pliocene unconformity (Top T140) is not interpreted to truncate the underlying reflectors, except within the incised valleys. The base Pliocene unconformity is mainly a surface of marine condensation (Martinsen et al., 1999). A contemporaneous hiatus has been interpreted on the Norwegian Sea margin (Eidvin et al., 2007). Many erosional surfaces are interpreted within the Pliocene prograding complex. The upper parts of Pliocene (T150 E-H) and Pleistocene (T160 A-C) units are all truncated. Along a Pleistocene horizon (Intra T160 B) a channel incision has been interpreted (Figure 37 b). The frequency of erosional events in the Pleistocene prograding complex appears to be higher than what is observed for the Pliocene package. Erosional surfaces within the Pliocene package are much harder to identify due to severe Pleistocene truncation of the upper parts. The multiple erosional events on clinoform surface may be related to frequent glacio-eustatic sea level changes.

The base Pleistocene unconformity is an extensive unconformity. It displays a clear angular relationship to the underlying deposits of Pliocene, Miocene, Oligocene, Eocene and Palaeocene age. The oldest Cenozoic deposits are cross cut closest to the Norwegian coast. The Pleistocene unconformity is an extensive erosional surface (e.g. Saga, 1985, 1986, 1987, 1988, 1991; Statoil, 1989). Rundberg (1989) attributed

the unconformity to subaerial exposure ca. 2.2 Ma during uplift along the Møre-Shetland axis. The unconformity was formed during the Pleistocene, a time of global climate cooling (Zachos, 2001). A Scandinavian ice cap grew and multiple ice sheets advances have been recorded onto the shelf (Sejrup et al., 2000). The first expansion onto the shelf has been suggested to have occurred about 1.2 Ma (Sejrup et al., 1995). Subaerial exposure is likely to have happened due to the observed erosional features at the tops of the clinoform. The interpreted unconformity is, however, most likely sculptured by glacial processes due to scouring observed on the base Pleistocene horizon (Top T150).

5.2.2 Submarine channel

Two incised valleys have been interpreted in this thesis (Figure 30). Various parts of the southernmost incised valley have already been described. Rundberg et al. (1995) interpreted the incision as fluvial formed in relation to a Miocene uplift event in the northernmost North Sea. The incision is up to 4 km wide and 200 m deep, making it a magnitude larger than a normal large fluvial stream. Martinsen et al. (1999) also suggested that the incision was formed in relation to the mid-Miocene unconformity. Due to the morphological pattern interpretation on 2D seismic lines they suggest it as a subaerial formed incision. The incision has been mapped from present day depths of 700 m down to 1800 m. Thus, for the entire incision to be subaerially exposed a highly unlikely. Gregersen (1998) interpreted the valley on a 3D seismic cube. He suggested the incision was formed as a proximal channel system continuing of a Western Norwegian river system. The deeper parts of the incision were suggested to be a submarine continuation. A sea-level fall was suggested, but not of the amplitude that would expose the basin floor by Gregersen (1998). Eidvin & Rundberg (2001) interpreted that the incision to cut into both Pliocene and Miocene deposits, and thus made it much younger than had previously been suggested. The Pliocene unit they suggested it cuts (basal Upper Pliocene) has in this thesis been interpreted below the downlap surface of Top T140 and thus included in the T140 unit. Eidvin & Rundberg (2001) suggested much like Gregersen (1998) that the incision formed by subaerial exposure and fluvial drainage along marginal parts of the northern North Sea with a submarine canyon continuation into the Møre Basin. The basin centred base Pliocene surface (Top T140) is not interpreted to truncate underlying reflector, apart from within the valley incisions. This indicates that the basinward continuation of the

incisions was of submarine nature. Incised valleys are typically formed during lowstand of base level. Localized erosion on the floodplains eventually leads to incising (Collinson, 1996). The sequence stratigraphic analysis suggests a base level fall through Early-Middle Miocene, with lowstand conditions during the Late Miocene (Figure 36). The provenance of the Miocene deposits in the north-eastern part of the area studied is suggested to be sourced from the north east. The northernmost incision is only easily recognizable on the seismic along the basin margin and its basinward continuation was possibly disrupted by the prograding sediments from north-east. The southernmost incision is located at the lowstand wedge's toe. Within the incision a parallel reflection pattern indicate that it has been filled by shales during the following highstand conditions. Sand content is also indicated by a chaotic reflection pattern at the channel floor and by the pull-up artefacts below the incision (Figure 13 a).

5.2.3 Sequence stratigraphy

The sequence stratigraphic analysis defined six unconformity bound sequences. Three of the unconformities were erosional events. Mainly deposits of lowstand systems tract have been defined. Highstand systems tracts were interpreted only within the first two sequences and for the fifth sequence. Transgressive systems tracts and highstand tracts are likely to have developed, but have been completely removed by erosion. The succession of Early-Middle Miocene FSST in the north, Late Miocene LST and the Pliocene HST follows a cyclic behaviour and could thus be considered as one sequence. Due to the formation of the large erosional incisions the Base Pliocene unconformity was also considered a sequence boundary. Martinsen et al. (1999) interpreted the incision as formed during the Mid-Miocene unconformity and thus included the Miocene and Pliocene deposits in the same sequence. The Miocene FSST and LST deposit in the north-east may be correlatable to the Norwegian Sea defined Middle Miocene Kai- and Late Miocene Molo Formations (Eidvin et al., 2007). During the Pliocene-Pleistocene highstand conditions the deep basin was completely filled by sediments up to the level were channels develop (Figure 37 b). During the Late Pliocene-Pleistocene sea level fluctuations are indicated from the shelf edge trajectories.

5.2.4 Sea level changes and uplift

Sedimentation deposition is the result from the interaction of sediment supply, its reworking and the accommodation space. Accommodation space is largely controlled by external processes such as variations in sea level and tectonic movements (Reading & Levell, 1996). Global eustatic sea level curves of Haq et al. (1988) and Miller et al. (2005) display frequent variations though the Cenozoic. The long term trend from Early Eocene till present is a generally decreasing global sea level. The accumulation of large Antarctic Ice Sheets and Northern Hemisphere Ice Sheets are attributed for frequent fluctuations (Miller et al., 2005). The identified sequence boundaries do not correspond with the fluctuating eustatic sea-level curves. The magnitude of short term variations rarely exceeds 50 m. Mid-Miocene subaerial exposure of the basin floor has been suggested (e.g. Martinsen et al., 1999). The Mid-Miocene basin floor presently lies at depths below 1200 m. Preceding Oligocene deposits are recorded as shallow as at 700 m depth. In order to explain subaerial exposure by attributing it to sea level fall, a 500 m drop would be required. This is a magnitude 10 times larger than fluctuations implied by eustatic sea level curves. Thus, a tectonic vertical component is frequently imposed.

It is generally agreed that the subsidence that has generation accommodation space for the post-rift succession in the North Sea is attributed to thermal subsidence, following the Late-Jurassic-Early Cretaceous rifting (e.g. Sclater & Christie, 1980; Glennie & Underhill, 1998; Ziegler & Dèzes, 2006). The subsidence has also been amplified by the continuous loading of sediments (Gabrielsen et al., 2001). Anomalous subsidence events that do not follow the expected post-rift thermal subsidence pattern has been suggested (Figure 43 a) (Kyrkjebø et al., 1999). Palaeocene uplift of Scandinavia (e. g. Rundberg, 1989; Martinsen et al., 1999; Kyrkjebø et al., 1999; Jordt et al., 2000) and Palaeocene uplift of the Shetland & British Isles (e. g. Jones & Milton, 1994; Galloway et al., 1993; Faleide et al., 2002) is commonly acknowledged as thermal uplift related to the North Atlantic rifting activity. A series of following Cenozoic regional uplifts events have also been suggested in the North Sea region:

- Eocene basin margin uplift (e. g. Knott et al., 1993; Galloway et al., 1993)
- Eocene uplift of Western Norway (Rundberg, 1989, Faleide et al., 2002).
- Oligocene uplift of Scandinavia (e. g. Rundberg, 1989; Jordt et al., 2000; Kyrkjebø et al., 1999, Faleide et al., 2002).
- Miocene uplift of southern Norway (e. g. Galloway et al., 1993; Jordt et al., 2000; Anell et al., 2009).
- Scandinavian uplift in the Early Pliocene (Rundberg, 1989, Jordt et al., 2000)
- Scandinavian uplift in the latest Pliocene-earliest Pleistocene (e. g. Rundberg, 1989; Kyrkjebø et al., 1999; Faleide et al., 2002; Japsen et al., 2011).

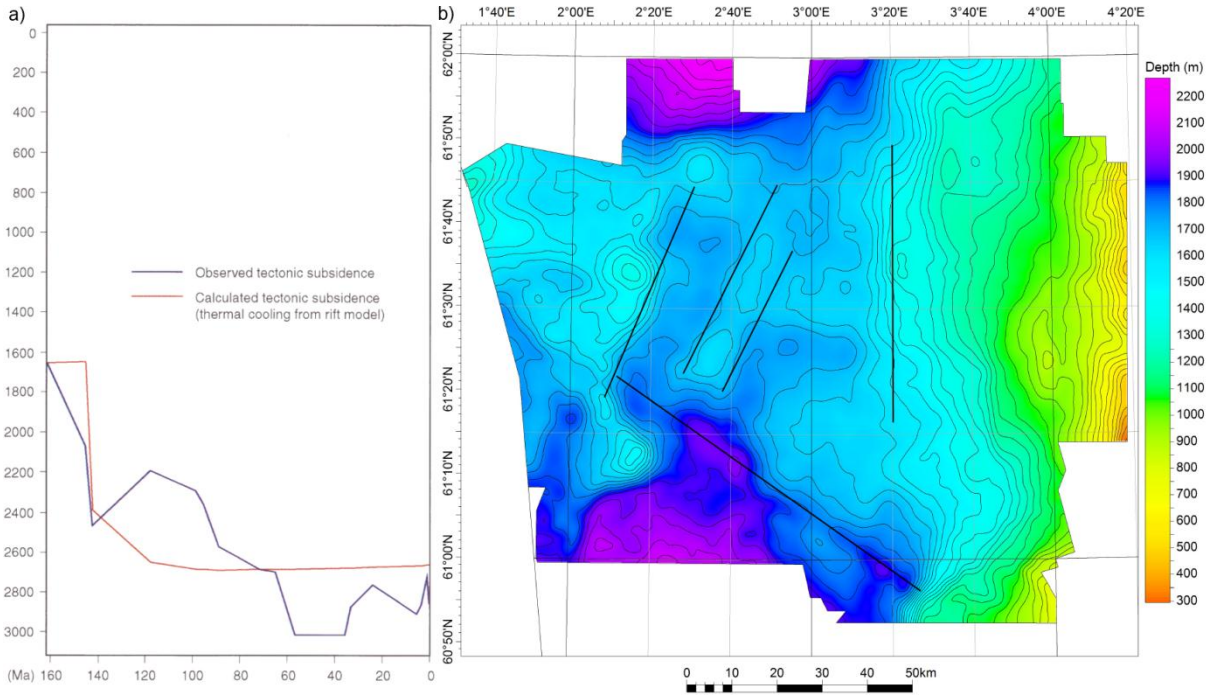

Figure 43 a) Tectonic subsidence curve of the northern North Sea compared with standard rift model (After Faleide et al., 2002). 43 b) Thickness map for the complete Cenozoic deposits in the northern North Sea. It illustrated the amount of post-rift subsidence within the northern North Sea.

It is possible to relate the three stages of erosion to three stages of uplift; in the Early, Mid and Late Cenozoic. Uplift in the Palaeocene and the Pliocene-Pleistocene coincide with an onset of major progradation of sedimentary wedges and increasing accumulation rates. In the Mid-Miocene sedimentary wedges have only been observed in the northernmost North Sea, close to the Møre Basin. Praeg et al. (2005)

suggested that along the north-western Atlantic Margin Early and Late Cenozoic uplift was coeval with offshore subsidence. This large scale tilting was implied to uplift source areas and cause the basinward progradation. From the thickness map of the complete Cenozoic sedimentary record (Figure 43 b) the amount of post-rift subsidence in the northern North Sea is illustrated. The lineaments may indicate active tectonic stresses influencing the Cenozoic deposition. However the lack of distinct faulting shows that there was no active rifting. The average thickness of preserved sediments is about 1500 m. Close to the Norwegian coast the thickness is only about 250 m. Thus the overall subsidence has been much greater in the basin centre than at the margin.

5.3 "Big picture"

5.3.1 Accumulation rate

The accumulation rates were calculated using input values of the volumes of preserved sediments, their area distribution and the age intervals in which the volumes were deposited. The calculation does not account for the unknown amount of eroded material, the palaeobathymetry during the deposition or post-depositional compaction. The effects of compaction were calculated to be about 6% for the Cretaceous clay sequence by input values of thickness and present day depth according to the methods of Waltham (2001). The compaction effects on the Cenozoic sequences are most likely less. The accumulation rates presented are thus minimum values and provide illustrative indications of which time periods account for the largest amount of deposition during the Cenozoic in the northern North Sea. A decrease of sediment input from Palaeocene-early Eocene to late Eocene and gentle increase in Oligocene, decrease in Miocene and a large increase in Pliocene-Pleistocene is in accordance with the accumulation rates for the North Sea calculated by Goledowski et al. (2012). From their calculations a dramatic increase in Pliocene-Pleistocene is recorded in the Danish and Dutch sectors of the North Sea and in the Norwegian Sea. The long term trend of lowering sea levels in the Late Ceonozoic (Miller et al., 2005) has contributed to increasing the source areas. Molnar (2004) suggested that accumulation rates increased on a global on or close to continents the latest 2-4 Ma. Increasing sedimentation suggests increasing rates of erosion and

Molnar (2004) related increasing erosion to climatic change. From Miocene until early Pliocene the global climate was cooling. In the early Pliocene a subtle warming trend has been suggested until 3,2 Ma, when further cooling resulted in the onset of the Northern Hemisphere Glaciation (NHG) (Zachos et al., 2001). The onset of continental glaciation in Scandinavia and the large accumulation rates in the North Sea is likely to be connected.

5.3.2 Pliocene sediment sources

The present North Sea is surrounded by landmass to the west, the south and the east. At the onset of the Pliocene the basin was narrower with more exposed hinterland (Figure 44). From the shelf edge trajectories (Figure 37 a) and the depocentre thickness maps (Figures 41 b and d) a north-westward progradation of the shelf is evident. To transport these astonishing amounts of sediments large fluvial systems must have existed. However, all traces of fluvial system have been removed by erosion. The fluvial system most likely transported sediments from the south or the east. In the southern North Sea Kuhlmann et al. (2004) suggested that the Pliocene and Early Pleistocene sediments of the North Sea were sourced from the same distributary system. The distributary system had at least two contributing source areas. They suggested source areas based on calculations of the source rock ages on and the clay mineralogy. Two source areas were suggested to provide sediments eroded from bedrocks up to 2 Ga and less than 1.5 Ga of age. The oldest sediments were mainly fine-grained with high illite and kaolinite content. They were suggested to be derived from the Scandinavian Shield via the Baltic River. The younger sediments were silt to fine sand with smectite clay minerals. They were suggested to derive from volcanic areas of southern Europe (Kuhlmann et al., 2004). The Baltic River was a drainage system that no longer exists. From the Miocene to the Pleistocene it used to transport sediments to the southern North Sea through the area now known as the Baltic Sea. Other drainage systems in the Northwest European that still exists includes the Elbe, Weser, Rhine, Meuse, Scheldt, Thames, Somme and Seine rivers (Gibbard, 1988). Sediments in the southern North Sea were mainly fed through the westward prograding Eridanos delta. Overeem et al. (2001) interpreted the Neogene development of the delta. The delta was not interpreted north of 58°N. During the Early Pliocene the delta prograded westward, in the Late Pliocene it shifted southward until it directed sediments towards the north-west in the Pleistocene

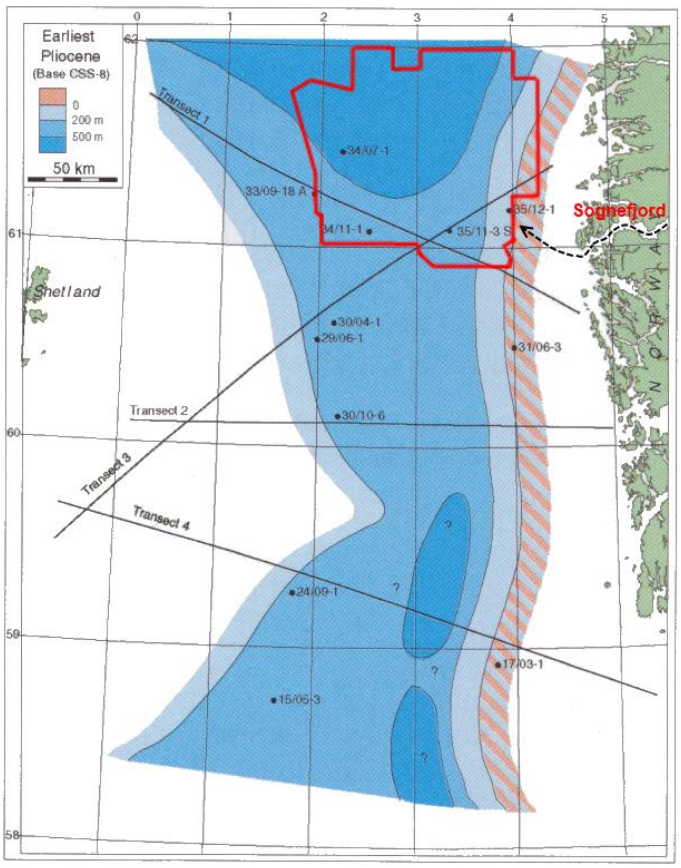

Figure 44. Palaeo-water depth map for the Early Pliocene (Faleide et al., 2002). The area of interest is marked in red. The dashed arrow illustrates the possible sediment supply from the Sognefjord.

(Overeem et al., 2001). The Pliocene sediments in the southern and northern North Sea are likely to have been supplied from separate provenance areas. On the mid-Norwegian continental shelf Late Pliocene-Pleistocene sedimentary succession of the Naust Formation has prograded basinward up to 150 km. This succession has been sourced from the adjacent Norwegian mainland. The Naust Formation has been interpreted to be glacially derived. Ottesen et al. (2009) argued that the high accumulation rate supported glacial environments. Similar conditions are likely to have prevailed at the basin margin of the northern North Sea as well. The nearby Sognefjord is a possible source of sediments. It has been formed by a combination of subaerial and subglacial processes. The fjord started forming along zones of structural weakness as V-shaped valleys by rivers incising the peneplain following the Palaeocene uplift. The fjords were formed mainly due to subaerial processes above sea level. With the onset of glaciation the fjords were further eroded and deepened below the sea level (Nesje & Whillans, 1994). Calculations from Nesje (2012) estimated that rock volumes of about 5400 km^3 have been removed from the Sognefjord drainage area following the onset of inland glaciations. These volumes are likely to have been transported by an ancient fluvial system and deposited along the eastern basin margin. In the area of study the Pliocene deposits make up 5276 km^3. This is a comparable digit to that of removed volumes from the Sognefjord drainage area. The Pliocene sediments were most likely sourced from the east and prograded towards the north-west due to this being the direction of deepening in the palaeo-North Sea Basin (Figure 44).

6. Conclusion

In the area of study over 22 000 km^3 of sediments were supplied into the post-rift subsiding North Sea Basin during the Cenozoic. The sediments were supplied by progradation from the basin margins during periods of uplift and lowstand. Six unconformities have been interpreted at the base of the Palaeocene, Oligocene, Miocene, Pliocene and Pleistocene, and in the Early Eocene. Three regional erosional phases are related to uplift in the Palaeocene, Miocene and Pleistocene. The supply from the eastern basin margin created the largest sedimentary wedges with the greatest accumulation rates in the Palaeocene-Early Eocene, Pliocene and Pleistocene. During the remainder of the Palaeogene the sediments were mainly supplied from the south-west. During the Miocene a sedimentary wedge prograded into the North Sea Basin supplied from the north-east. In the rest of the basin the sand bodies of the Utsira Formation were deposited. Along the eastern basin margin delta deposition supplied the sediments. Two large incised valleys formed from the Western Norway into the Møre Basin prior to the onset of Pliocene progradation. During the north-westward progradation of Pliocene-Pleistocene clinoforms the deposition was dominated by shelf and slope processes. Submarine fans were deposited in the northernmost area. In the Pleistocene sediments of Palaeocene-Pleistocene age were truncated by glacial erosion.

The Palaeogene stratigraphy has been deformed by polygonal faulting and shale diapirism. The shale diapirs formed in the same time interval as the deposition of the Utsira Formation. The polygonal faulting is thought to have occurred prior to the diapirism. Both post-depositional processes are formed along a NW-SE trending axes.

This established methodologies of seismic stratigraphy, sequence stratigraphy and shelf edge trajectories have been better constrained with the application of 3D seismic data. Mapping and visualisation in 3D improves the evaluation of time and space relationships of geological events.

Bibliography

Ahmadi, Z. M., Sawyers, M., Kenyon-Roberts, S., Stanworth, C. W., Kugler, K. A., Kristensen, J., & Fugelli, E. M. G. (2003). Paleocene. In D. Evans, C. Graham, A. Armour & P. Bathurst (Eds.), *The Millennium Atlas: Petroleum geology of the central and northern North Sea.* (p. 235-260). London: The Geological Society of London.

Anell, I., Thybo, H., & Artemieva, I. M. (2009). Cenozoic uplift and subsidence in the North Atlantic region: Geological evidence revisited. *Tectonophysics, 474*(1–2), 78-105.

Anell, I., Thybo, H., & Rasmussen, E. (2012). A synthesis of Cenozoic sedimentation in the North Sea. *Basin Research*, *24*(2), 154-179.

Barnes, A. E. (2007). Redundant and useless seismic attributes. *Geophysics, 72*(3), 33-38.

Berggren, W. A., Kent, D. V., Swisher, C. C., Aubry, M. P. (1995). A revised Cenozoic geochronology and chronostratigraphy. In W. A. Berggren, D. V. Kent, M. P. Aubry, & J. Hardenbo (Eds.), *Geochronology, Time Scales, and Global Stratigraphic Correlation* (Special Publication 54, p. 129-212). Tulsa: Society for Sedimentary Geology.

Berndt, C., Bünz, S., & Mienert, J. (2003). Polygonal fault systems on the mid-Norwegian margin: a long term source for fluid flow. In P. Van Rensbergen, R. R. Hillis, A. J. Maltman & C. K. Morley (Eds.), *Subsurface Sediment Mobilization* (Special Publications 216, p. 283-290). London: The Geological Society of London.

Bowman, M. B. J. (1998). Cenozoic. In K. W. Glennie (Ed.), *Petroleum Geology of the North Sea – Basic concepts and recent advances* (Fourth edition, p. 350-375). Oxford: Blackwell Science.

Brekke, H., & Olaussen, S. (2007). Høyt hav og lave horisonter – Jordas kritt-tid; 146-66 Ma. In I. B. Ramberg, I. Bryhni, A. Nøttvedt (Eds.) *Landet blir til – Norges geologi* (Second Edition, p. 416-439). Trondheim: Norsk Geologisk Forening.

Brekke, H., Sjulstad, H. I., Magnus, C., & Williams, R. W. (2001). Sedimentary environments offshore Norway — an overview. In O.J. Martinsen & T. Dreyer (Eds.), *Norwegian Petroleum Society Special Publications* (Vol. 10, p. 7-37). Elsevier.

Bullimore, S., Henriksen, S., Liestøl, F. M., & Helland-Hansen, W. (2006). Clinoform stacking patterns, shelf edge trajectories and facies associations in Tertiary coastal deltas, offshore Norway: Implications for the prediction of lithology in prograding systems. *Norwegian Journal of Geology, 85*, 169-187.

Carmot (2010). The seismic merge and velocity process.

Carmot (2012). General information about our products. Obtained 21.09.12, from http://www.carmotseismic.no/products.html

Cartwright, J. A. (1994). Episodic basin-wide hydrofracturing of overpressured Early Cenozoic mudrock sequences in the North Sea Basin. *Marine and Petroleum Geology, 11*(5), 587-607.

Cartwright, J., James, D., & Bolton, A. (2003). The genesis of polygonal fault systems: a review. In P. Van Rensbergen, R. R. Hillis, A. J. Maltman & C. K. Morley (Eds.), *Subsurface Sediment Mobilization* (Special Publications 216, p. 223-244). London: The Geological Society of London**.**

Catuneanu, O., Abreu, V., Bhattacharya, J. P., Blum, M. D., Dalrymple R. W., Eriksson P. G., . . . Winker, C. (2009). Towards the standardization of sequence stratigraphy. *Earth-Science Reviews, 92*(1–2), 1-33.

Catuneanu, O., Galloway, W. E., Kendall C. G. St. C., Miall, A. D., Posamentier, H. W., Strasser, A., Tucker, M. E. (2011). Sequence stratigraphy: Methodology and Nomenclature. *Newsletter on stratigraphy 44*(3), 173-245.

Chopra, S., & Larsen, G. (2000) Acquisition footprint – Its detection and removal. *CSEG Recorder, 25*(8), 16-20.

Clausen, J. A., Gabrielsen, R. H., Reksnes, P. A., & Nysæther, E. (1999). Development of intraformational (Oligocene-Miocene) faults in the northern North Sea: influence of remote stress and doming of Fennoscandia. *Journal of Structural Geology, 21,* 1457-1475.

Collinson, J. D. (1996). Alluvial sediments. In H. G. Reading (Ed.), *Sedimentary Environments: Processes, Facies and Stratigraphy* (Third Edition, p. 37-82). Oxford: Blackwell Publishing.

Coward, M. P., Dewey, J., Hempton, M., & Holroyd, J. (2003). Tectonic evolution. In D. Evans, C. Graham, A. Armour & P. Bathurst (Eds.), *The Millennium Atlas: Petroleum geology of the central and northern North Sea.* (p. 17-33) London: The Geological Society of London.

Daber, R., Ditcha, E. M., Gustafsson, L. E., Knudsen, E., Pepper, R., Bejarano, G. (2008). Seismic-to-Simulation Software – Interpreter's Guide to Seismic Attributes. Houston: Schlumberger Information Solutions.

Dalland, A., Worsley, D., & Ofstad K. (1988). A lithostratigraphic scheme for the Mesozoic and Cenozoic succession offshore mid- and northern Norway. NPD-bulletin No 4. Oljedirektoratet.

Deegan, C. E. & Scull, B. J. (1977). A standard lithostratigraphic nomenclature for the central and northern North Sea. NPD-bulletin No 1. Oljedirektoratet.

Dmitrieva E., Jackson, C. A. L., Huuse, M. & McCarthy, A. (2012). Paleocene deep-water depositional systems in the North Sea Basin: a 3D seismic and well data case study, offshore Norway. *Petroleum Geoscience, 18*(1), 97-114.

Eidvin, T., & Rundberg, Y. (2001). Late Cainozoic stratigraphy of the Tampen area (Snorre and Visund fields) in the northern North Sea, with emphasis on the chronology of early Neogene sands. *Norwegian Journal of Geology, 81*, 119-160.

Eidvin, T., Bugge, T., & Smelror, M. (2007). The Molo Formation, deposited by coastal progradation on the inner Mid-Norwegian continental shelf, coeval with the Kai Formation to the west and the Utsira Formation in the North Sea. *Norwegian Journal of Geology, 87*, 75-142.

Eidvin, T. (2009). A biostratigraphic, strontium isotopic and lithostratigraphic study of the upper part of Hordaland Group and lower part of Nordland Group in well 34/7-2, 34/7-12 and 34/7-R-1 H from the Tordis Field in the Tampen area (northern North Sea). Scientific report. Norwegian Petroleum Directorate.

Eidvin, T., & Øverland, J. A. (2009). Tolket Tordis feil. *Norsk Sokkel, 2*, 35-36.

Emery, D., & Myers, K. J. (1996). *Sequence Stratigraphy*. Oxford: Blackwell Science.

Etris, E. L., Crabtree, N. J., Dewar J. (2001). True depth conversion: more than a pretty picture. *CSEG Recorder 26*(9), 11-22.

Faleide, J. I., Kyrkjebø, R., Kjennerud, T., Gabrielsen, R. H., Jordt, H., Fanavoll, S., & Bjerke, M. D. (2002). Tectonic impact on sedimentary processes during Cenozoic evolution of the northern North Sea and surrounding areas. In A. G. Doré, J. A. Cartwright, M. S. Stoker, J. P. Turner, & N. White (Eds.), *Exhumation of the North Atlantic Margin: Timing, Mechanisms and Implications for Petroleum Exploration* (Special Publication 196, p. 235-269). London: The Geological Society of London**.**

Fraser, S. I., Robinson, A. M., Johnson, H. D., Underhill, J. R., Kadolsky, D. G. A., Connell, R., Johannesen, P., & Ravnås, R. (2003). Upper Jurassic. In D. Evans, C. Graham, A. Armour & P. Bathurst (Eds.), *The Millennium Atlas: Petroleum geology of the central and northern North Sea.* (p. 157-189) London: The Geological Society of London.

Fyfe, J. A., Gregersen, U., Jordt, H., Rundberg, Y., Eidvin, T., Evans D., . . . Andersen, P. (2003). Oligocene to Holocene. In D. Evans, C. Graham, A. Armour & P. Bathurst (Eds.), *The Millennium Atlas: Petroleum geology of the central and northern North Sea.* (p. 279-287) London: The Geological Society of London.

Gabrielsen, R., Kyrkjebø, R., Faleide, J., Fjeldskaar, W., & Kjennerud, T. (2001). The Cretaceous post-rift basin configuration of the northern North Sea. *Petroleum Geoscience,* 7(2) 137-154.

Galloway, W. E., Garber, J. L., Xijin L., & Sloan, B. J. (1993). Sequence stratigraphic and depositional framework of the Cenozoic fill, Central and Northern North Sea Basin. *Petroleum Geology Conference series, 4*, 33-43.

Galloway, W. E. (2002). Paleogeographic setting and depositional architecture of a sand-dominated shelf depositional system, Miocene Utsira Formation, North Sea Basin. *Journal of Sedimentary Research, 72*(4), 476-490.

Gibbard, P. L., Rose, J., & Bridgland, D. R. (1988). The History of the Great Northwest European Rivers during the Past Three Million Years. *Philosophical Transactions of the Royal Society B, 318*, 559-602.

Glennie, K. W., & Underhill, J. R. (1998). Origin, Development and Evolution of Structural Styles. In K. W. Glennie (Ed.), *Petroleum Geology of the North Sea – Basic concepts and recent advances* (Fourth edition, p. 42-84). Oxford: Blackwell Science.

Glennie, K. W., Higham, J., & Stemmerik, L. (2003). Permian. In D. Evans, C. Graham, A. Armour & P. Bathurst (Eds.), *The Millennium Atlas: Petroleum geology of the central and northern North Sea.* (p. 91-103) London: The Geological Society of London.

Goledowski, B., Nielsen, S. B., & Clausen, O. R. (2012). Patterns of Cenozoic sediment flux from western Scandinavia. *Basin Research, 24*, 377–400.

Gradstein, F.M., Ogg, J.G., & Smith, A.G. (2004). A Geologic Time Scale. (p. 589) Cambridge: Cambridge University Press.

Gradstein, F. M., Anthonissen, E., Brunstad, H., Charnock, M., Hammer, Ø., Hellem, T., & Lervik K. S. (2010). Norwegian Offshore Stratigraphic Lexicon (NORLEX). *Newsletter on Stratigraphy, 44*(1), 73-86.

Gregersen, U. (1998). Upper Cenozoic channels and fans on 3D seismic data in the northern North Sea. *Petroleum Geoscience, 4*(1), 67-80.

Gregersen, U., & Johannessen, P. N. (2007). Distribution of the Neogene Utsira Sand and the succeeding deposits in the Viking Graben area, North Sea. *Marine and Petroleum Geology, 24*(10), 591-606.

Gregersen, U., Michelsen, O., & Sørensen, J. C. (1997). Stratigraphy and facies distribution of the Utsira Formation and the Pliocene sequences in the northern North Sea. *Marine and Petroleum Geology, 14*(7–8), 893–914.

Gulf (1982). 35/8-2 well completion report.

Hansen, J., Jerram, D. A., McCaffrey, K., & Passey, S. R. (2009). The onset of the North Atlantic Igneous Province in a rifting perspective. *Geological Magazine, 146,* 309-325.

Haq, B., Hardenbol, J., & Vail, P. B. (1987). Chronology of Fluctuating Sea Levels Since the Triassic. *Science, 235*, 1156-1167.

Helland-Hansen, W., & Hampson, G. J. (2009) Trajectory analysis: concepts and applications. *Basin Research 21*, 454-483.

Hovland, M. (1981). Characteristics of pockmarks in the Norwegian Trench. *Marine and Petroleum Geology, 39*, 103-117.

Hovland, M., Gardner, J. V., & Judd, A. G. (2002). The significance of pockmarks to understanding fluid flow processes and geohazards. *Geofluids, 2*, 127-136.

Hronusov, V. (2006). Global Paleogeographic Views. Obtained 05.06.2012, from http://www.google.com/gadgets/directory?synd=earth&hl=no&preview=on&cat=ocean&url=http://www.google.com/mapfiles/mapplets/earthgallery/Global_Paleogeographic_Views.xml

Husmo, T., Hamar, G. P., Høiland, O., Johannessen, E. P., Rømuld, A., Spencer, A. M., & Titterton, R. (2003). Lower and Middle Jurassic. In D. Evans, C. Graham, A. Armour & P. Bathurst (Eds.), *The Millennium Atlas: Petroleum geology of the*

central and northern North Sea. (p. 129-155) London: The Geological Society of London.

Hydro (2006). Final Well Report 35/2-1, Peon.

Ichron (2010). North Viking Graben and Tampen Spur Stratigraphic Database.

ICS (2010). International Stratigraphic Chart. Obtained 05.03.2012, from http://www.stratigraphy.org/ics%20chart/StratChart2010.pdf

Isaksen, D., & Tonstad, K. (1989). A revised Cretaceous and Tertiary lithostratigraphic nomenclature for the Norwegian North Sea. NPD-bulletin No 5. Oljedirektoratet.

Japsen, P., Chalmers, J. A., Green, P. F., & Bonow, J. M. (2011). Elevated, passive continental margins: Not rift shoulders, but expressions of episodic, post-rift burial and exhumation. *Global and Planetary Change, 90-91,* 73-86.

Johansen T. (2012). Seismikkbåtene var først - Oljealderen begynte i 1963. *Petromagasinet, 6.*

Johnson, H. D., & Baldwin, C. T. (1996). Shallow clastic seas. In H. G. Reading (Ed.), *Sedimentary Environments: Processes, Facies and Stratigraphy* (Third Edition, p. 232-280). Oxford: Blackwell Publishing.

Jolley, D. W., Keane, P. J., Merker, A. M., Minnis, J., Rusca, V., Titterton, R., Underwoord, J. (1987). Saga 34/7-8 Norwegian North Sea well: Biostratigraphy of the interval 450m-2766TD. Robertson Research International Limited.

Jones, R. W., & Milton, N. J. (1994). Sequence development during uplift: Palaeogene stratigraphy and relative sea-level history of the Outer Moray Firth, UK North Sea. *Marine and Petroleum Geology, 11*(2), 157-165.

Jones, E., Jones, R., Ebdon, C., Ewen, D., Milner, P., Plunkett, J., . . . Slater, P. (2003). Eocene. In D. Evans, C. Graham, A. Armour & P. Bathurst (Eds.), *The Millennium Atlas: Petroleum geology of the central and northern North Sea.* (p. 261-277) London: The Geological Society of London.

Jordt, H., Faleide, J. I., Bjørlykke, K., & Ibrahim, M. T. (1995). Cenozoic sequence stratigraphy of the central and northern North Sea Basin: tectonic development, sediment distribution and provenance areas. *Marine and Petroleum Geology, 12*(8), 845-879.

Jordt, H. (1996). The Cenozoic geological evolution of the Central and Northern North Sea based on seismic sequence stratigraphy. PhD thesis, University of Oslo.

Jordt, H., Thyberg, B. I., Nøttvedt, A. (2000). Cenozoic evolution of the central and northern North Sea with focus on differential vertical movements of the basin floor and surrounding clastic source areas. In A. Nøttvedt (Ed.) *Dynamics of the Norwegian Margin* (Special Publications 167, p. 219-243). London: The Geological Society of London**.**

Keary, P., & Brooks, M. (1991). *An Introduction to Geophysical Exploration* (Second Edition). Oxford: Blackwell Science.

Knott, S. D., Burchell, M. T., Jolley, E. J., & Fraser, A. J. (1993). Mesozoic to Cenozoic plate reconstructions of the North Atlantic and hydrocarbon plays of the Atlantic Margins. In J. R. Parker (Ed.), *Petroleum Geology of Northwest Europe: Proceedings of the 4th Conference*. (p. 953-974) London: The Geological Society of London.

Kristing, T., & Andersen, E. S. (2007). Exploring the Norwegian Channel – The Peon Discovery. AAPG and AAPG European Region Energy Conference and Exhibit 2007, Athens, Greece.

Kuhlmann, G., de Boer, P., Pedersen, R. B., & Wong, T. (2004). Provenance of Pliocene sediments and paleoenvironmental changes in the southern North Sea region using Samarium–Neodymium (Sm/Nd) provenance ages and clay mineralogy. *Sedimentary Geology, 171*, 205–226.

Kyrkjebø, R., Fjeldskaar, W., Faleide, J. I., Gabrielsen, R. H. (1999). The post-rift (Cretaceous-Tertiary) vertical tectonic movements in the northern North Sea as obtained by 2D backstripping. PhD thesis, University of Bergen.

Lambeck, K. (1993). Glacial rebound of the British Isles – II. A high resolution, high-precision model. *Geophysical Journal International, 115*, 960-990.

Landrø, M. (2010) Anvendt geofysikk – Et innføringskurs i de vanligste geofysiske metodene som blir brukt for å kartlegge jordas bergarter.

Løseth, H., Wensaas, L., Arntsen, B., & Hovland, M. (2003). Gas and fluid injection triggering shallow mud mobilization in the Hordaland Group, North Sea. In P. Van Rensbergen, R. R. Hillis, A. J. Maltman & C. K. Morley (Eds.), *Subsurface Sediment Mobilization* (Special Publications 216, p. 139-157). London: The Geological Society of London**.**

Maltman, A. J., & Bolton, A. (2003). How sediments become mobilized. In P. Van Rensbergen, R. R. Hillis, A. J. Maltman & C. K. Morley (Eds.), *Subsurface Sediment Mobilization* (Special Publications 216, p. 9-20). London: The Geological Society of London**.**

Marfurt, K.J., Scheet, R.M., Sharp, J.A., & Harper, M.G., (1998). Suppression of the acquisition footprint for seismic sequence attribute mapping. *Geophysics, 63*(3), 1024-1035.

Marshall, J. E. A., & Hewett, A. J. (2003). Devonian. In D. Evans, C. Graham, A. Armour & P. Bathurst (Eds.), *The Millennium Atlas: Petroleum geology of the central and northern North Sea.* (p. 65-80) London: The Geological Society of London.

Martinsen, O. J., & Dreyer, T. (2001). Sedimentary environments offshore Norway — Palaeozoic to recent: an introduction. In O.J. Martinsen & T. Dreyer (Eds.), *Norwegian Petroleum Society Special Publications* (Vol. 10, p. 1-5). Elsevier.

Martinsen, O. J., Boen, F., Charnock, M. A., Mangerud, G. & Nøttvedt, A. (1999). Cenozoic development of the Norwegian margin 60-64°N: sequences and sedimentary response to variable basin physiography and tectonic setting. In A. J. Fleet, & S. A. R. Boldy (Eds.) *Petroleum Geology of Northwest Europe: Proceedings of the 5th Conference*, 293-304.

Martinsen, O., & Nøttvedt A. (2007). Av hav stiger landet – Paleogene og neogene (kenozoikum), kontinentene av i dag formes; 66-2,7 Ma. In I. B. Ramberg, I. Bryhni, A. Nøttvedt (Eds.) *Landet blir til – Norges geologi* (Second Edition, p. 440-477). Trondheim: Norsk Geologisk Forening.

Miller, K. G., Kominz, M. A., Browning, J. V., Wright, J. D., Mountain, G. S., Katz, M. E., . . . Pekar, S. F. (2005). The Phanerozoic Record of Global Sea-Level Change. *Science, 310*, 1293-1298.

Mitchum, R. M., & Vail, P., R. (1977). Seismic Stratigraphy and Global Changes of Sea Level, Part 7: Seismic Stratigraphic Interpretation Procedure. In: C.E. Payton (Ed.), *Seismic Stratigraphy – Applications to Hydrocarbon Exploration (*AAPG Memoir 26, p. 135–144). Tulsa: American Association of Petroleum Geologists.

Mitchum, R. M., Vail, P. R., & Sangree, J. B. (1977). Seismic Stratigraphy and Global Changes of Sea Level, Part 6: Stratigraphic Interpretation of Seismic Reflection Patterns in Depositional Sequences. In: C.E. Payton (Ed.), *Seismic Stratigraphy – Applications to Hydrocarbon Exploration* (AAPG Memoir 26, p. 117–133). Tulsa: American Association of Petroleum Geologists.

Molnar, P. (2004). Late Cenozoic increase in accumulation rates of terrestrial sediment: How may climate have affected erosion rates? *Annual Review of Earth and Planetary Sciences, 32,* 67-89.

Nesje, A. (2012). Hva er en fjord, og hvordan blir den til. Obtained 27.11.2012, from http://www.fjords.com/sognefjord1.shtml

Nesje, A., & Whillans, I. M. (1994). Erosion of Sognefjord, Norway. *Geomorphology, 9*, 33-45.

NPD (2010). Helhetlig forvaltningsplan for Nordsjøen og Skagerrak – Statusbeskrivelse for petroleumsvirksomheten med hovedvekt på norsk sokkel.

NPD (2012). Regulations to Act relating to petroleum activities. General provisions, Section 85, Procedures and duty of secrecy**.** Obtained 05.03.2012, from http://www.npd.no/en/regulations/regulations/petroleum-activities/

NPD FactPages (2012). Obtained 12.10.2012, from http://factpages.npd.no/factpages/Default.aspx?culture=en

NPD FactMap (2012). Obtained 12.10.2012 , from http://npdmap1.npd.no/website/npdgis/viewer.htm

Nygård, A., Sejrup, H. P., Haflidason, H., Lekens, W. A. H., Clark, C. D., & Bigg, G. R. (2007). Extreme flow and sediment output rates of the Norwegian Channel Ice Stream during the last glaciation. *Geology, 35*(5), 395-398

Ogg, J.G., Ogg, G., & Gradstein, F.M. (2008). The Concise Geologic Time Scale. (p. 177) Cambridge: Cambridge University Press.

Ottesen, D., Rise, L., Andersen, E. S., Bugge, T., & Eidvin, T. (2009). Geological evolution of the Norwegian continental shelf between 61ºN and 68ºN during the last 3 million years. *Norwegian Journal of Geology, 89*, 251-265.

Overeem, I., Weltje, G. J., Bishop-Kay, C., Kroonenberg, S. B. (2001). The Late Cenozoic Eridanos delta system in the Southern North Sea Basin: a climate signal in sediment supply? *Basin Research, 13*(3), 293-312.

Reading, H. G., & Collinson, J. D. (1996). Clastic coasts. In H. G. Reading (Ed.), *Sedimentary Environments: Processes, Facies and Stratigraphy* (Third Edition, p. 154-231). Oxford: Blackwell Publishing.

Reading, H. G., & Levell, B. K. (1996) Controls on the sedimentary rock record. In H. G. Reading (Eds.), *Sedimentary Environments: Processes, Facies and Stratigraphy* (Third Edition, p. 5-36). Oxford: Blackwell Publishing.

Riis, F., & Fjeldskaar W. (1992). On the magnitude of the Late Tertiary and Quaternary erosion and its significance for the uplift of Scandinavia and the Barents Sea. In R. M. Larsen, H. Brekke, B. T. Larsen & E. Talleraas (Eds.), *Norwegian Petroleum Society Special Publications* (Vol. 1, p. 163-185): Elsevier.

Rundberg, Y. (1989). Tertiary sedimentary history and basin evolution of the Norwegian North Sea between 60° – 62°N – An integrated approach. PhD thesis, University of Trondheim.

Rundberg, Y., Olaussen, S., & Gradstein, F. (1995). Incision of Oligocene strata: evidence for northern North Sea uplift and key to the formation of the Utsira sands. *Geonytt, 22*.

Rundberg, Y., & Eidvin, T (2005). Controls on depositional history and architecture of the Oligocene-Miocene succession, northern North Sea Basin. In B. Wandås, J. P. Nystuen, E. A. Eide, & F. M. Gradstein (Eds.), *Norwegian Petroleum Society Special Publications* (Vol. 12, p. 207-239). Elsevier.

Saga (1977). Final Well Report 35/3-1.

Saga (1985). Final Well Report 34/7-1.

Saga (1986). Final Well Report 34/7-8.

Saga (1987). Well 34/4-6 Biostratigraphic Summary Report.

Saga (1988). Final Well Report 34/7-13

Saga (1991). Final Well Report 34/7-15 S

Salvador, A. (1994). *International Stratigraphic Guide - A guide to stratigraphic classification, terminology, and procedure* (Second Edition). Boulder, Colorado: The Geological Society of America.

Sclater, J. G., & Christie, P. A. F. (1980). Continental stretching: An explanation of the post-Mid Cretaceous subsidence of the Central North Sea Basin. *Journal of Geophysical Research, 85*, 3711-3739.

Sejrup, H. P., Aarseth, I., Halfidason, H., Løvlie, R., Braten, Å, Tjøstheim, G, . . . Ellingsen, K. L (1995). Quarternary of the Norwegian Channel; paleoceanography and glaciation history. *Norwegian Journal of Geology, 75*, 65-87.

Sejrup, H. P., King, E. L., Aarseth, I., Haflidason, H., & Elverhøy, A. (1996). Quarternary erosion and depositional processes: western Norwegian fjords, Norwegian Channel and North Sea Fan. In M. De Batist & P. Jacobs (Eds.), *Geology of siliciclastics shelf seas* (Special Publications 117, p. 187-202). London: The Geological Society of London**.**

Sejrup, H. P., Larsen, E., Landvik, J., King, E. L., Haflidason, H., Nesje, A. (2000). Quaternary glaciations in southern Fennoscandia: evidence from southwestern Norway and the northern North Sea region. *Quaternary Science Reviews, 19,* 667-685.

Skogseid, J., Planke, S., Faleide, J. I., Pedersen, T., Eldholm, O., & Neverdal, F. (2000). NE Atlantic continental rifting and volcanic margin formation. In A. Nøttvedt (Ed.) *Dynamics of the Norwegian Margin* (Special Publications 167, p. 295-326). London: The Geological Society of London**.**

Statoil (1989). PL 152 Well 33/12-7 Completion Report.

Statoil (2010). Final Well Report 35/2-2 and 35/2-2 T2 PEON, PL 318 and 269.

Steel, R., & Olsen, T. (2002). Clinoforms, Clinoform Trajectories and Deepwater Sands. In J.M. Armentrout & N.C. Rosen (Eds.), *Sequence Stratigraphic models for exploration and production: Evolving Methodology, Emerging Models and Application Histories* (p. 367-381). Houston: Special Publication GCS - Society of Economic Paleontologists and Mineralogists.

Stenløk, J. (2008). Sammenfallende seismikkområder - unødvendig innsamling eller en nødvendighet? En undersøkelse av seismisk datainnsamling mellom 60° - 62°N. Stavanger: Oljedirektoratet.

Stewart, I. J. (1987) A revised stratigraphic interpretation of the Early Palaeogene of the Central North Sea. In J. Brooks & K. Glennie (Eds.), *Petroleum Geology of North West Europe*. (p. 557-576) London: Graham & Trotman.

Stow, D. A. V., Reading, H. G., & Collinson, J. D. (1996). Deep seas. In H. G. Reading (Ed.), *Sedimentary Environments: Processes, Facies and Stratigraphy* (Third Edition, p. 395-453). Oxford: Blackwell Publishing.

Torsvik, T. H., & Cocks, L. R. M. (2005). Norway in space and time: A Centennial cavalcade. *Norwegian Journal of Geology, 85*, 73-86.

Van Rensbergen, P., Hillis, R. R., Maltman, A. J., Morley, C. K. (2003). Subsurface sediment mobilization: introduction. In P. Van Rensbergen, R. R. Hillis, A. J. Maltman, & C. K. Morley (Eds.), Subsurface Sediment Mobilization (Special Publication 216, p. 1-8). London: The Geological Society of London**.**

Walday, M., & Kroglund T. (2002). The North Sea – bottom trawling and oil/gas exploration. In N. Liamine (Ed.), *Europe's biodiversity - biogeographical regions and seas*. (pp. 31) European Environment Agency.

Waltham, D. (2001). Decompaction Excel Worksheet. Royal Holloway.

Wheeler, H. E. (1958). Time stratigraphy. *Bulletin of the American Association of Petroleum Geologists 42*, 1047-1063.

Wien, S. T., & Kjennerud, T. (2005). 3D cretaceous to Cenozoic palaeobathymetry of the northern North Sea. In B. T. G. Wandås, J. P. Nystuen, E. A. Eide & F. M. Gradstein (Eds.), *Norwegian Petroleum Society Special Publications* (Vol. 12, p. 241-253). Elsevier.

Zachos, J., Pagani, M., Sloan, L., Thomas, E., & Billups, K. (2001). Trends, Rhythms, and Aberrations in Global Climate 65 Ma to Present. *Science, 292*, 686-693.

Zanella, E., Coward, M. P., & McGrandle, A. (2003). Crustal structure. In D. Evans, C. Graham, A. Armour & P. Bathurst (Eds.), *The Millennium Atlas: Petroleum geology of the central and northern North Sea.* (p. 35-42) London: The Geological Society of London.

Ziegler, P. A. (1988). Crustal Separation Between Eurasia and North America-Greenland: Opening of the Arctic-North Atlantic Ocean. In P. A. Ziegler (Ed.), *Evolution of the Arctic-North Atlantic and the Western Tethys* (AAPG Memoir 43, p. 97-119). Tulsa: American Association of Petroleum Geologists.

Ziegler, P. A., & Dèzes, P. (2006). Crustal Evolution of Western and Central Europe. In D. G. Gee & R. A. Stephenson (Eds.), *European Lithosphere Dynamics* (Memoirs 32, p. 43-56). London: The Geological Society of London.

APPENDIX A

Unit K10-K120

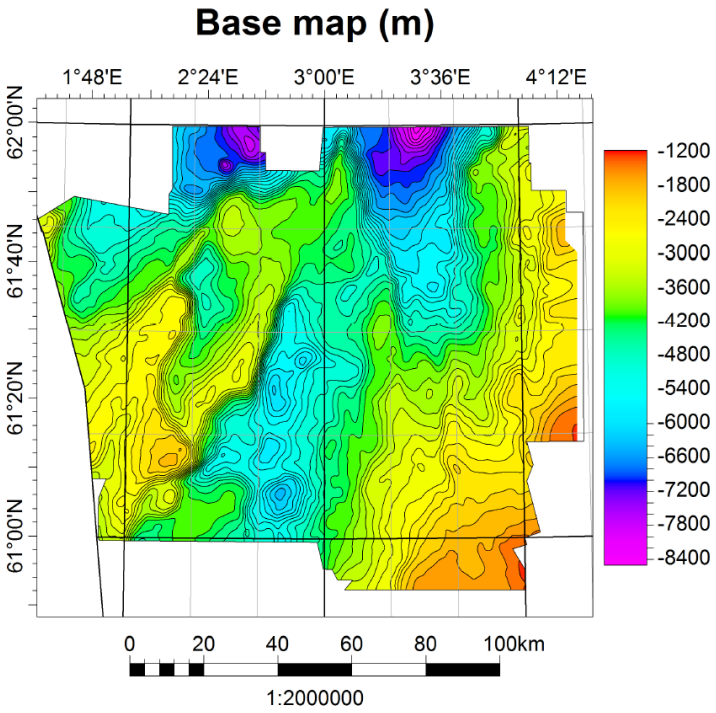

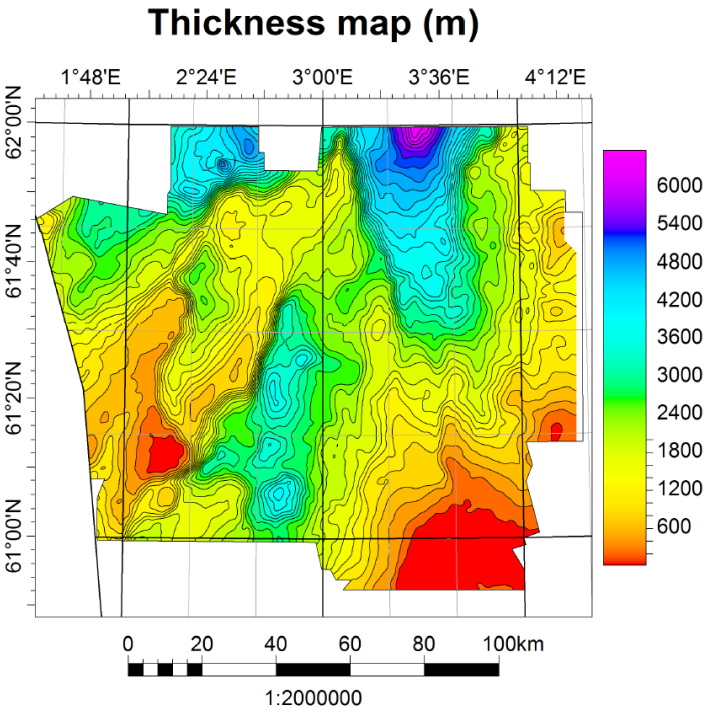

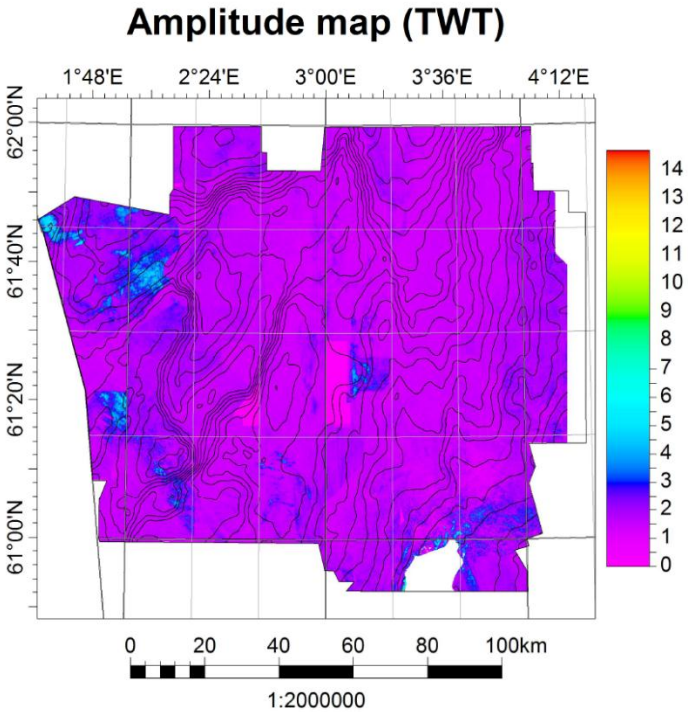

Unit	K10-K120
Groups	Cromer Knoll & Shetland
Epoch	Cretaceous
Age (Ma)	145,5 – 65,5
Maximum thickness	6651,2 m
Average thickness	2020,2 m
Volume	28 933 km^3
Av. sediment. rate	2,44 cm/ka
Max sediment. rate	8,31 cm/ka

Contour increments: Base map (200 m), Thickness map (200 m), Amplitude map (200 ms).

Amplitude map displays RMS Amplitude.

Unit T10

Base map (m)

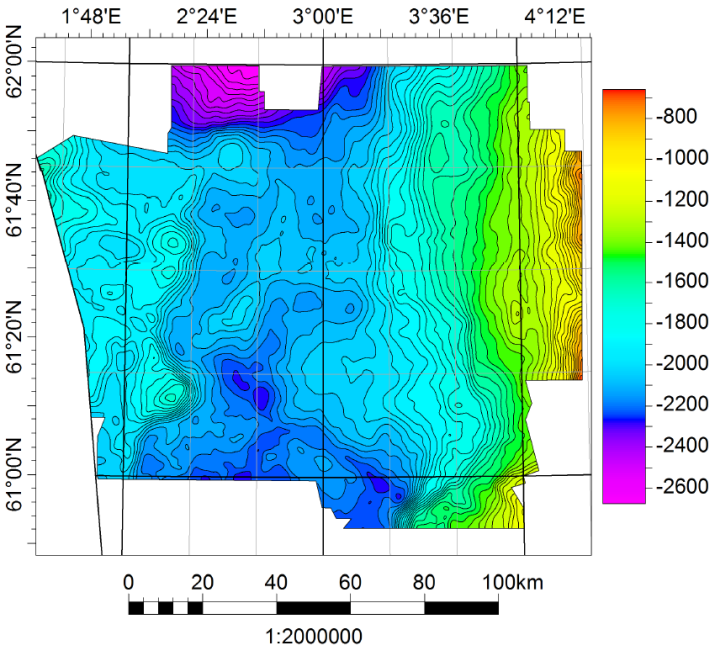

Thickness map (m)

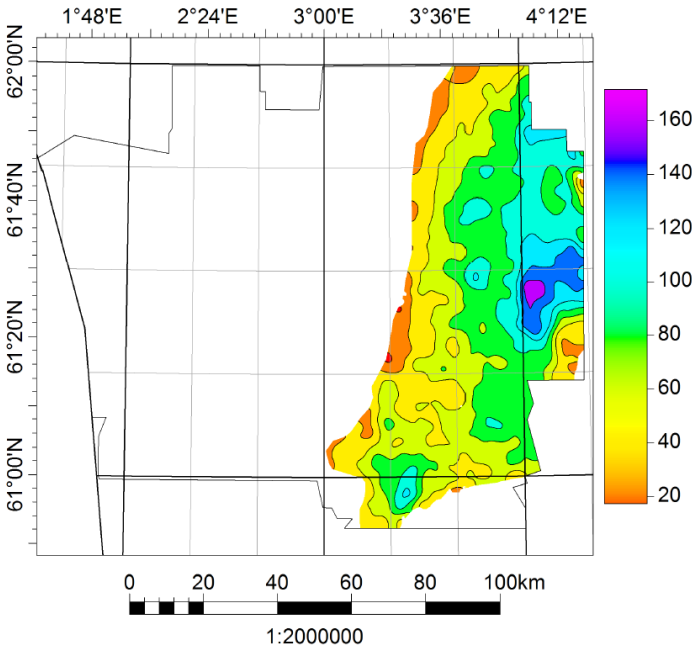

Amplitude map (TWT)

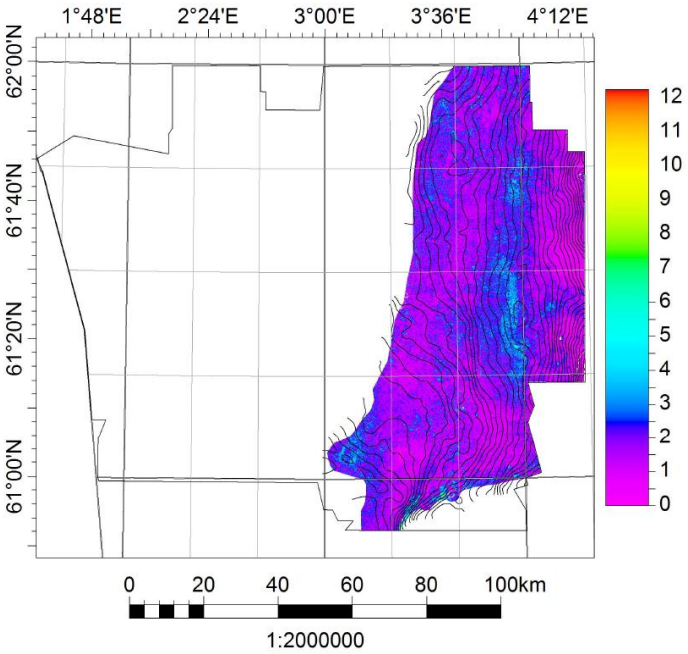

Unit	T10
Formation	Våle
Epoch	Early Paleocene
Age (Ma)	65,5 – 61,1
Maximum thickness	192,3 m
Average thickness	80,3 m
Volume	417 km^3
Av. sediment. rate	3,71 cm/ka
Max sediment. rate	4,37 cm/ka

Contour increments: Base map (40 m), Thickness map (20 m), Amplitude map (40 ms).

Amplitude map displays RMS Amplitude.

Unit T20-T50

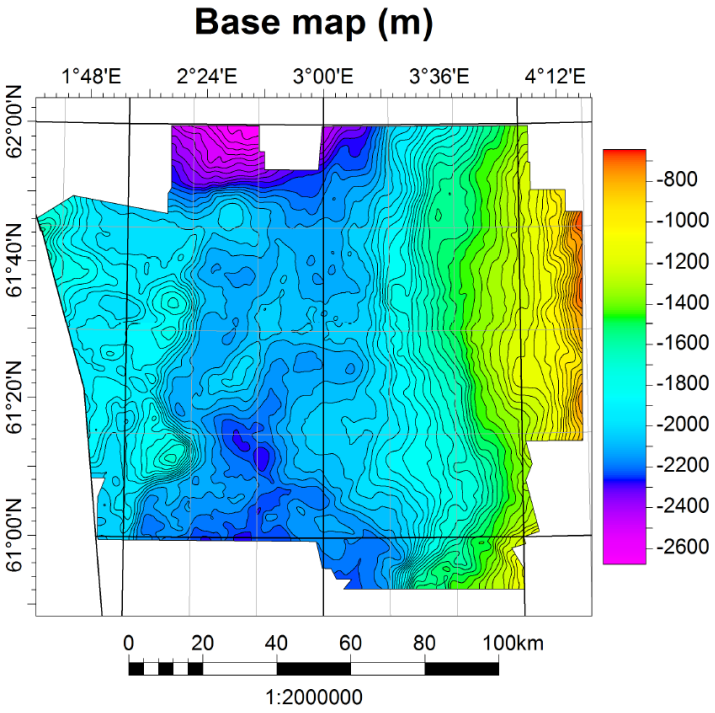

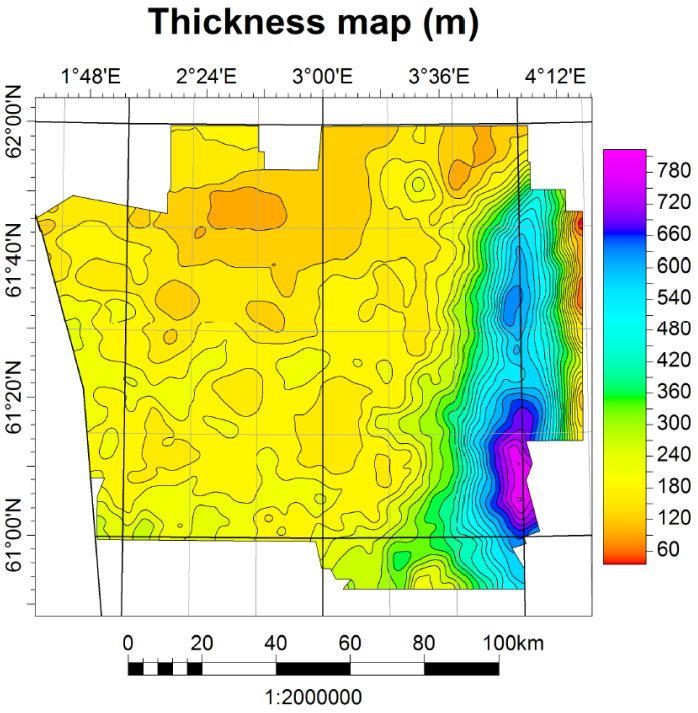

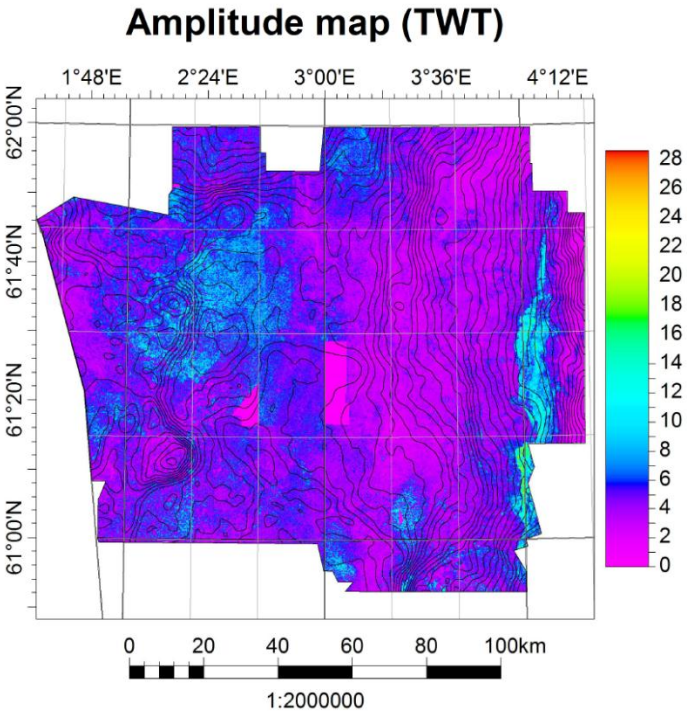

Unit	T20-T50
Group	Rogaland (w/o Våle FM)
Epoch	Late Paleocene – Early Eocene
Age (Ma)	61,1 – 54,0
Maximum thickness	851,7 m
Average thickness	252,5 m
Volume	3 688 km^3
Av. sediment. rate	3,50 cm/ka
Max sediment. rate	12,00 cm/ka

Contour increments: Base map (40 m), Thickness map (30 m), Amplitude map (40 ms).

Amplitude map displays Maximum Magnitude.

Unit T60-T100

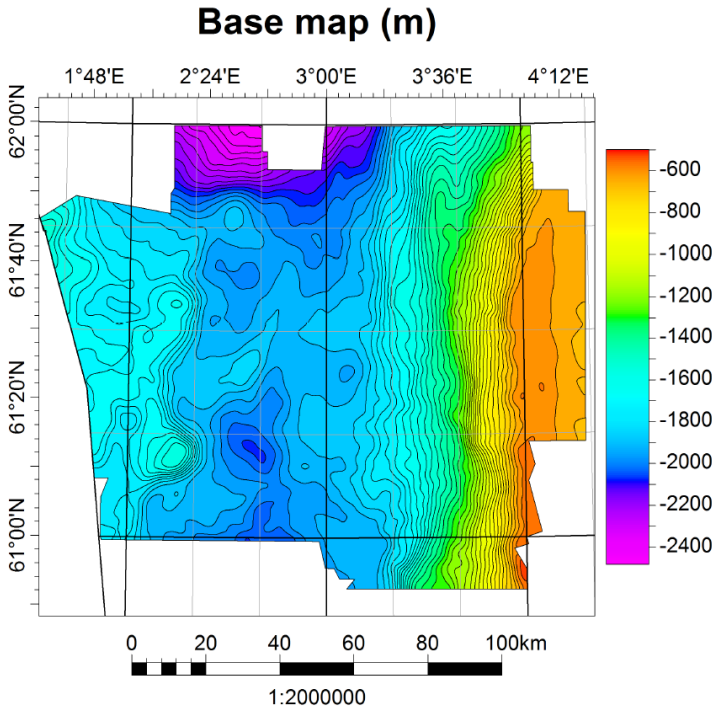

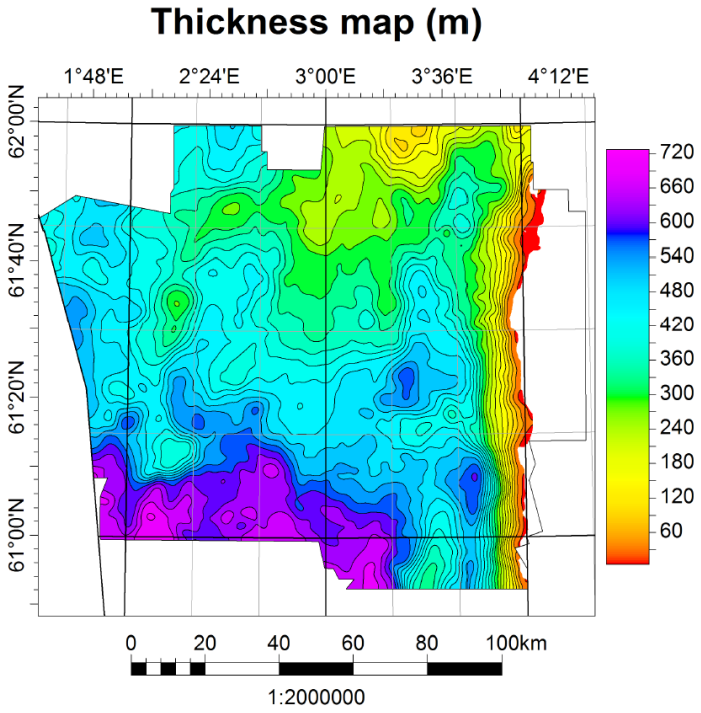

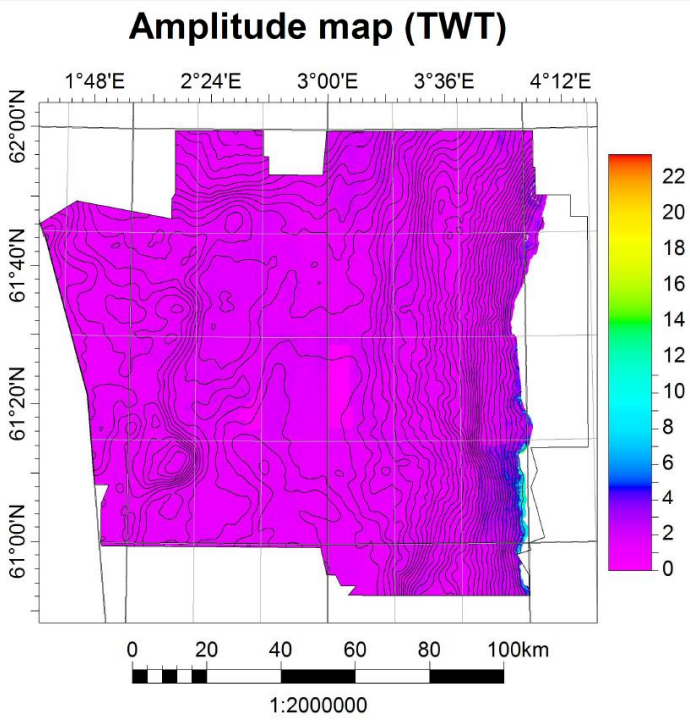

Unit	T60-T100
Group	Hordaland
Epoch	Early Eocene – Early Oligocene
Age (Ma)	54,0 – 31,1 ± 2,8
Maximum thickness	751,3 m
Average thickness	442,9 m
Volume	5 692 km^3
Av. sediment. rate	1,85 cm/ka
Max sediment. rate	3,29 cm/ka

Contour increments: Base map (40 m), Thickness map (30 m), Amplitude map (40 ms).

Amplitude map displays RMS Amplitude.

Unit T110

Base map (m)

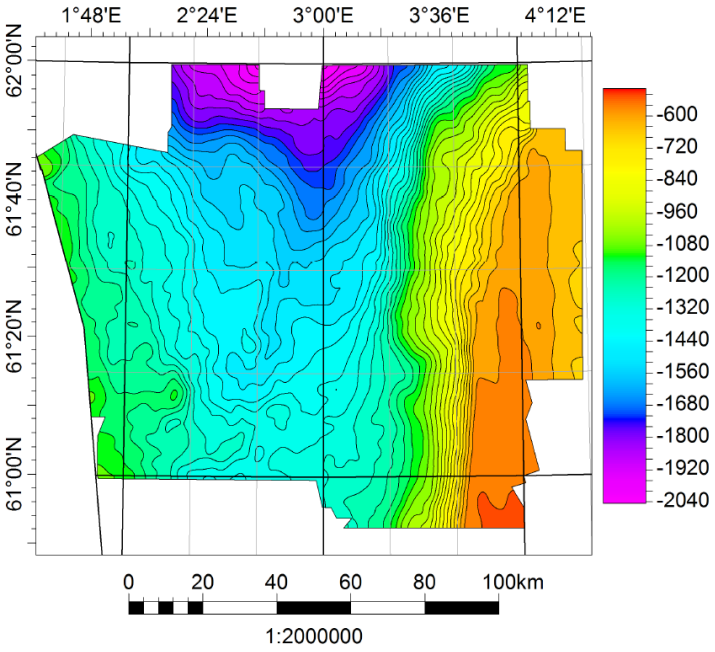

Thickness map (m)

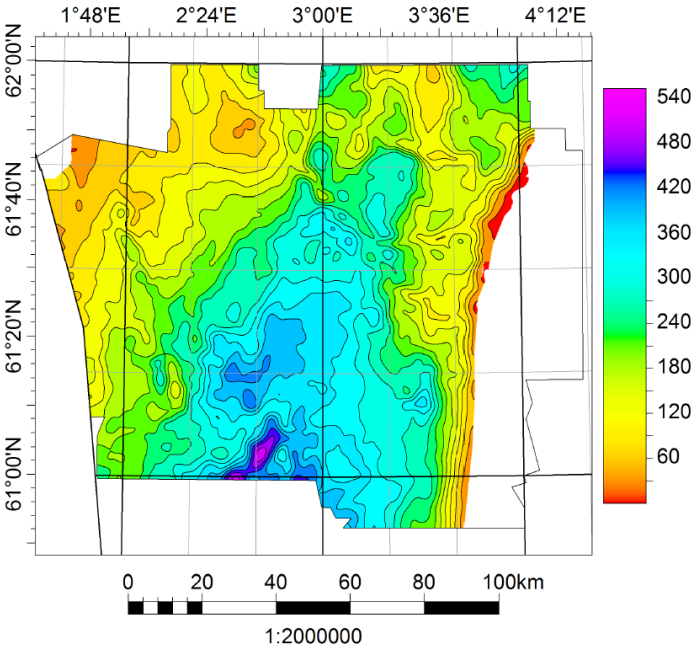

Amplitude map (TWT)

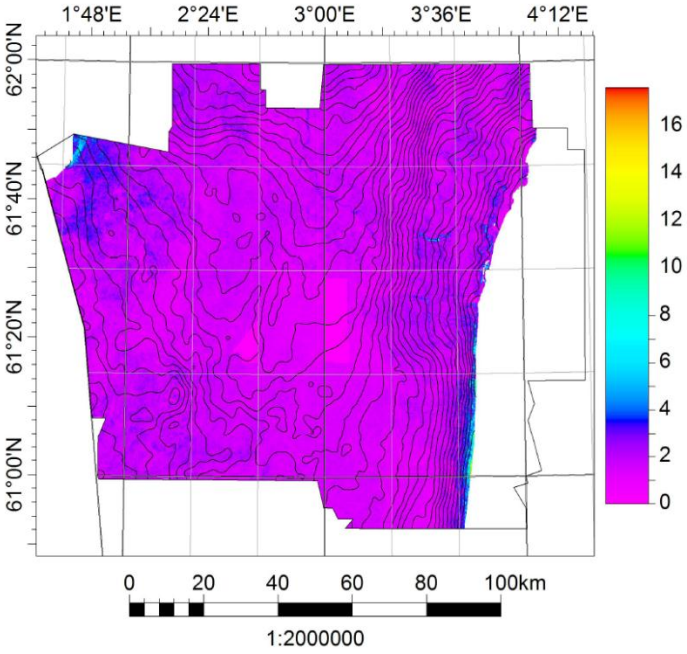

Unit	T110
Group	Hordaland
Epoch	Late Oligocene
Age (Ma)	31,1 ± 2,8 - 23,03
Maximum thickness	573,8 m
Average thickness	227,2 m
Volume	2 815 km^3
Av. sediment. rate	2,80 cm/ka
Max sediment. rate	7,07 cm/ka

Contour increments: Base map (40 m), Thickness map (30 m), Amplitude map (40 ms).

Amplitude map displays RMS Amplitude.

Unit T120-130

Base map (m)

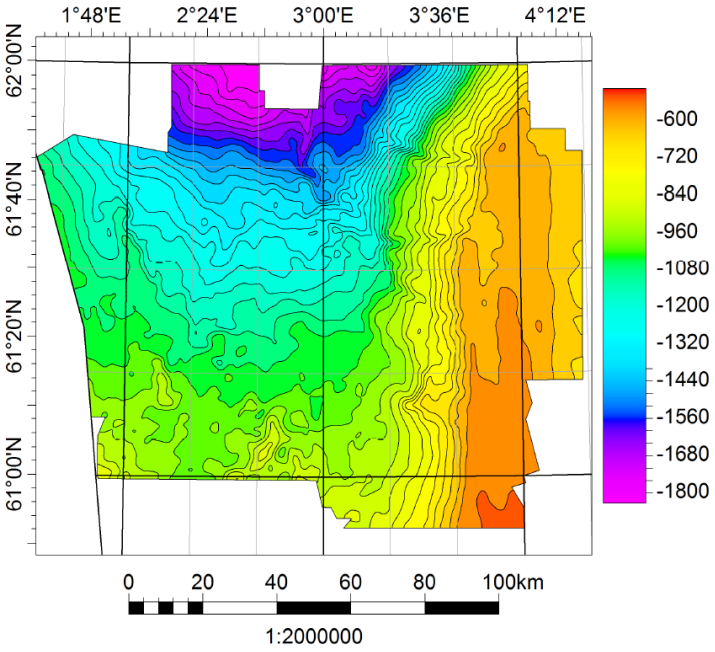

Thickness map (m)

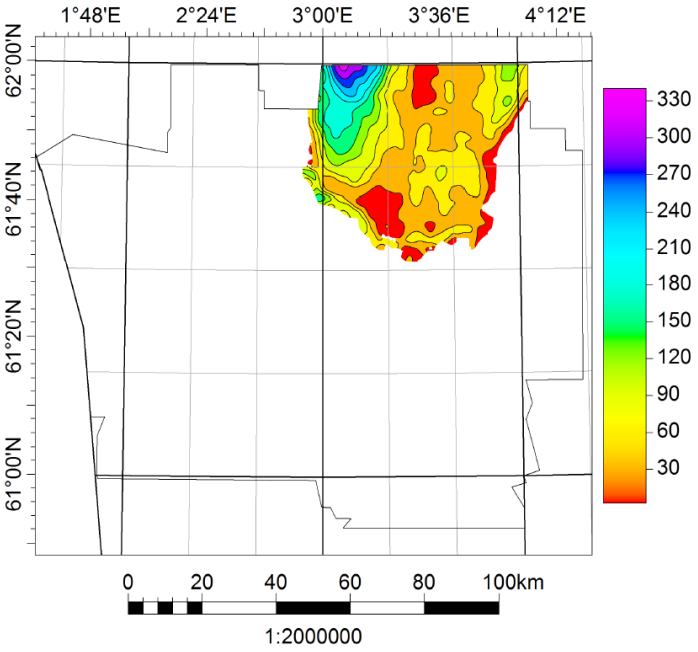

Amplitude map (TWT)

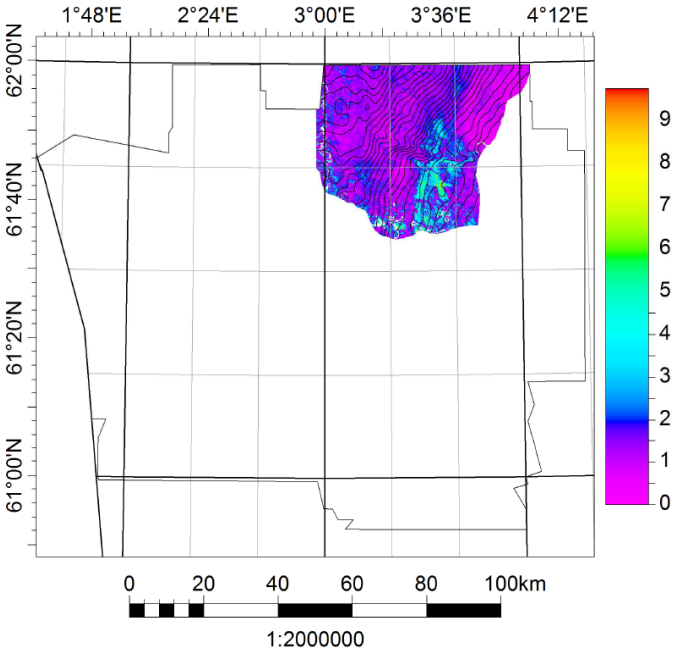

Unit	T120-T130
Group	Nordland
Epoch	Early - Middle Miocene
Age (Ma)	23,03 – 11,61
Maximum thickness	340,2 m
Average thickness	81,1 m
Volume	247 km^3
Av. sediment. rate	0,91 cm/ka
Max sediment. rate	3,56 cm/ka

Contour increments: Base map (m), Thickness map (m), Amplitude map (ms).

Amplitude map displays RMS Amplitude

Unit T140

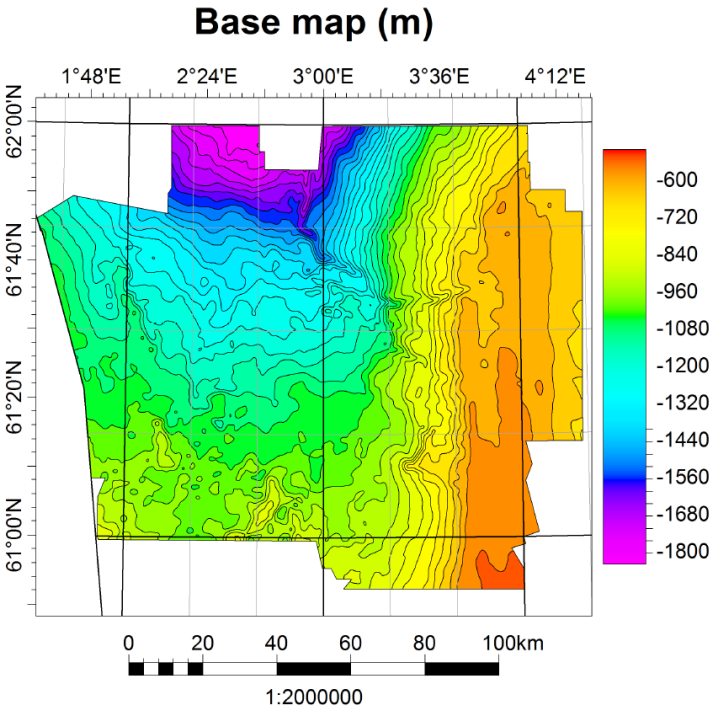

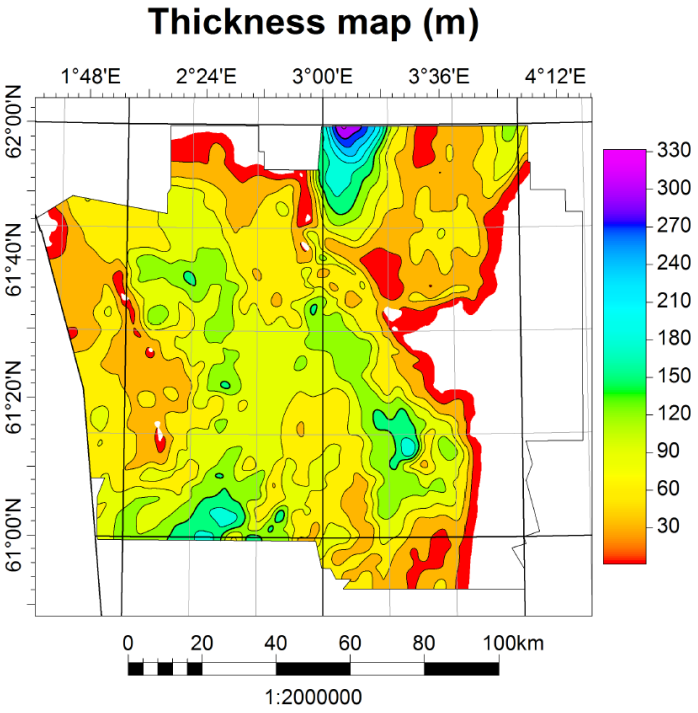

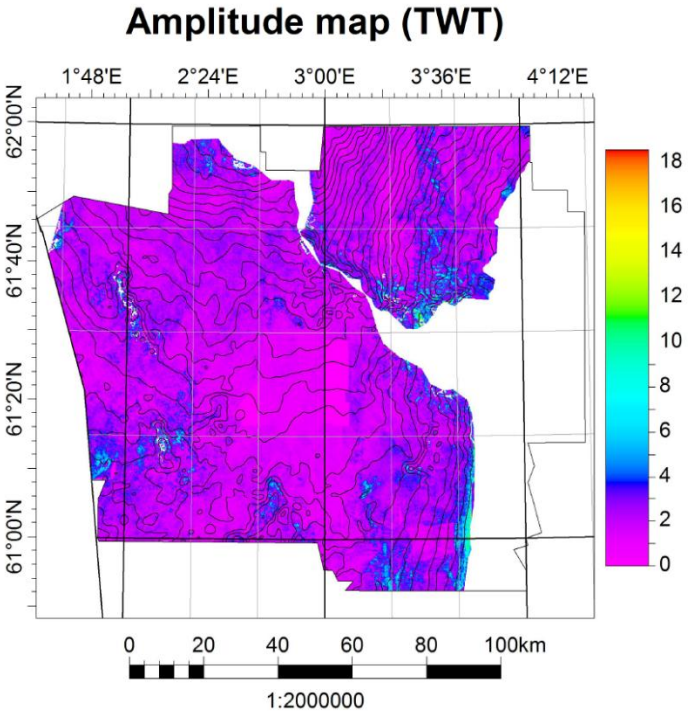

Unit	T140
Formation	Utsira
Epoch	Late Miocene
Age (Ma)	11,61 – 5,33
Maximum thickness	328,9 m
Average thickness	83,3 m
Volume	987 km^3
Av. sediment. rate	1,33 cm/ka
Max sediment. rate	5,51 cm/ka

Contour increments: Base map (m), Thickness map (m), Amplitude map (ms).

Amplitude map displays RMS Amplitude.

Unit T150 A

Base map (m)

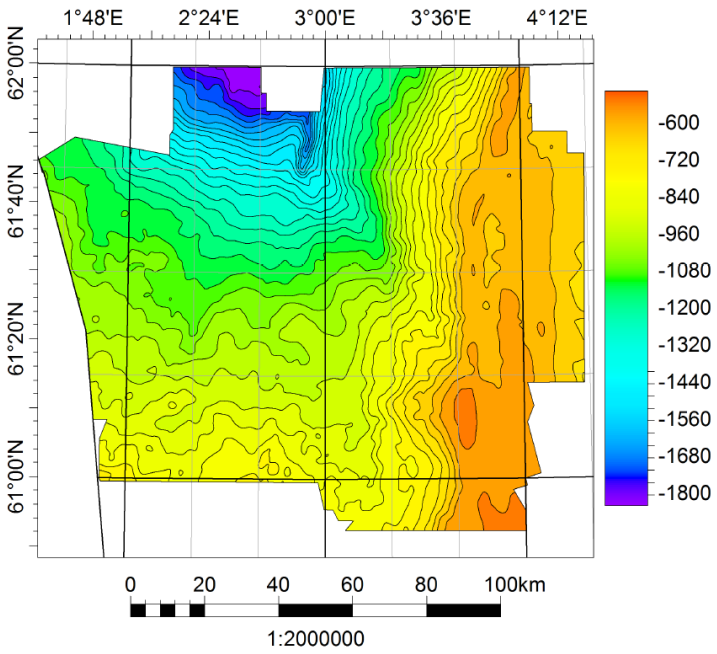

Thickness map (m)

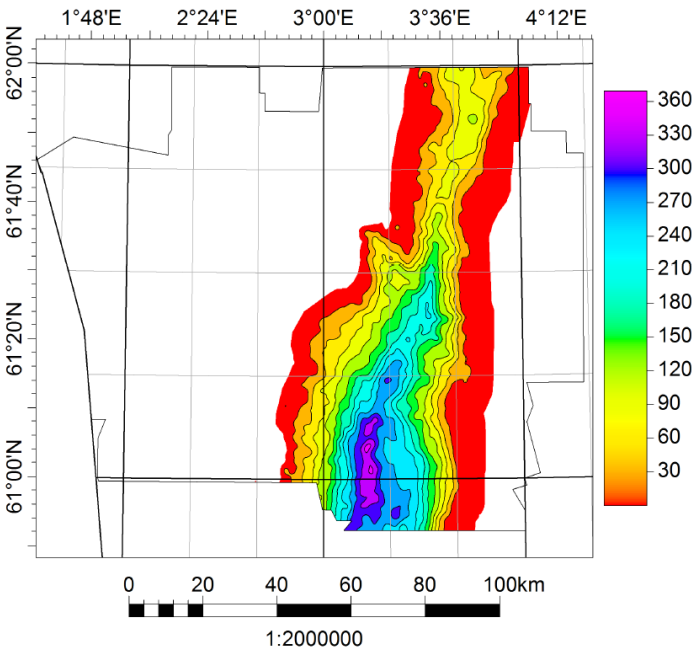

Amplitude map (TWT)

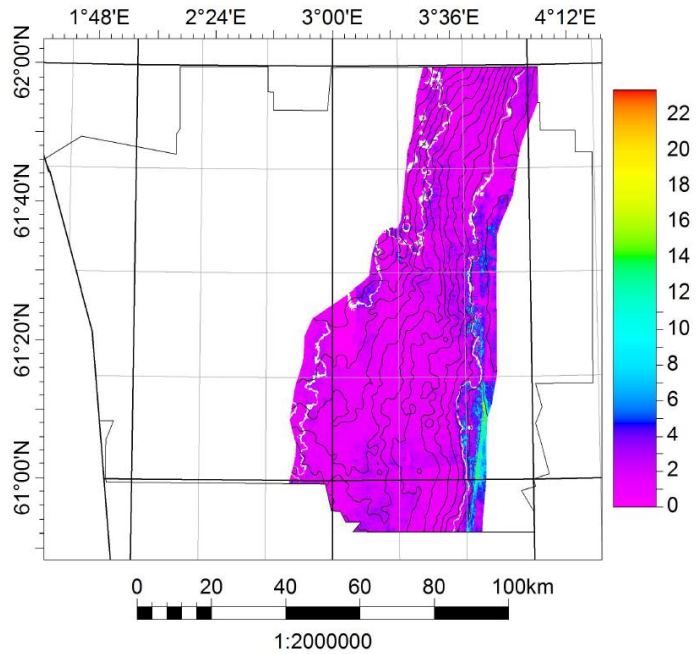

Unit	T150 A
Group	Nordland
Epoch	Pliocene
Age (Ma)	5,33 – 2,59
Maximum thickness	369,0 m
Average thickness	100,0 m
Volume	532 km^3
Av. sediment. rate	16,01 cm/ka
Max sediment. rate	41,11 cm/ka

Contour increments: Base map (40 m), Thickness map (30 m), Amplitude map (40 ms).

Amplitude map displays RMS Amplitude.

Unit T150 B

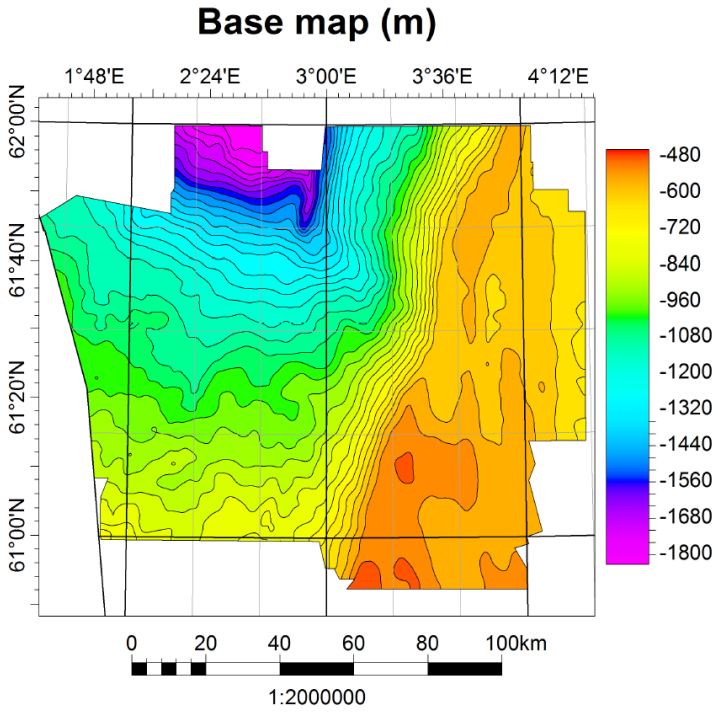

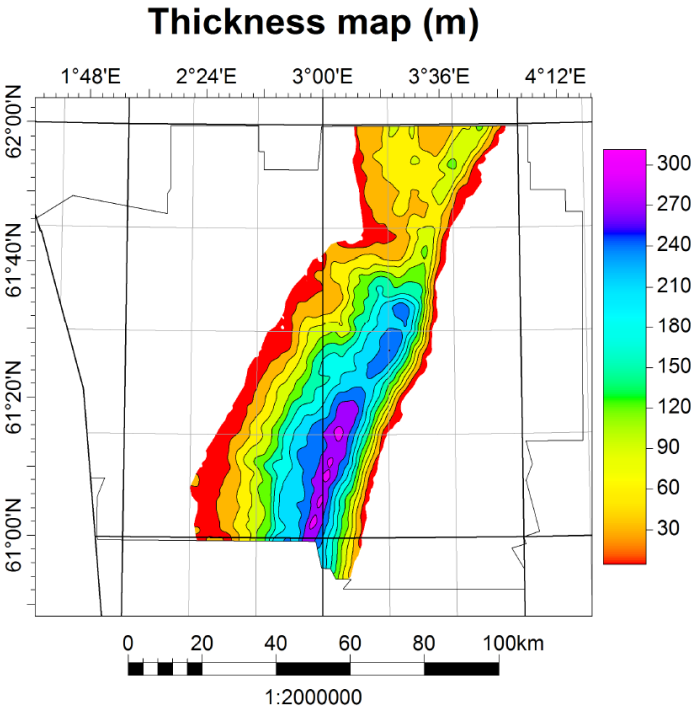

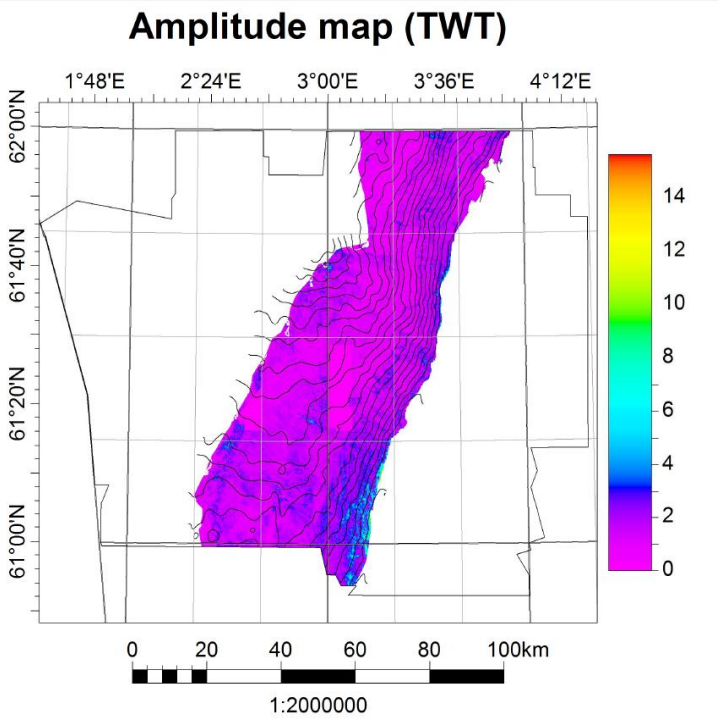

Unit	T150 B
Group	Nordland
Epoch	Pliocene
Age (Ma)	5,33 – 2,59
Maximum thickness	334,8 m
Average thickness	116,4 m
Volume	536 km^3
Av. sediment. rate	16,01 cm/ka
Max sediment. rate	41,11 cm/ka

Contour increments: Base map (40 m), Thickness map (30 m), Amplitude map (40 ms).

Amplitude map displays RMS Amplitude.

Unit T150 C

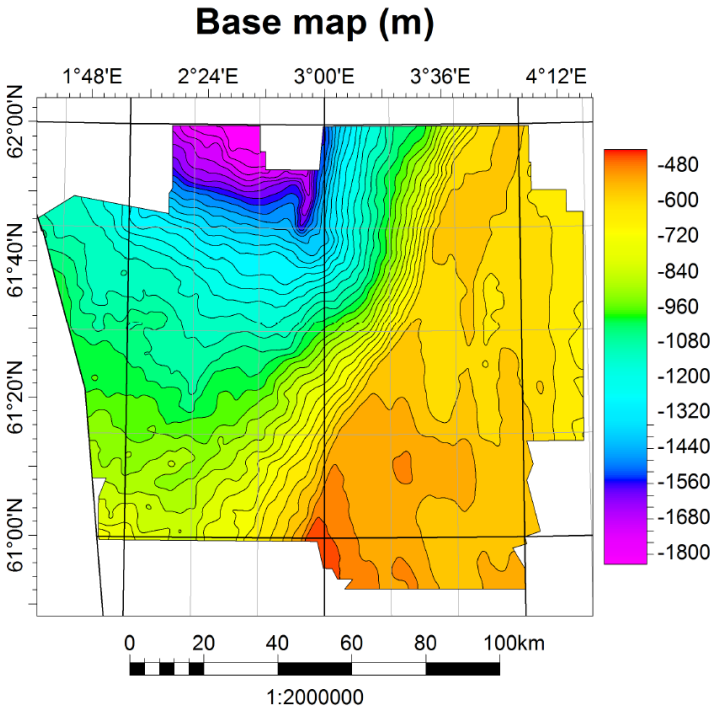

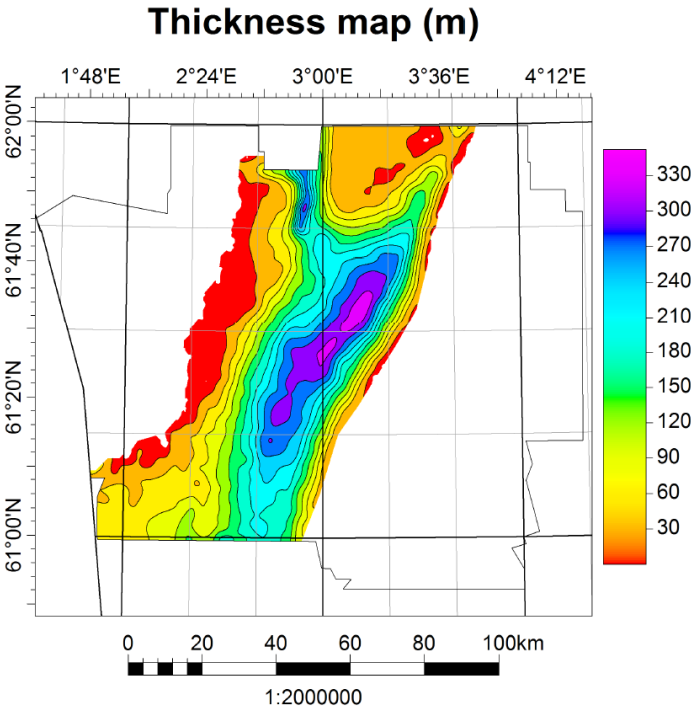

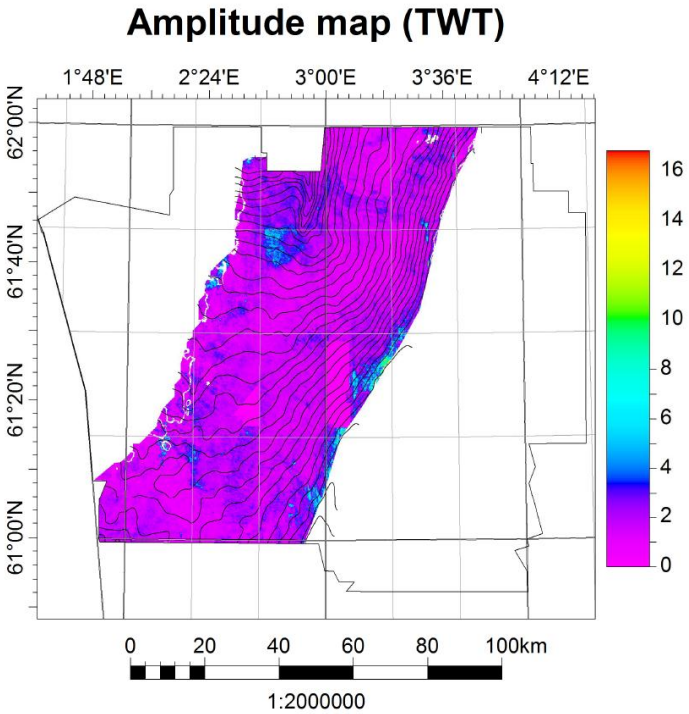

Unit	T150 C
Group	Nordland
Epoch	Pliocene
Age (Ma)	5,33 – 2,59
Maximum thickness	391,4 m
Average thickness	130,4
Volume	780 km^3
Av. sediment. rate	16,01 cm/ka
Max sediment. rate	41,11 cm/ka

Contour increments: Base map (40 m), Thickness map (30 m), Amplitude map (40 ms).

Amplitude map displays RMS Amplitude.

Unit T150 D

Base map (m)

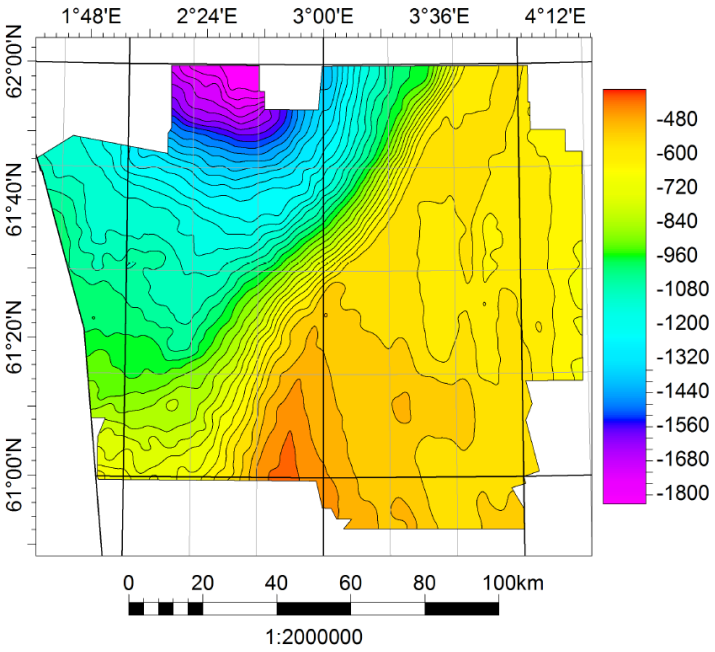

Thickness map (m)

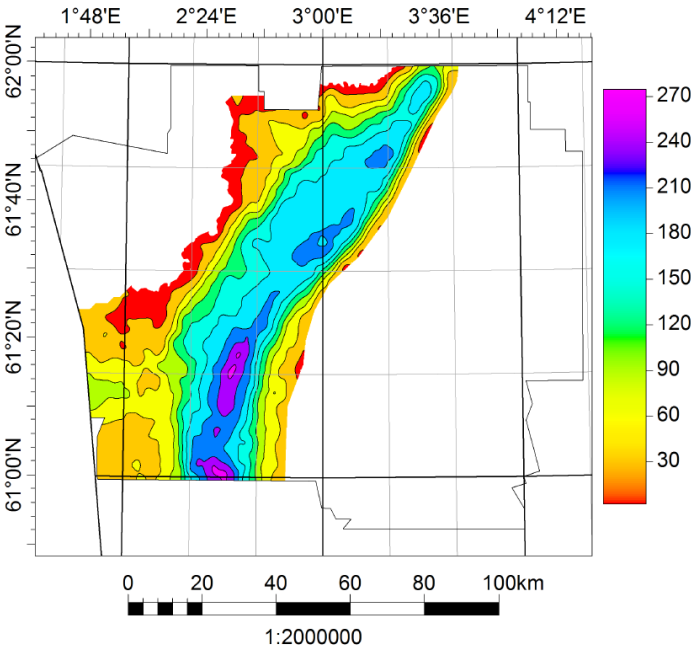

Amplitude map (TWT)

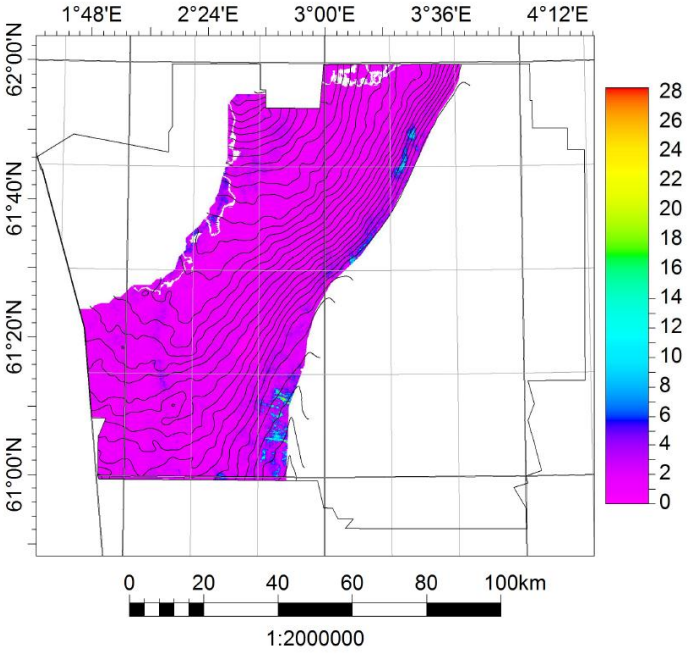

Unit	T150 D
Group	Nordland
Epoch	Pliocene
Age (Ma)	5,33 – 2,59
Maximum thickness	330,0 m
Average thickness	119,7 m
Volume	664 km^3
Av. sediment. rate	16,01 cm/ka
Max sediment. rate	41,11 cm/ka

Contour increments: Base map (40 m), Thickness map (30 m), Amplitude map (40 ms).

Amplitude map displays RMS Amplitude.

Unit T150 E

Base map (m)

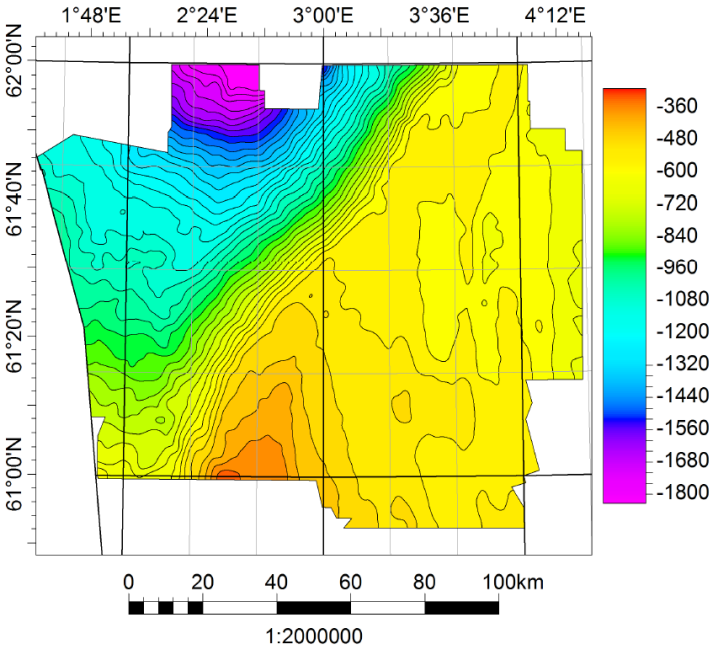

Thickness map (m)

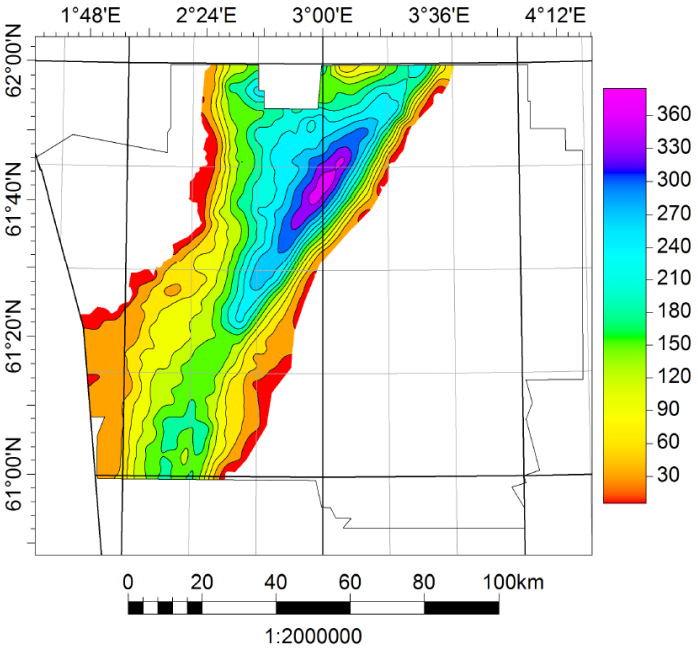

Amplitude map (TWT)

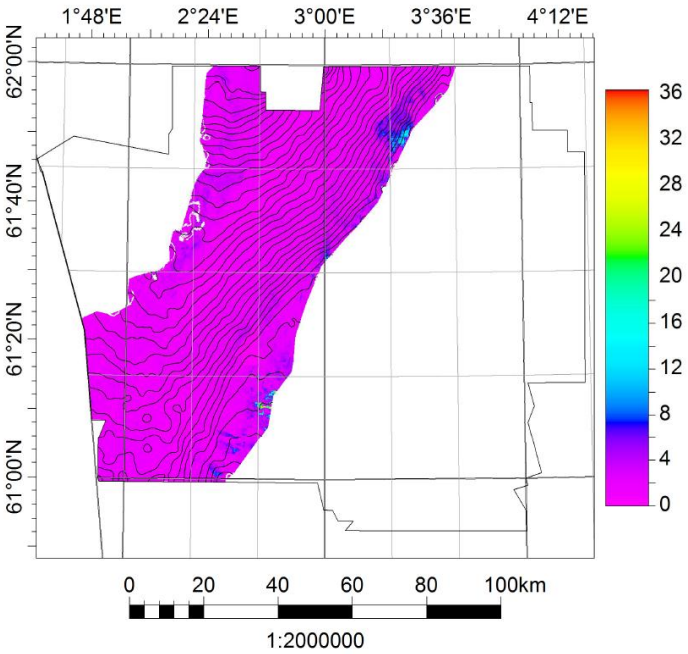

Unit	T150 E
Group	Nordland
Epoch	Pliocene
Age (Ma)	5,33 – 2,59
Maximum thickness	399,3 m
Average thickness	143,2 m
Volume	785 km^3
Av. sediment. rate	16,01 cm/ka
Max sediment. rate	41,11 cm/ka

Contour increments: Base map (40 m), Thickness map (30 m), Amplitude map (40 ms).

Amplitude map displays RMS Amplitude.

Unit T150 F

Base map (m)

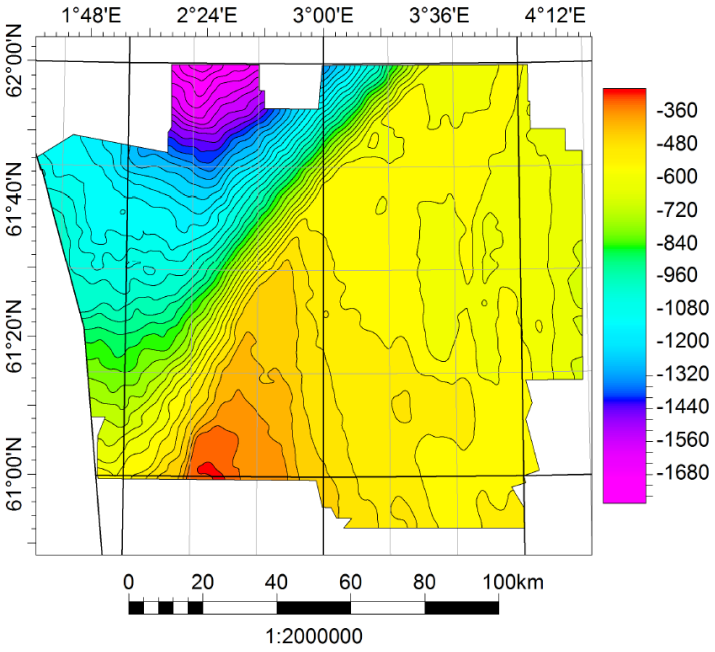

Thickness map (m)

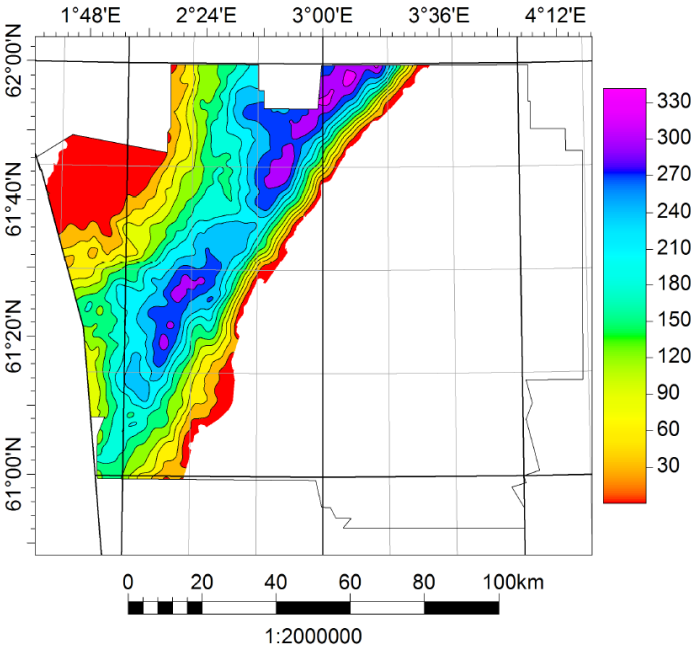

Amplitude map (TWT)

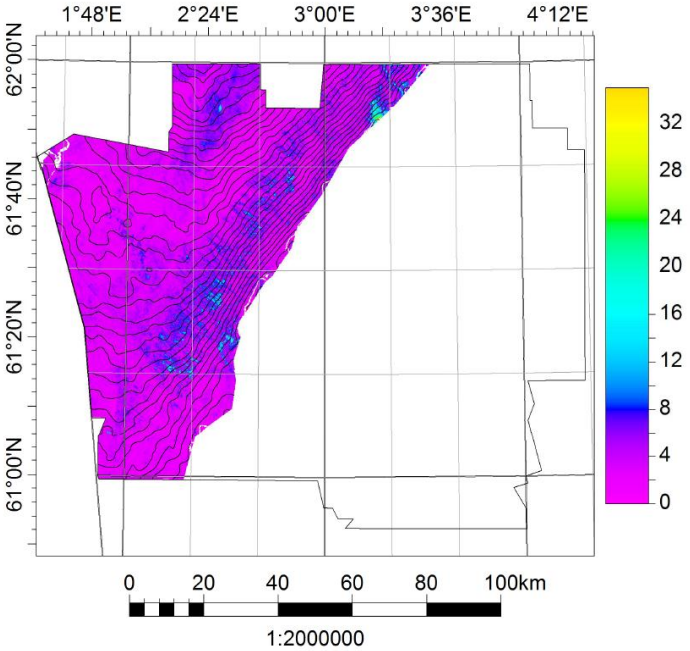

Unit	T150 F
Group	Nordland
Epoch	Pliocene
Age (Ma)	5,33 – 2,59
Maximum thickness	359,6 m
Average thickness	155,5 m
Volume	862 km^3
Av. sediment. rate	16,01 cm/ka
Max sediment. rate	41,11 cm/ka

Contour increments: Base map (40 m), Thickness map (30 m), Amplitude map (40 ms).

Amplitude map displays Maximum Magnitude.

Unit T150 G

Base map (m)

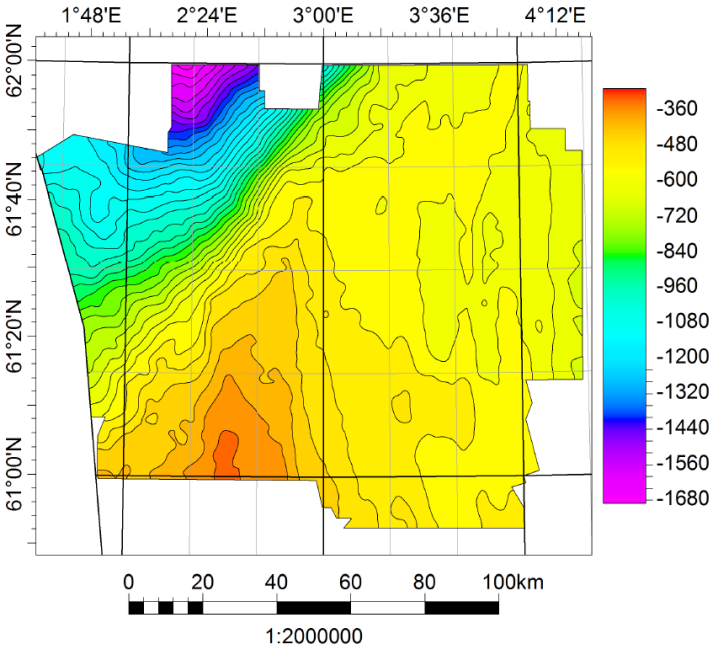

Thickness map (m)

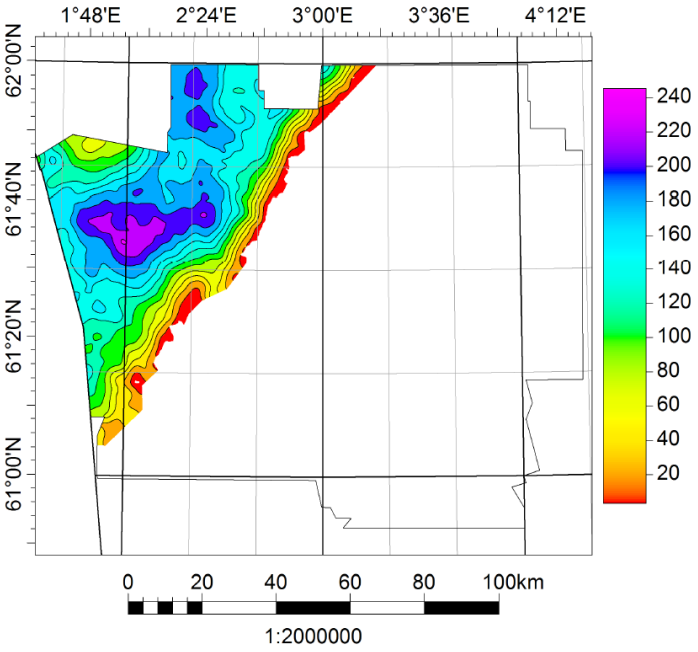

Amplitude map (TWT)

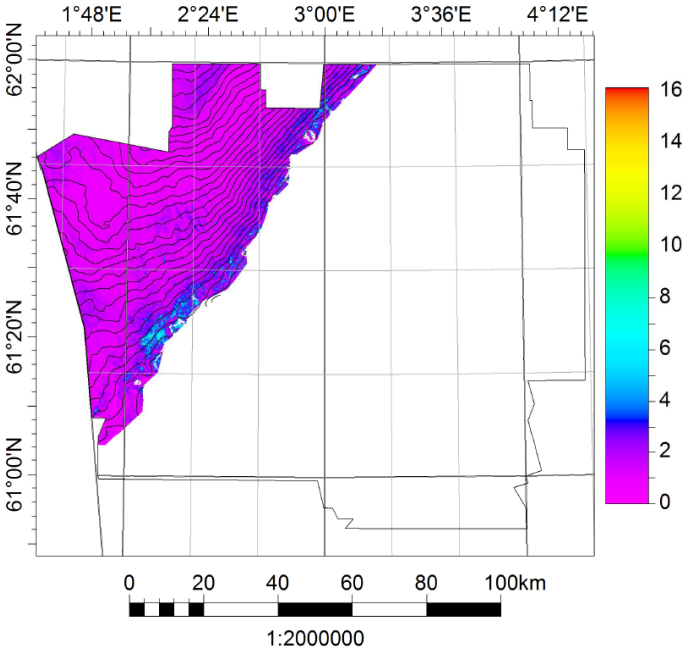

Unit	T150 G
Group	Nordland
Epoch	Pliocene
Age (Ma)	5,33 – 2,59
Maximum thickness	441,8 m
Average thickness	137,0 m
Volume	522 km^3
Av. sediment. rate	16,01 cm/ka
Max sediment. rate	41,11 cm/ka

Contour increments: Base map (40 m), Thickness map (20 m), Amplitude map (40 ms).

Amplitude map displays RMS Amplitude.

Unit T150 H

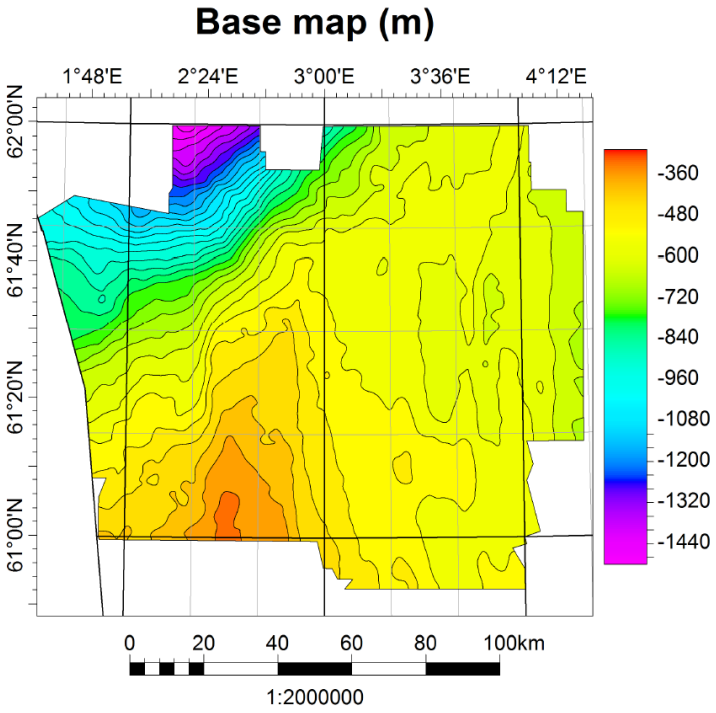

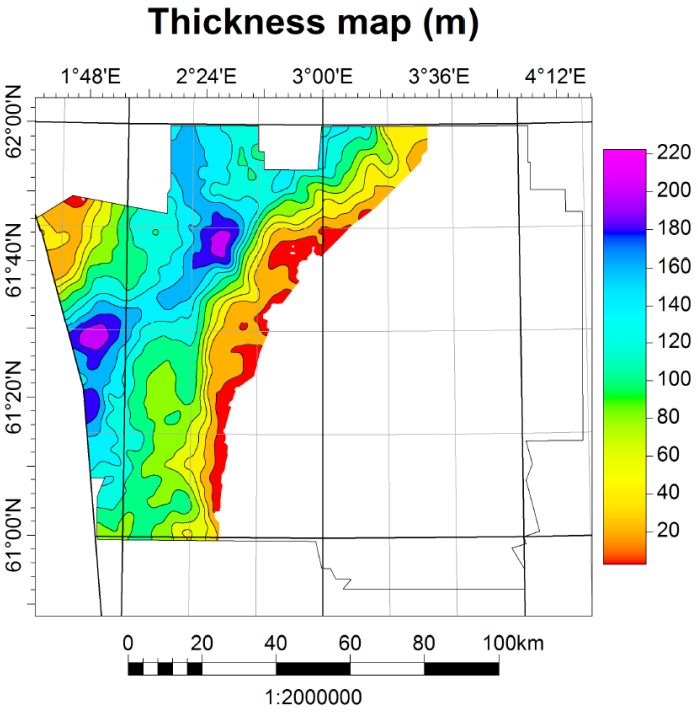

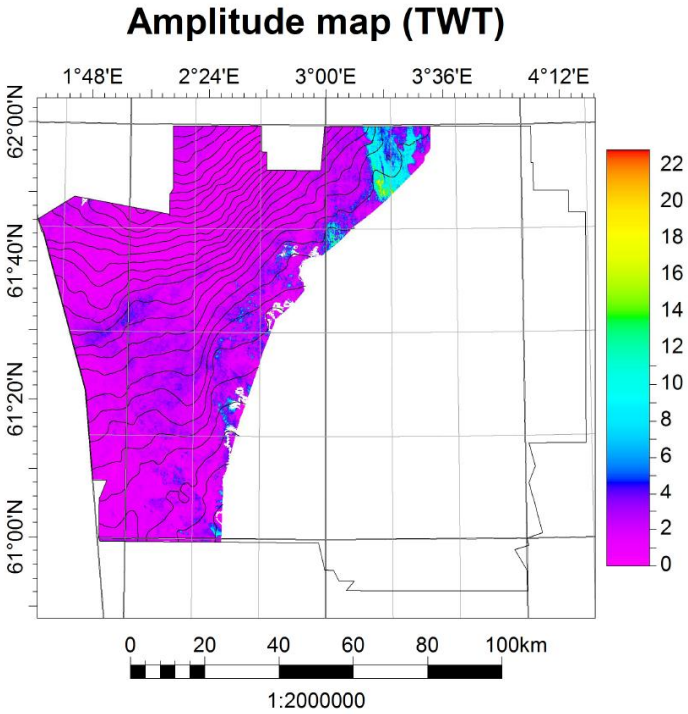

Unit	T150 H
Group	Nordland
Epoch	Pliocene
Age (Ma)	5,33 – 2,59
Maximum thickness	237,8 m
Average thickness	102,8 m
Volume	594 km^3
Av. sediment. rate	16,01 cm/ka
Max sediment. rate	41,11 cm/ka

Contour increments: Base map (40 m), Thickness map (20 m), Amplitude map (40 ms).

Amplitude map displays RMS Amplitude.

Unit T160 A

Base map (m)

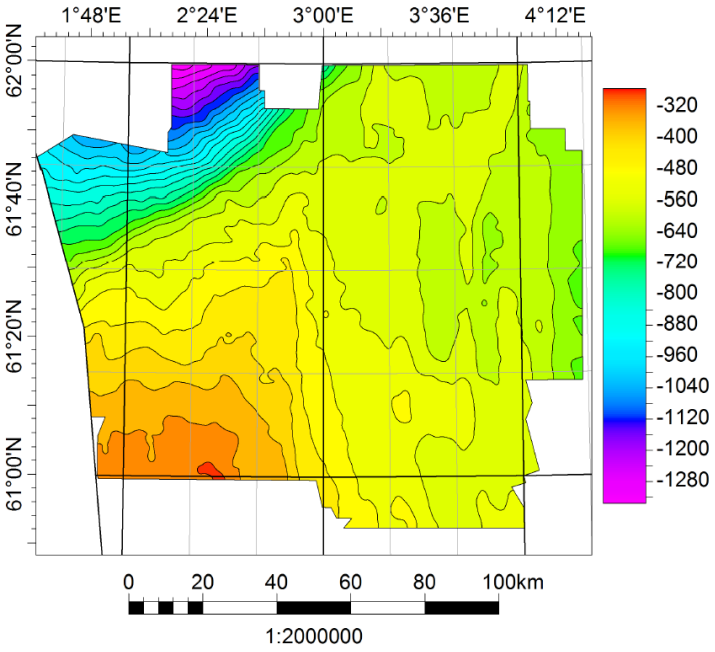

Thickness map (m)

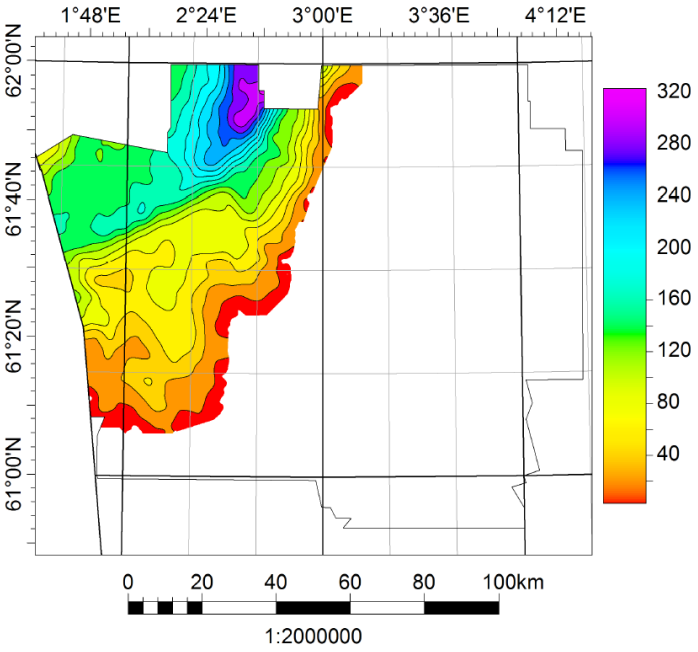

Amplitude map (TWT)

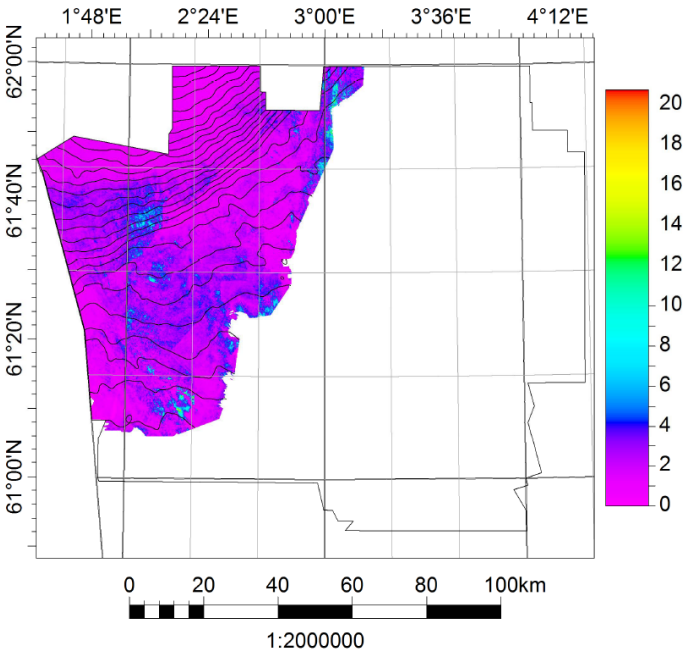

Unit	T160 A
Group	Nordland
Epoch	Pleistocene
Age (Ma)	2,59 – 0
Maximum thickness	341,7 m
Average thickness	103,9 m
Volume	529 km^3
Av. sediment. rate	8,34 cm/ka
Max sediment. rate	37,31 cm/ka

Contour increments: Base map (40 m), Thickness map (20 m), Amplitude map (40 ms).

Amplitude map displays RMS Amplitude.

Unit T160 B

Base map (m)

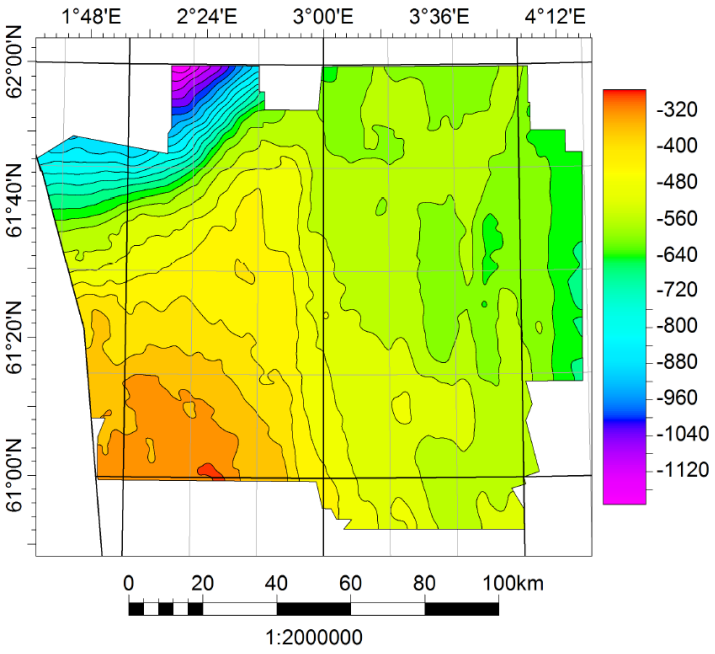

Thickness map (m)

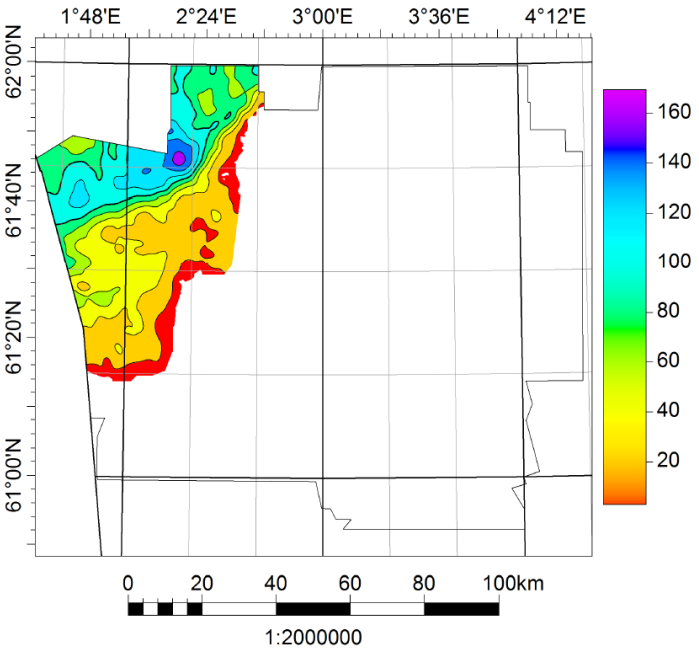

Amplitude map (TWT)

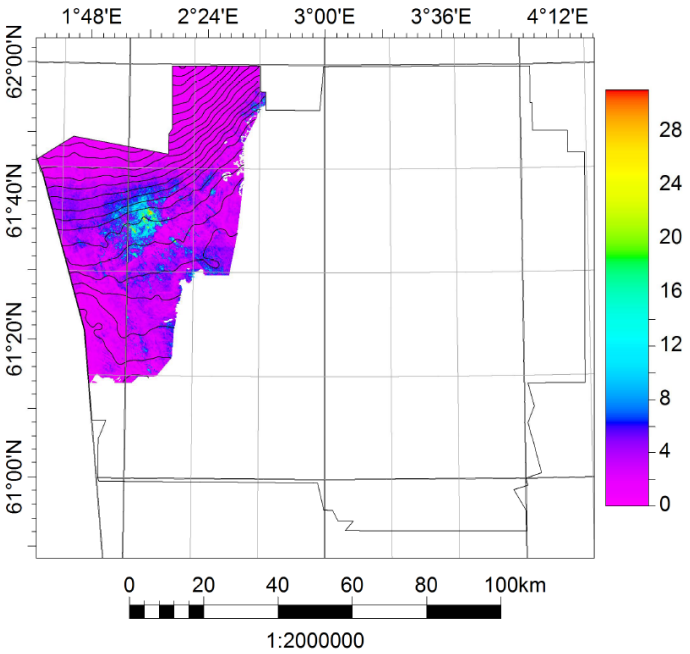

Unit	T160 B
Group	Nordland
Epoch	Pleistocene
Age (Ma)	2,59 – 0
Maximum thickness	175,3 m
Average thickness	63,0 m
Volume	184 km^3
Av. sediment. rate	8,34 cm/ka
Max sediment. rate	37,31 cm/ka

Contour increments: Base map (40 m), Thickness map (20 m), Amplitude map (40 ms).

Amplitude map displays RMS Amplitude.

Unit T160 C

Base map (m)

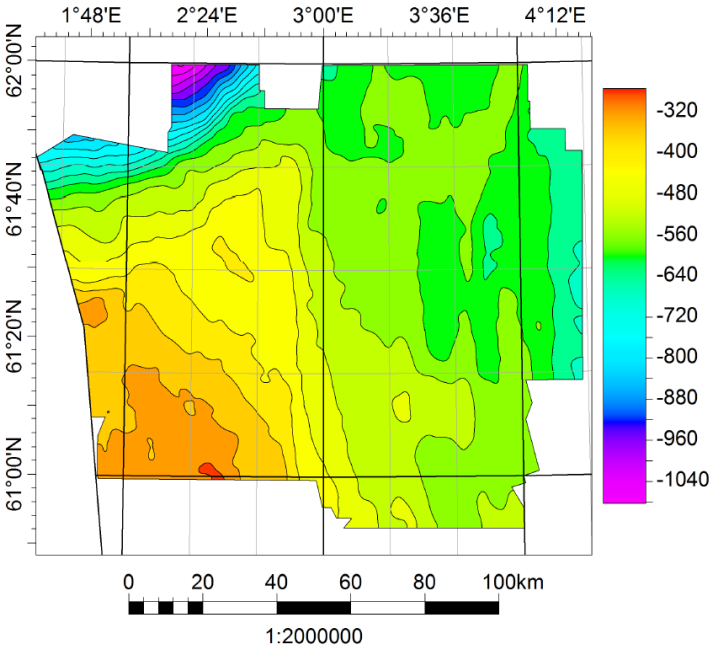

Thickness map (m)

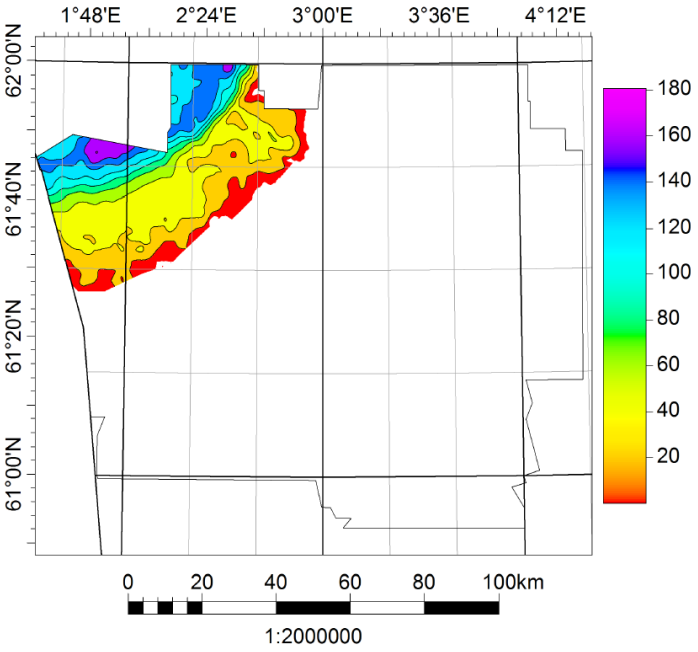

Amplitude map (TWT)

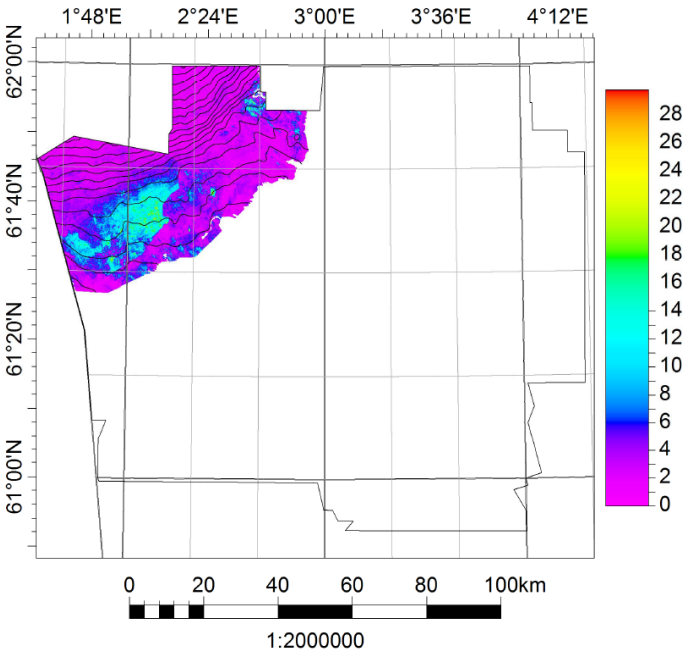

Unit	T160 C
Group	Nordland
Epoch	Pleistocene
Age (Ma)	2,59 – 0
Maximum thickness	187,8 m
Average thickness	65,7 m
Volume	159 km^3
Av. sediment. rate	8,34 cm/ka
Max sediment. rate	37,31 cm/ka

Contour increments: Base map (40 m), Thickness map (20 m), Amplitude map (40 ms).

Amplitude map displays RMS Amplitude.

Unit T160 D

Base map (m)

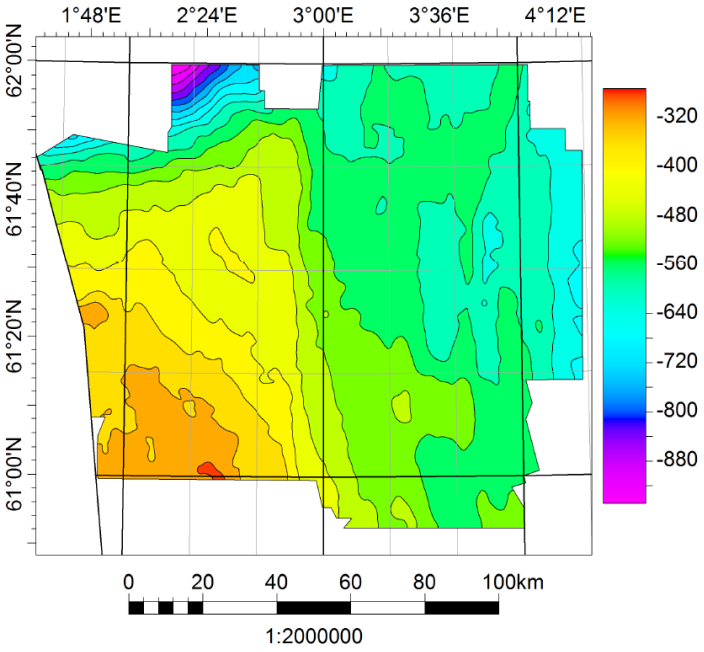

Thickness map (m)

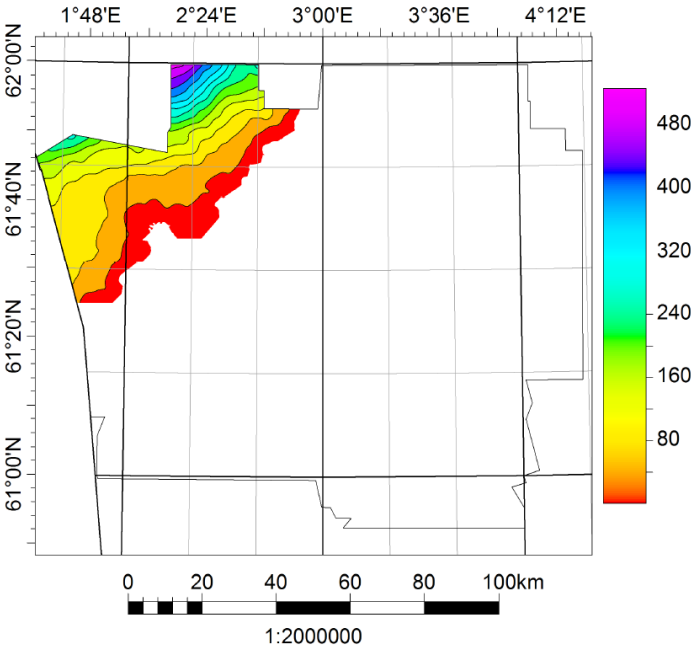

Amplitude map (TWT)

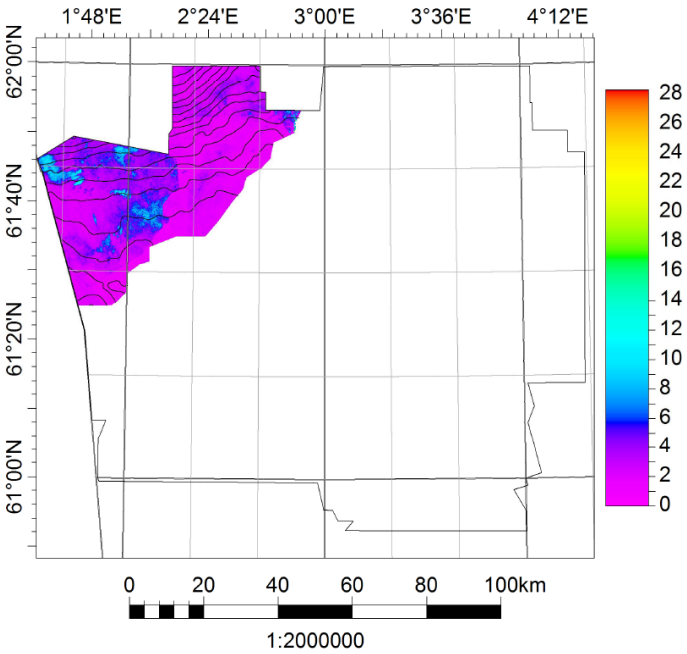

Unit	T160 D
Group	Nordland
Epoch	Pleistocene
Age (Ma)	2,59 – 0
Maximum thickness	537,0 m
Average thickness	115,2 m
Volume	246 km^3
Av. sediment. rate	8,34 cm/ka
Max sediment. rate	37,31 cm/ka

Contour increments: Base map (40 m), Thickness map (20 m), Amplitude map (40 ms).

Amplitude map displays RMS Amplitude.

Unit T160 E

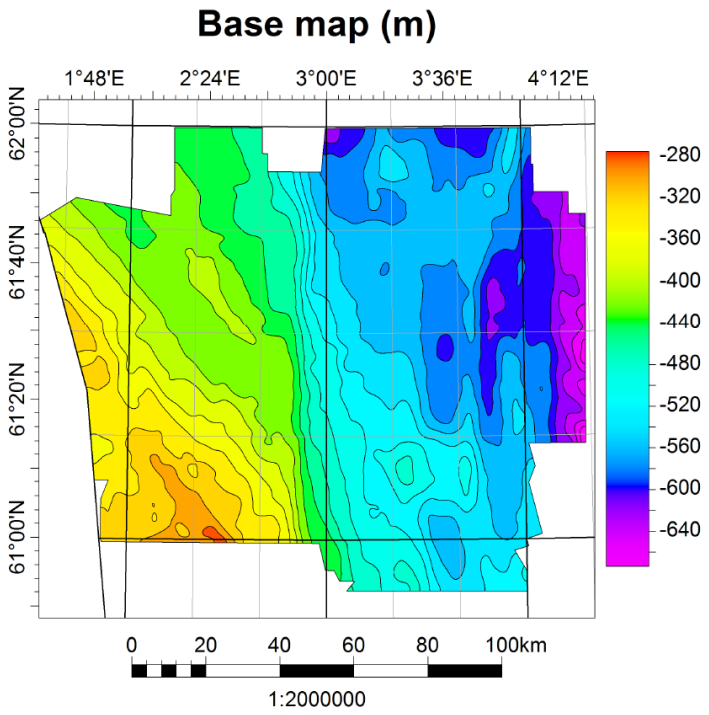

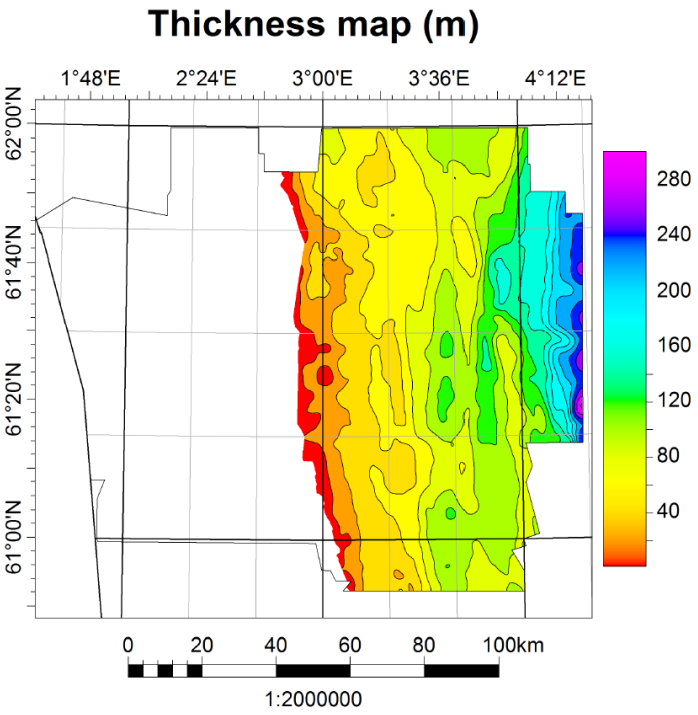

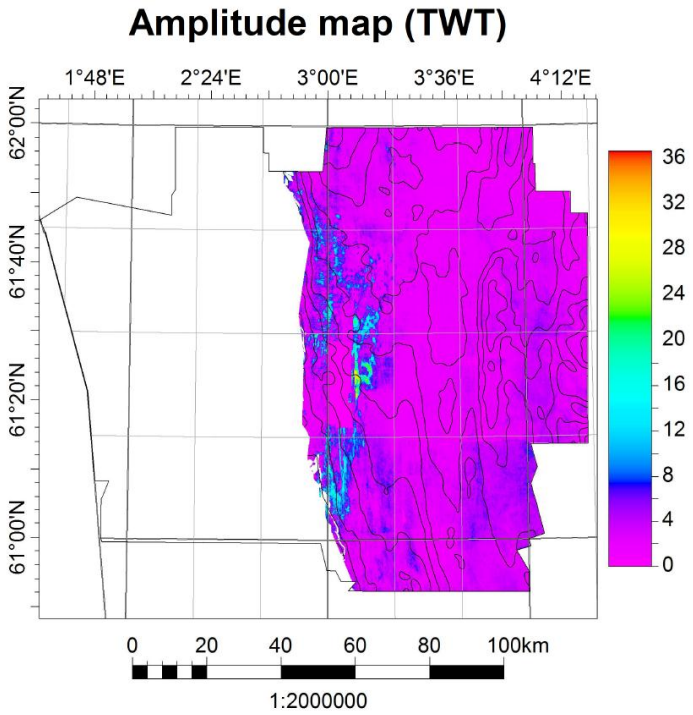

Unit	T160 E
Group	Nordland
Epoch	Pleistocene
Age (Ma)	2,59 – 0
Maximum thickness	325,7 m
Average thickness	92,0 m
Volume	766 km^3
Av. sediment. rate	8,34 cm/ka
Max sediment. rate	37,31 cm/ka

Contour increments: Base map (20 m), Thickness map (20 m), Amplitude map (20 ms).

Amplitude map displays RMS Amplitude.

Unit T160 F

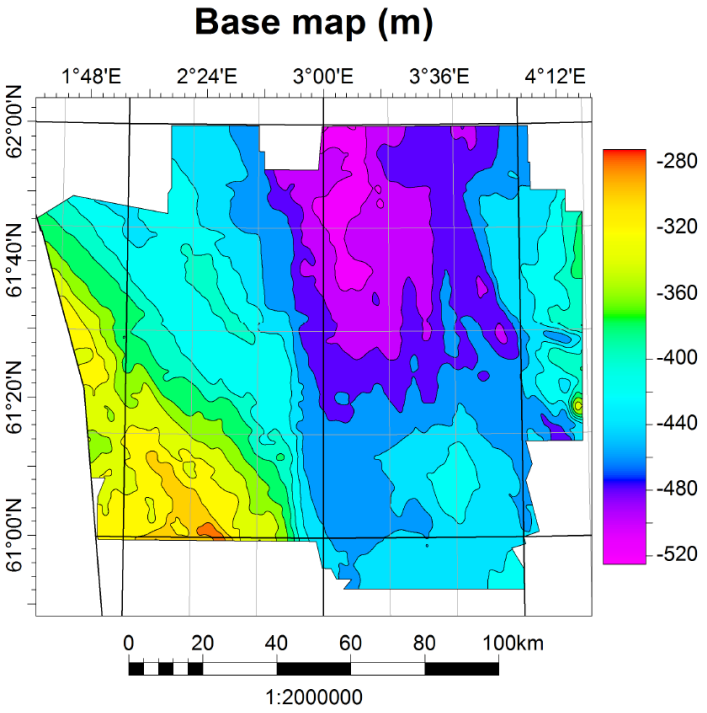

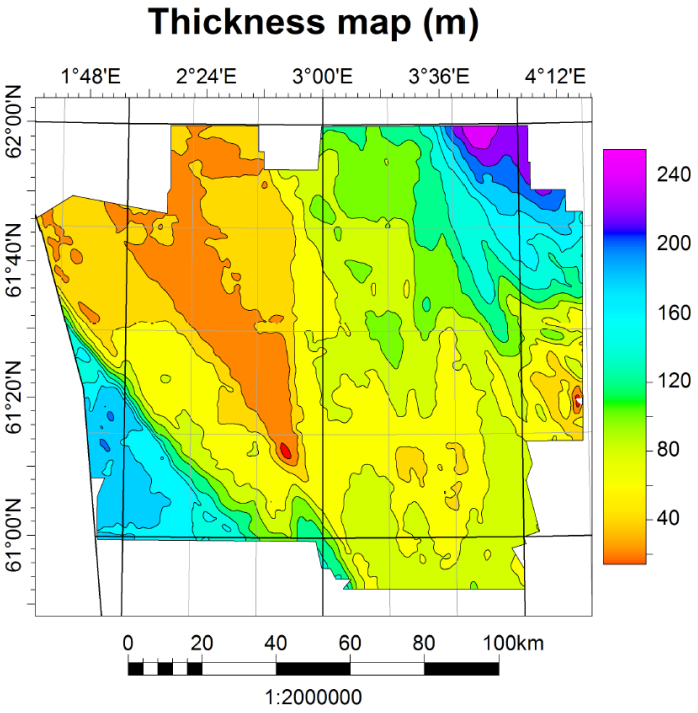

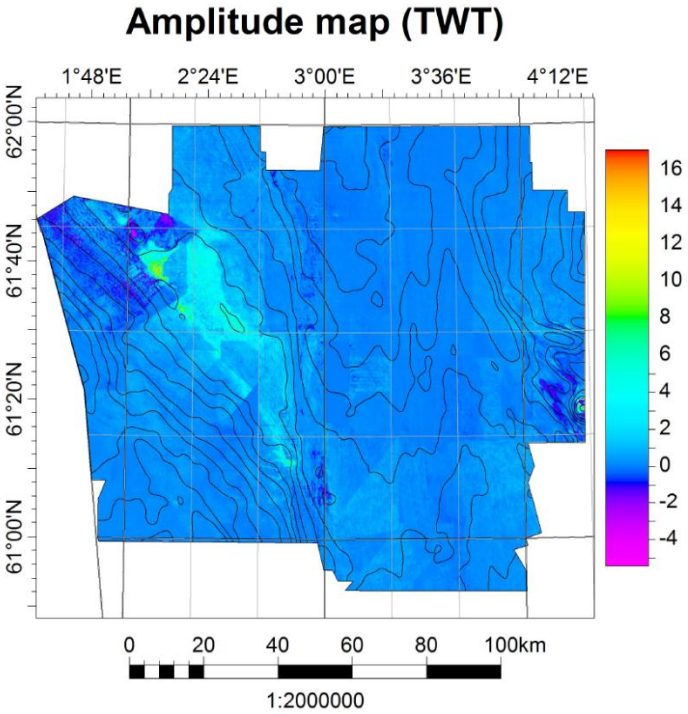

Unit	T160 F
Group	Nordland
Epoch	Pleistocene
Age (Ma)	2,59 – 0
Maximum thickness	333,9 m
Average thickness	90,4 m
Volume	1 320 km^3
Av. sediment. rate	8,34 cm/ka
Max sediment. rate	37,31 cm/ka

Contour increments: Base map (20 m), Thickness map (20 m), Amplitude map (20 ms).

Amplitude map displays Mean Amplitude.

Seabed

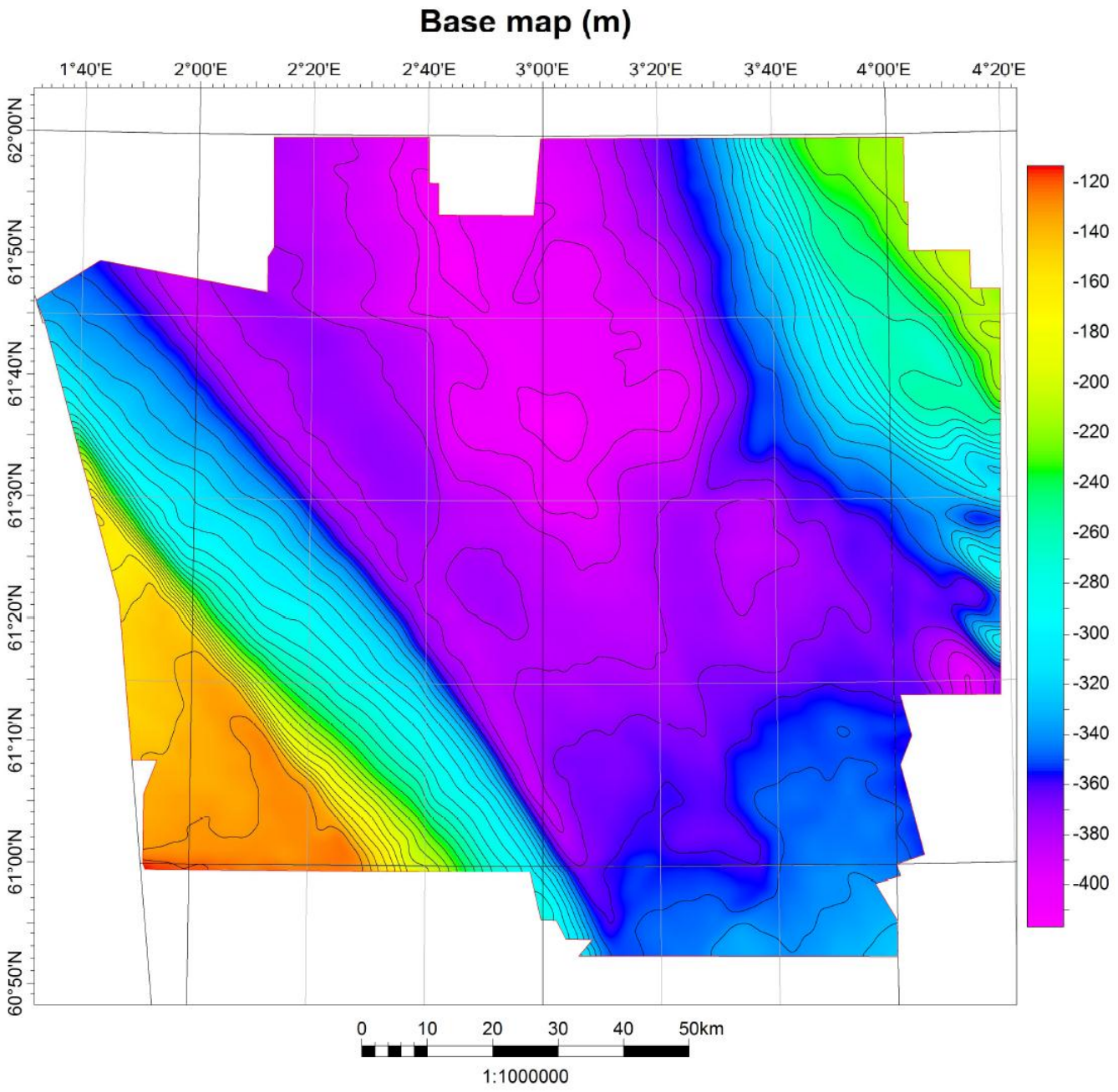

Contour increment: 20 m.

APPENDIX B

Accumulation rates table

Unit	Volume (km^3)	Area (km^2)	Thickness of unit (cm)		Age of deposition (ka)			Accumulation rate (cm/ka)	
			Max	Average	from	to	Δ	Max	Average
T160	3204	14840,8	96631	21855	2590	0	2590	37,3093	8,3359
T150	5276	12024,2	112640	35961	5330	2590	2740	41,1095	16,0136
T140	987	11821,6	34581	8329	11610	5330	6280	5,5065	1,3299
T120-T130	247	2370,6	40664	13347	23030	11610	11420	3,5608	0,9136
T110	2816	12380,9	57380	22720	31150	23030	8120	7,0665	2,8009
T60-T100	5692	13453,6	75130	44290	54000	31150	22850	3,2880	1,8517
T20-T50	3688	14840,8	85170	25250	61100	54000	7100	11,9958	3,5001
T10	417	1089,0	19230	8030	65500	61100	4400	4,3705	3,7106
K10-K120	28934	14840,8	665120	202020	145500	65500	80000	8,3140	2,4370

Table B. Overview of the input data for the calculation of accumulation rates. The calculated results are displayed in the two columns to the right.

APPENDIX C

Well table

Well	Water depth	Cuttings depth	Total depth	Youngest Age	Oldest Age	Completion date	Source
31/2-8	346	500	3375	N/A	Triassic	18.08.1982	NPD
33/6-1	306	450	3900	N/A	Late Triassic	06.07.1979	NPD
33/9-10	162	280	3715	N/A	Late Triassic	12.06.1978	NPD
33/9-11	287	590	3528	N/A	Early Jurassic	28.08.1978	NPD
33/9-12	148	370	2952	Late Oligocene	Late Triassic	03.08.1987	Ichron
33/9-15	253	430	3007	N/A	Middle Jurassic	08.06.1992	NPD
33/9-16	227	410	2870	N/A	Middle Jurassic	20.01.1993	NPD
33/9-18	145	770	3253	Late Oligocene	Late Jurassic	20.12.1994	NPD & Ichron
33/9-9	145	254	3106	Early Eocene	Late Triassic	17.11.1977	Ichron
34/10-15	164	250	2400	Early Eocene	Late Triassic	12.12.1982	Ichron
34/10-30	158	230	3785	Pleistocene	Triassic	12.05.1986	Well Report
34/10-37	140	1530	2873	N/A	Middle Jurassic	22.02.1995	NPD
34/10-37 A	140	2060	2950	N/A	Middle Jurassic	03.04.1995	NPD
34/11-3	208	1120	4482	Late Oligocene	Early Jurassic	16.01.1997	NPD & Ichron
34/4-5	379	510	3917	Early Eocene	Late Triassic	06.04.1984	NPD & Ichron
34/4-6	400	540	3282	Pleistocene	Late Triassic	27.03.1986	Well Report
34/4-7	354	480	2950	N/A	Late Triassic	12.05.1987	NPD
34/7-1	353	480	2905	Pleistocene	Late Triassic	24.07.1984	Well Report
34/7-34	292	1200	2701	N/A	Early Jurassic	10.03.2009	NPD
34/7-8	312	439	2766	Pleistocene	Triassic	11.04.1986	Well Report
34/7-9	330	480	3240	Late Oligocene	Late Triassic	12.06.1986	Ichron
34/8-4 S	309	1170	4150	N/A	Triassic	09.06.1991	NPD
35/10-2	373	1470	4677	Late Oligocene	Early Jurassic	22.08.1996	NPD & Ichron
35/1-1	408	890	4540	Pliocene	Late Triassic	18.07.2002	NPD & Ichron
35/11-2	372	1030	4025	Late Oligocene	Early Jurassic	04.12.1987	NPD & Ichron
35/11-4	355	1010	3127	Late Oligocene	Early Jurassic	29.12.1990	NPD & Ichron
35/11-5	355	1020	3769	N/A	Early Jurassic	03.11.1991	NPD
35/1-2 S	409	1290	4202	N/A	Early Jurassic	19.12.2010	NPD
35/2-1	409	544	713	M. Pleistocene	Pliocene	28.08.2005	Well Report
35/2-2	398	543	640	M. Pleistocene	Early Pliocene	26.07.2009	Well Report
35/3-1	304	520	4475	Pliocene	Middle Jurassic	26.10.1976	NPD & Ichron
35/3-2	272	470	4400	Pliocene	Early Cretaceous	26.10.1980	NPD & Ichron
35/3-4	258	890	4089	Early Oligocene	Early Cretaceous	06.06.1981	NPD & Ichron
35/3-6	225	1310	3366	N/A	Late Jurassic	02.04.2002	NPD
35/6-2 S	344	588	3700	N/A	Early Cretaceous	04.04.2009	NPD
35/8-2	376	580	4336	Pliocene	Early Jurassic	21.05.1982	NPD & Ichron
36/1-2	226	360	3256	Pliocene	Pre-Devonian	27.10.1975	NPD & Ichron

Table C. Overview over all wells used in the thesis with the water depth at the well location, the depth of the first cuttings returned to the surface, the total depth of the wells, the youngest and oldest strata penetrated, the well's completion date and the source of the information.